



HAL
open science

Observational and modelling approaches to study urban climate: application on Pakistan

Sajjad Hussain Sajjad

► **To cite this version:**

Sajjad Hussain Sajjad. Observational and modelling approaches to study urban climate: application on Pakistan. Earth Sciences. Université de Strasbourg, 2013. English. NNT : 2013STRAH021 . tel-01044727

HAL Id: tel-01044727

<https://theses.hal.science/tel-01044727v1>

Submitted on 24 Jul 2014

HAL is a multi-disciplinary open access archive for the deposit and dissemination of scientific research documents, whether they are published or not. The documents may come from teaching and research institutions in France or abroad, or from public or private research centers.

L'archive ouverte pluridisciplinaire **HAL**, est destinée au dépôt et à la diffusion de documents scientifiques de niveau recherche, publiés ou non, émanant des établissements d'enseignement et de recherche français ou étrangers, des laboratoires publics ou privés.



**ÉCOLE DOCTORALE SCIENCES DE LA TERRE, DE L'UNIVERS ET
DE L'ENVIRONNEMENT
LABORATOIRE IMAGE VILLE ENVIRONNEMENT
FACULTÉ DE GÉOGRAPHIE**

A thesis submitted in fulfillment to obtain the degree of
Doctor of Sciences from Université de Strasbourg
Discipline: Geography
Specialization: Urban Climate

by

Mr. Sajjad Hussain SAJJAD

Title of thesis:

**OBSERVATIONAL AND MODELLING APPROACHES
TO STUDY URBAN CLIMATE: APPLICATION ON
PAKISTAN**

16.04.2013

Jury Members:

Research Director:

Prof. Alain CLAPPIER – Laboratoire Image Ville Environnement, Université de Strasbourg (UDS) – France

Internal Reporter:

Prof. Jean-Luc PONCHE – Laboratoire des Matériaux, Surfaces et Procédés pour la Catalyse, UDS – France

External Reporters:

Prof. Syed Shoaib RAZA – Pakistan Institute of Engineering and Applied Sciences, Islamabad - Pakistan

Prof. Salman QURESHI – Department of Geography, Humboldt University of Berlin – Germany

Invited Member:

Dr. Nadège BLOND – Centre National de la Recherche Scientifique, CNRS – France



Declaration of authorship

I Mr. Sajjad Hussain SAJJAD hereby declare that this thesis entitled '*Observational and Modelling Approaches to Study Urban Climate: Application on Pakistan*' is written by me and the work presented in it is my own. I confirm that:

- While in candidature at this university, this work was wholly done for the fulfilment of the degree of PhD at the Faculté de Géographie.
- Where any part of this thesis has previously been submitted for publications or conference presentations either at this University or any other institution, this has been clearly stated.
- Where I have consulted the published work of others, this is always clearly attributed.
- Where I have quoted from the work of others, the source is always given. Whenever I have taken some text from work of others to use as a reference, it is always clearly attributed by citing it properly. With exception of such quotations or referenced work, this thesis is entirely my own work.
- I have acknowledged all the sources of help used for the purpose of this work.

Signed:

Date: 16.04.2013

Abstract

Currently, the cities are the source for the planetary flow of energy and materials which are used to construct cities and ensures their functions. As major human activities are concentrated in urban areas, about 70 per cent of world energy is consumed in cities. The cities are also main source of emissions of several pollutants and greenhouse gases through combustion reactions of fossil fuels. They are also sources of emission of heat into the urban atmosphere because of using energy for cooling or heating of the buildings.

Urbanization affects the physical mechanisms of urban area by reducing the vegetation fraction, modification of the surface roughness, surface albedo and absorption of solar radiation. Urbanization usually causes a change in all elements of the surface energy balance. During the day, urban areas (buildings, roads and other infrastructure) receive the solar radiation. A part of the solar radiation is absorbed by built-up area of the city and the rest is reflected in the atmosphere. Warmed surface of an urban area emit infra-red radiation which can be trapped by reflection/absorption in the urban canyon. The heat from anthropogenic and natural sources also leads to change the urban energy balance. As a result, urban areas become warmer than areas where there is no city and it is generally referred as the urban heat island (UHI). Urban heat island can have the consequences for human health and thermal comfort. It modifies the photochemistry of the city and has an effect on urban air pollution. It initiates or affects the formation of convective storms. It contributes to modify the energy demand for heating or cooling of the buildings. There are several factors that may affect the UHI such as geographical location (climate, topography, rural surrounds) of the city, size of the city, functions of the city, form of the city (materials, geometry, green space) and synoptic weather (clouds, wind) of the city. Because of these factors, the UHI greatly vary from city to city.

At global scale, the average surface temperature is increasing. The rate of global warming averaged over the last 50 years (1956–2005) was $0.13^{\circ}\text{C} \pm 0.03^{\circ}\text{C}$ per decade (Trenberth et al., 2007). During 1979-2004, the minimum and maximum temperature at global scale is also observed increasing by 0.29°C per decade (Vose et al., 2005). At regional scales, in most parts of Pakistan, the average temperature trends also showed increasing trends during 1951-2000 (APN CAPaBLE, 2005) i.e., 0.243°C per decade in west Balochistan and 0.022°C per decade in central and south Punjab. So, the urban areas are being affected in three ways: by global changes, by regional changes and by local urban effects (such as UHI).

Several studies examining the relationship between urbanization and variation in local temperature were published mainly by focusing on UHI. Based on population size, Pakistan is one of the largest countries in the world that have 180 million of population. Currently, in South Asia, Pakistan has the highest percentage of population living in urban areas. According to an estimate, by 2050, 59.4% of total population of the country will be living in urban areas (equivalent to global percentage by 2060). The cities of Pakistan may have an impact on their local climates.

The objective of this work is to study the urban climate, mainly by focusing on urban temperature trends. The specific focus is to understand the reasons of increase in minimum temperature through observational and modelling techniques. For this purpose, the temperatures data from 1950 to 2004 measured on several meteorological stations of Pakistan is studied and analyzed.

Daily averaged annual and seasonal minimum (T_{min}) and maximum (T_{max}) temperature data of 37 meteorological observatories of Pakistan (17 urban, 7 town and 13 rural) from 1950 to 2004 is first homogenized and then analyzed. In order to identify the urbanization effect on local temperature trends, the data is divided into two different time periods, 1950-1979 (period 1) and 1980-2004 (period 2). The urban stations refer to the major cities declared as metropolitan areas by the government and the cities with population density more than 5000 persons/km². The town stations refer to the cities with population density between 1000 to 5000 persons/km² and the rural stations with population density less than 1000 persons/km².

The results show that after 1980s T_{min} and T_{max} increase faster than the period before 1980s at urban areas. During 1980–2004, the increase in T_{min} at major urban stations is observed higher than the smaller towns and rural stations. During 1980–2004, T_{max} increased more at town and rural stations than urban stations and at rural stations, during this period T_{min} decreased and T_{max} increased more than the period 1950–1979. The highest growth in T_{min} and T_{max} at urban and town stations is observed in spring season. At rural stations, it is observed in winter for T_{min} and in spring for T_{max} during 1980–2004. The increase in T_{min} at urban areas of Pakistan is observed 0.43°C per decade that is 0.14 °C per decade higher than the per decade increase (0.29°C) in global minimum temperature during 1980–2004. However, during the same period, per decade increase in T_{max} at urban areas of Pakistan is measured 0.33°C that is close to the per decade increase in global T_{max} which is 0.29°C.

Several hypotheses have been proposed to explain why minimum temperature increases more than maximum temperature on global scale. In this work, we tried to understand why this effect is magnified in urban areas. For this, the effect of the size of the

city, changing land use and the building height on the evolution of minimum and maximum temperatures in urban areas has been studied by using the FVM (Finite Volume Model) model and the simulations are run by taking into account all the possible combinations of urban scenarios. FVM is a three-dimensional non-hydrostatic model which can calculate the evolution of meteorological characteristics (wind speed and direction, pressure, air temperature, and density and moisture) on big cities or regions. FVM is able to correctly simulate the interaction between cities and the atmosphere. The scenarios are constructed by changing the percentage of urban fraction, height of the building and radius of the city. The simulations are run for three days starting at 00:00 (GMT) on 19th day of each month and ending at 00:00 (GMT) on 22nd day of each month. For each month, 48 possible combinations of simulation scenarios are run ($4*4*3$) and in total, 576 simulations ($48*12$) are run for a year.

The main results show that the urban fraction u , city size r and building's height h influence the urban temperatures. T_{min} and T_{max} increase when urban fraction u , city size r and building height h increase. But it is noticed that T_{max} increases more than the T_{min} when u increases, T_{min} increases more than the T_{max} when r increases and T_{min} increases more than the T_{max} when h increases. Among all urban factors (urban fraction u , city size r and building's height h), city size is the major factor that mainly contributes to increase the minimum temperature more than the maximum temperature in urban areas. However, the contribution of city size to increase the minimum temperature compared to the maximum temperature in urban areas varies from season to season. In winter, in 98% cases of the simulation scenarios of city size r showed higher increase in T_{min} compared to T_{max} and it represents in 58% cases in spring, in 51% cases in autumn and only in 30% cases in summer.

Résumé

Actuellement, les villes sont les sources de flux planétaires d'énergie et de matériaux, qui sont utilisés pour construire les villes et assure leurs fonctions. Comme les principales activités humaines sont concentrées dans les zones urbaines, environ 70 pour cent de l'énergie mondiale est consommée dans les villes. Les villes sont ainsi la principale source d'émission de plusieurs polluants et de gaz à effet de serre et ce via les réactions de combustion des combustibles fossiles. Elles sont également sources d'émission de chaleur dans l'atmosphère urbaine, liée au refroidissement ou au chauffage des bâtiments.

L'urbanisation affecte les mécanismes physiques de la zone urbaine en réduisant la fraction de végétation, la modification de la rugosité de surface, l'albédo de la surface et l'absorption du rayonnement solaire. L'urbanisation provoque généralement une modification de tous les éléments du bilan énergétique de surface. Pendant la journée, les zones urbaines (bâtiments, routes et autres infrastructures) reçoivent le rayonnement solaire. Une partie du rayonnement solaire est absorbée par zone bâtie de la ville et le reste se reflète dans l'atmosphère. Réchauffée la surface urbaine émet un rayonnement infra-rouge qui peut être piégé par réflexion/absorption dans le canyon urbaine. Le dégagement de chaleur par des sources anthropiques et de sources naturelles amène également à modifier le bilan énergétique urbain. En conséquence, les zones urbaines deviennent plus chaudes que les zones où il n'y a pas de ville et ce qui est généralement nommé comme îlot de chaleur urbain (ICU). Un îlot de chaleur urbain peut avoir des conséquences sur la santé humaine et sur le confort thermique. Il modifie la photochimie de la ville et a ainsi un effet sur la pollution de l'air urbain. Il initie ou affecte la formation des orages de convection. Il contribue à modifier la demande d'énergie pour le chauffage ou le refroidissement des bâtiments. Plusieurs facteurs peuvent influencer ICU comme la localisation géographique (climat, topographie, rurale entoure) de la ville, taille de la ville, fonctions de la ville, la forme de la ville (matériaux, géométrie, espaces verts) et les conditions météorologiques synoptiques (nuages, vent). En raison de ces facteurs, ICU grandement varié d'une ville à l'autre.

A l'échelle globale, la température moyenne à la surface augmente. Le taux de réchauffement de la planète en moyenne au cours des 50 dernières années (1956-2005) a été de $0,13 \text{ °C} \pm 0,03 \text{ °C}$ par décennie (Trenberth et al., 2007). Au cours de la période 1979-2004 l'augmentation de températures minimales et maximales à l'échelle mondiale est même

observée plus élevée à 0,29 °C par décennie (Vose et al., 2005). À l'échelle régionale, dans la plupart des régions du Pakistan, les tendances de la température moyenne ont aussi montré une augmentation du 0,011 °C par décennie au cours de la période 1951-2000 (APN CAPaBLE, 2005) i.e. 0,243 °C par décennie dans l'ouest du Baloutchistan et de 0,022 °C par décennie dans le centre et le sud du Pendjab. Ainsi, les zones urbaines sont touchées de trois manières: par les changements globaux, par des changements régionaux et locaux par des effets urbains (ICU).

Plusieurs études portant sur la relation entre l'urbanisation et la variation de la température locale ont été publiées ces études portent principalement sur ICU. Selon la taille de la population, le Pakistan est l'un des plus grands pays du monde qui a 180 millions d'habitants. Actuellement, en Asie du Sud, le Pakistan a le pourcentage le plus élevé de la population vivant dans les zones urbaines. Selon une estimation, en 2050, 59,4% de la population totale du pays vivront dans les zones urbaines (ce qui équivaut au pourcentage mondial d'ici à 2060). Les villes du Pakistan pourraient avoir un impact sur le climat local.

L'objectif majeur de ce travail est d'étudier le climat urbain, principalement en mettant l'accent sur les tendances de la température. Il s'agit principalement de l'augmentation des températures grâce à des techniques d'observation et de modélisation. A cet effet, des données températures de 1950 à 2004 ont été étudiées sur plusieurs stations de mesure au Pakistan.

Les données de températures annuelles et saisonnières moyennes quotidiennes minimales (T_{min}) et maximales (T_{max}) de 37 observatoires météorologiques du Pakistan (17 urbain, 7 petite ville et 13 rurale) pour la période 1950-2004 ont d'abord été homogénéisées, puis analysées. Afin d'identifier l'effet de l'urbanisation sur les tendances de la température locale, les données ont été divisées en deux périodes distinctes, 1950-1979 (période 1) et 1980-2004 (période 2) et les résultats sont présentés par types de station. Les stations urbaines correspondent aux grandes villes déclarées comme des métropoles par le gouvernement et à des densités de population de plus de 5000 personnes/km². Les stations de petites villes correspondent à des villes de densité de population entre 1000 à 5000 personnes/km². Les stations rurales correspondent à des surfaces où la densité de population reste inférieure à 1000 personnes/km².

Les résultats montrent qu'après les années 1980, T_{min} et T_{max} tendent à augmenter plus vite que la période d'avant 1980 sur les zones urbaines. Au cours de la période 1980-2004, l'augmentation annuelle de T_{min} sur les stations urbaines est observée plus élevée que sur les stations des petites villes et les stations rurales. Au cours de la période 1980-2004, T_{max} a augmenté plus sur les stations des petites villes et les stations rurales que sur les stations

urbaines. Pendant 1980-2004, T_{min} a diminué et T_{max} a augmenté sur les stations rurales plus que pendant le période 1950-1979. La plus forte croissance de T_{min} et T_{max} sur les stations urbaines et de petites villes est observée au printemps. Sur les stations rurales, elle est observée en hiver pour T_{min} et au printemps pour T_{max} pendant le période 1980-2004. L'augmentation de T_{min} sur les zones urbaines du Pakistan est mesurée à 0,43 °C/décennie ce qui est 0,14 °C/décennie plus que l'accroissement de la température minimum global au cours de la même période. L'augmentation de T_{max} sur les zones urbaines du Pakistan est proche de l'augmentation de T_{max} observée à l'échelle globale.

Plusieurs hypothèses ont été émises pour expliquer pourquoi température minimale augmente plus que température maximale à l'échelle globale. Dans ce travail, nous avons essayé de comprendre pourquoi cet effet est amplifié sur les zones urbaines. Pour cela, l'effet de la taille de la ville, le changement de l'utilisation des sols et la hauteur du bâtiment sur l'évolution des températures minimales et maximales des zones urbaines a été étudié en utilisant le model FVM (Finite Volume Model) et des simulations ont faites en tenant compte de toutes les combinaisons possibles de scénarios urbains. FVM est un modèle en trois dimensions non-hydrostatique qui peut permet de calculer l'évolution des caractéristiques météorologique (la vitesse du vent et des orientations, pression, température de l'air, et densité et de l'humidité) sur les grandes agglomérations ou des régions. FVM est capable de simuler correctement l'interaction entre les villes et l'atmosphère. Les scénarios ont construit en changeant le pourcentage de la fraction urbaine, la hauteur des bâtiments et le rayon de la ville. Les simulations ont été effectuées pour trois jours à partir de 00:00 (GMT) le 19e jour de chaque mois et se terminant à 00:00 (GMT) le 22e jour de chaque mois. Pour chaque mois, 48 combinaisons possibles de scénarios de simulation sont exécutés (4*4*3) et au total, 576 simulations (48*12) sont exécutés pendant un an.

Les résultats centre montrent que la fraction urbaine u , la taille de la ville r et la hauteur du bâtiment h influencent les températures urbaines. T_{min} et T_{max} augmente lorsque fraction urbaine u , taille de la ville r et hauteur du bâtiment h augmente. Mais on remarque que T_{max} augmente plus que le T_{min} quand u augmente, T_{min} augmente plus que T_{max} lorsque r augmente et T_{min} augmente plus que T_{max} lorsque h augmente. Parmi tous les facteurs urbains (fraction urbaine u , taille de la ville r et hauteur du bâtiment h), la taille de la ville est le facteur majeur qui contribue principalement à augmenter la température minimale plus que température maximale dans les zones urbaines. Toutefois, la contribution de la taille de la ville dans l'augmentation relative de la température minimale par rapport à la température maximale dans les zones urbaines varie saison par saison. En hiver 98% des scénarios de

simulation de taille de la ville r montrent une plus grande augmentation de T_{min} par rapport à T_{max} , ils représentent 58% des cases en printemps, 51% des cases en automne et 30% des cases en été.

Acknowledgement

I owe my special and the most sincere gratitude to Professor Alain Clappier for providing me the best opportunity to work in his team under his pleasant supervision. His supreme efforts, regular guidance and encouragement made me able to learn the advances in urban climate studies through modelling approaches and finally succeeded to complete this thesis. I would like to express my sincere gratefulness and highly acknowledge to Dr. Nadège Blond for her full time assistance, guidance and providing me the plenty of her valuable time to let me understand the urban climate processes, techniques to analyse the data and the use of atmospheric model. I am obliged for her great patience, encouragement all the way of my studies and repeatedly correcting me whenever I made the mistakes during my Master and PhD thesis – thanks a lot dear Nadège.

My exceptional thanks are for Higher Education Commission (www.hec.gov.pk), Government of Pakistan for granting me fully funded scholarship for my Master and PhD studies in France. I am highly thankful to the administration of University of Sargodha (www.uos.edu.pk) – Pakistan for providing me the opportunity to avail this chance.

I acknowledge Réseau Alsace de Laboratoires en Ingénierie et Sciences pour l'Environnement (REALISE) and Région Alsace, France for providing the computers and other computing material. I am grateful of all members of the management of SFERE (Société Française d'Exportation des Ressources Éducatives) for their wonderful arrangements for my admission, residences and addressing all the matters on priority basis. I am thankful to the administration of Pakistan Meteorological Department for providing the meteorological data of different meteorological observatories of Pakistan. I am also thankful to Dr. Khalid Mahmood (Chairman), Zahid Naveed Ahmed and all other colleagues of Department of Earth Sciences for their moral support and looking after the administrative matters related to me at the university during my absence from the department.

I also wish to express thanks to Prof. Enric Aguillar, Center for Climate Change (C3), Universitat Rovira I Virgili, Tarragona – Spain for his great help to homogenize the time series data of several stations of Pakistan and allowing me to use some important text and figures out of his publication in my thesis. Indeed, his support helped us to properly homogenize the time series data. I am highly thankful to Dr. Alberto Martilli, Senior Scientist, CIEMAT for his guidance in Chapter 4. His ideas made me able to properly parameterize the

urban zones and then to use them in the model to extract the contribution of each parameter. I also thank to Prof. Sèrge Occhietti, Faculté de Géographie, Université de Nancy2 – France for his support during my Master studies. My special thanks also go to Louiza Salam, Dominique Lebesson and Pierre-Jean Cholley (my Master Class fellows) for giving me their precious time for the preparation of my exams whenever I felt difficulty to understand French language. Off course, their support at that time made me able to successfully complete my Master from Université de Nancy2. I am also gratified of all my Professors of Department of Geography and Center for South Asian Studies, University of the Punjab, Lahore – Pakistan for their contributions in my higher education and research activities. I am thanks to *Prof. Dr. Raas Masood* from University of the Punjab, Lahore and Madam *Shakeela Khanum Rasheed* from All Pakistan Women Association (APWA) who managed a scholarship for my Master studies at University of the Punjab, Lahore during 1999-2000 and it was due to their support that I succeeded to keep continuing my studies.

I would like to thank all the members of Faculté de Géographie and Laboratoire Image Ville Environnement (LIVE) of this university especially Christian Webber (Directrice du LIVE), Christophe Enaux (Directeur adjoint du LIVE), Estelle Baehrel (Assistante de Direction) and Jean-Luc Mercier for their administrative and academic supported during my stay at the lab. I am also thankful to my respectable colleagues ‘Manon Kohler, Dasaraden Mauree’ who helped me a lot in my research. Their valuable comments, suggestions and discussions about my research helped me to improve my work. I am really thankful to everybody here in lab for their moral and respectful cooperation during my stay here at this lab. I am also grateful to all my friends in Pakistan who always had the best wishes for me and supported me in all the ways during my academic career.

I can’t forget to say lot of thanks to dear Uncle Suleman Asif who was the prime sources of inspiration for me and off course one of the great personality to whom I met in my life. Although I have fulfilled his dream of my PhD, I am sad too as he is not with us today. May Almighty Allah rest his soul in peace.

At the end, I would like to especially thank to my loving parents, my sisters, brothers and all my relatives who supported me from my primary education to higher education. Among all, I am highly thankful to my wife Kalsoom for helping and praying for me all the times. It’s because of financial, moral and encouraging supports and scarifications of my family members, today I became able to finish my higher degree from France otherwise I may never succeed. Thanks a lot everybody.

Strasbourg – France

CONTENTS

Declaration of Authorship	i
Abstract	ii
Résumé	v
Acknowledgement	ix
List of figure	xiv
List of Tables	xvii
Abbreviations	xix
List of Appendix	xxi
Chapter 1: Introduction	01
1.1 Introduction	01
1.2 Urbanization in Pakistan	06
1.3 Objective of the study	09
1.4 Structure of the thesis	10
Chapter 2: Energy balance, urban heat island and its measuring techniques	11
2.1 Introduction	11
2.2 The Atmospheric Boundary Layer	12
2.3 Radiation budget	17
2.3.1 Earth-Atmospheric radiation budget	18
2.3.2 The urban energy budget	20
2.4 Urban Heat Island (UHI)	24
2.4.1 Causes of UHI	25
2.4.2 Consequences of UHI	27
2.5 UHI studying approaches and measuring techniques	29
2.5.1 Field measurements	29
2.5.2 GIS and Remote Sensing	31
2.5.3 UHI modelling approaches	32

Chapter 3: A comparative analysis of the change in temperature on urban, town and rural areas **36**

	Abstract	36
3.1	Introduction	37
3.2	Data and methodology	42
3.2.1	Meteorological data	42
3.2.2	Homogenization of data	45
3.2.3	Metadata	47
3.2.4	Homogeneity assessment	47
3.2.5	Mann-Kendall test	56
3.2.6	Principal Component Analysis	57
3.2.7	Calculation of temperature trends	60
3.3	Results and discussion	60
3.3.1	Analysis of variation in minimum and maximum temp.	60
3.4	Discussion	67
3.5	Conclusion	68

Chapter 4: Urban size, landuse change and building height effect on urban temperature **71**

	Abstract	71
4.1	Introduction	72
4.2	Methodology	79
4.2.1	Model description	79
4.2.2	Model setup for simulation	80
4.2.3	Model input and data acquisition	81
	4.2.3.1 Topographical data	81
	4.2.3.2 Landuse data input	82
	4.2.3.3 Meteorological data	84
4.2.4	Preparation of simulation scenarios	85

4.2.4.1	Preparation of landuse scenarios	86
4.2.4.2	Preparation of city size scenarios	86
4.2.4.3	Preparation of building height scenarios	87
4.2.4.4	Computation of temperature variations for urban parameters	87
4.2.4.5	Computation of contribution of urban parameters in temperature variation	88
4.3	Results and Discussion	89
4.4	Conclusion	97
Chapter 5: Conclusion		99
5.1	Major outcome of the study	99
5.2	Future Perspective	102
Appendices		104
References		125
Curriculum Vitae		147

List of Figures

Figure No.	Title	Page No.
1.1	Percentage of urban population of major countries of South Asian region.	7
1.2	Percentage of Pakistan's urban population during 1950 – 2050	8
2.1	A typical midlatitude vertical temperature profile; (b) Schematic of the planetary boundary layer.	14
2.2	Urban heat island processes at mesoscale and microscale.	14
2.3	The effect of terrain roughness on wind speed.	16
2.4	A scheme of mechanical and thermal effect due to presence of buildings in urban areas.	16
2.5	Schematic representation of global-mean energy budget (W m^{-2}).	19
2.6	Schematic of the volumetric averaging approach to urban energy balance.	23
2.7	Generalized cross-section of a typical urban heat island.	24
2.8	The UHI types and their measuring approaches.	30
3.1	Topographic Map of Pakistan.	39
3.2	Pakistan climates classification and associated mean annual rainfall.	40
3.3	Location of meteorological stations on the map of Pakistan	43
3.4	Schematic representation of homogenization procedures for monthly to annual climate records.	46
3.5	Quality of raw data of minimum temperature measured at Bunji and Rohri during 1950 to 2004.	49
3.6	Annual and seasonal average of daily minimum temperature of Quetta airport for 1950 to 2004. Detection of break points (on left) and adjustment of data (on right).	53
3.7	Annual and seasonal average of daily minimum temperature of	54

	Lahore city for 1950 to 2004. Detection of break points (on left) and adjustment of data (on right).	
3.8	A presentation of data points of annual average of daily minimum temperature of a reference and a candidate series representing the trends before and after homogenization.	55
3.9	Abrupt changes in time series of monthly averaged minimum and maximum temperature of Lahore (urban).	57
3.10	Principal Component Analysis results on the differences of temperatures trends between phase 2 and phase 1. (a) Variables graph, (b) individuals graph.	59
3.11	dT_n trends as a function of dT_x trends for urban, town and rural stations. Per year trends computed for 1950–1979 (a) ; for 1980–2004 (b); mean trends computed for all urban, town and rural stations for phase 1 and phase 2 (c). The values of dT_n and dT_x are in °C/year.	64
3.12	Illustration of per year variance in $dT_{n(1980-2004)} - dT_{n(1950-1979)}$ as a function of per year variance in $dT_{x(1980-2004)} - dT_{x(1950-1979)}$ for each station as well as for average of each type of stations for <i>annual</i> (a); <i>winter</i> (b); <i>spring</i> (c); <i>summer</i> (d); and <i>autumn</i> €.	65-66
4.1	Relationship between maximum heat island intensity ($\Delta T_{ur(max)}$) and population (P) for European and North American settlements.	73
4.2	Effect of city size (in population on day and night time surface UHI magnitude. Tokyo (T); Beijing (BE); Shanghai (SH); Seoul (SE); Pyongyang (P); Bangkok (BA); Manila (M); Ho Chi Minh City (H).	73
4.3	Changes in temperature differences between urbanized and rural areas in the years 1975–2004. (a) Difference in mean annual temperature ($dMAT$); (b) difference in monthly mean maximum temperature (dMT_{max}); (c) difference in monthly mean minimum temperature (dMT_{min}); and (d) relationships between the temperature differences and degree of urbanization.	74

4.4	Relationship between built-up ratio, distance from the city centre and annual mean maximum UHI intensities along South–North cross-section in Debrecen, Hungary	78
4.5	Raw topography tile and the processed topography map.	82
4.6	Raw landuse tile and processed landuse map for the selected domain.	83
4.7	Wind at 5 meter above the ground. The color contours represent the topography in meters above sea level.	85
4.8	Scheme of the city size scenarios.	86
4.9	Effect of urban areas on local temperature by varying the city size r for 20.04.2005 at 09:00 GMT	90
4.10	Effect of urban areas on local temperature with varying city size r for 20.04.2005 at 17:00 GMT.	91

List of Tables

Table No.	Title	Page No.
2.1	Characteristics of urban boundary-layer regions.	15
2.2	Radiative properties of typical urban materials and areas.	21
2.3	Scales of atmospheric motion.	33
3.1	Values of Thom's Discomfort Index calculated for Celsius temperature scales	41
3.2	Geographical descriptions of meteorological stations of Pakistan	44
3.3	Break-Points detection of minimum temperature	51
3.4	Break-Points detection of maximum temperature	52
3.5	Annual and seasonal temperature trends computed for the periods 1950–1979, 1980–2004 and for the difference between the two periods. dT_n and dT_x correspond to change in minimum and maximum temperatures, whereas An, Wi, Sp, Su, Au correspond to the Annual, Winter, Spring, Summer and Autumn.	62
3.6	Percentage of stations showing positive trends for annual and seasonal minimum and maximum temperature at urban, town and rural stations for the period 1950–1979 and 1980–2004.	62
3.7	Annual trends ($^{\circ}\text{C dec}^{-1}$) of mean, minimum and maximum temperatures for global and regional (Pakistan) land areas.	68
3.8	Annual trends ($^{\circ}\text{C dec}^{-1}$) of mean, minimum and maximum temperatures for global and regional (Pakistan) land areas.	68
3.9	Annual trends ($^{\circ}\text{C dec}^{-1}$) of mean, minimum and maximum temperatures for average of urban, town and rural stations of Pakistan.	68
4.1	UHI magnitudes and spatial extensions for the eight selected Asian mega cities.	75
4.2	Annual averages, minimum and maximum values and % of positive values out of all the simulations for dT_{min}/du , dT_{max}/du , dT_{min}/dr , dT_{max}/dr , dT_{min}/dh and dT_{max}/dh .	92

4.3	Net annual temperature difference between $dT_{min}/du - dT_{max}/du$; $dT_{min}/dr - dT_{max}/dr$; $dT_{min}/dh - dT_{max}/dh$ based on average of all the months.	93
4.4	Monthly average, maximum and minimum value, monthly and seasonal percentage of positive dT_{min} based on all the simulation scenarios of each month.	95
4.5	Evolution of urban surface area of Lahore from 1972 to 2010.	96
4.6	Per decade change in minimum and maximum temperature for dT/dt (eq. 4.1) for the two periods 1972 to 1980 and 1980 to 2004 obtained through annual average of all the simulation scenarios by using FVM model.	96
4.7	Comparison of per decade change in minimum and maximum temperature at Lahore based on observational data of Lahore city and the output of the model. Here P1 is representing first period (1972-1980) and P2 is representing for second period (1980-2004).	97

Abbreviations

GHGs	Greenhouse gases
OECD	Organisation for Economic Co-operation and Development
GDP	Gross domestic product
Mtoe	Megaton oil equivalent
GNP	Gross national product
K	Kelvin
UHI	Urban heat island
cal	Calorie
FVM	Finite Volume Mesoscale
E-A	Earth-Atmosphere
ABL	Atmospheric Boundary Layer
UBL	Urban boundary layer
UCL	Urban canopy layer
RSL	Roughness sub-layer
CFL	Constant-flux layer
ML	Mixed layer
TKE	Turbulent kinetic energy
SW	Short-wave
LW	Long-wave
UC	Urban canyon
MW	Megawatts
VOCs	Volatile organic compounds
SODAR	SOund Detection And Ranging

GIS	Geographical Information System
MODIS	Moderate Resolution Imaging Spectro-Radiometer
TM	Landsat Thematic Mapper
ETM+	Enhanced Thematic Mapper Plus
LST	Land-surface temperature
NDVI	Normalized Difference Vegetation Index
LULC	Landuse/land cover
PBL	Planetary Boundary Layer
CFD	Computational Fluid Dynamics
UCM	Urban canopy model
SNHT	Standard normal homogeneity test
MTOE	Million tons of oil equivalents
ACS	Air Conditioner Systems
PMD	Pakistan Meteorological Department
WMO	World meteorological organization
QC	Quality control
PCA	Principal Component Analysis
GMT	Greenwich Meridian Time
NCDC	National Climatic Data Center
NCEP	National Center for Environmental Predictions
DEM	Digital Elevation Model
GLC	Global land cover
WRF	Weather Research Forecasting

List of Appendix

Appendix 2.1	The factors affecting urban heat island	104
Appendix 3.1	Change in global T_{min} and T_{max} from 1950 to 1993	105
Appendix 3.2	Comparison between temperature of urban and rural areas	106
Appendix 3.3	dT_n and dT_x during 1950-1979	107
Appendix 3.4	dT_n and dT_x during 1980-2004	108
Appendix 4.1	Population density of the largest cities	109
Appendix 4.2	The mesoscale model governing equations	110
Appendix 4.3	Impact of variation in urban fraction on local temperature	118
Appendix 4.4	Impact of variation in urban fraction on local temperature	119
Appendix 4.5	Impact of variation in building height on local temperature	120
Appendix 4.6	Impact of variation in building height on local temperature	121
Appendix 4.7	$dT_{r12-r08}/dr$; $dT_{r16-r12}/dr$ and $dT_{r20-r16}/dr$	122
Appendix 4.8	$dT_{u80-u70}/du$; $dT_{u90-u80}/du$ and $dT_{u95-u90}/du$	123
Appendix 4.9	$dT_{h30-h25}/dh$ and $dT_{h25-h20}/dh$	124

DEDICATED TO MY FAMILY
AND
DEAR UNCLE SULEMAN ASIF

CHAPTER 1

INTRODUCTION

1.1 Introduction

Before the middle of eighteenth century, the levels of urbanization throughout the world were low and the existence of large cities was only as elements of the urban systems of large national states and empires (Jones and Kandel, 1992). The major developments in urbanization are associated with industrialization that progressed a lot as a result of the shift in primary power sources for manufacturing. During mid of the 19th century, the shift in power source from hand and water power to steam power brought an industrial revolution. By 1870, the steam power

capacity in manufacturing increased by replacing the water-power (Fenichel, 1979; Rosenberg and Trajtenberg, 2004; Kim, 2005). Such turmoil of industrial revolution caused an arisen in economic development and expressive urbanization. Moreover, the advancement of engineering in mechanical and construction industries also caused the development and expansion of existing of new cities, respectively. As a result, in twentieth century the world witnessed the rapid urbanization throughout the world and especially in third world countries. The global urban population in 1900 was 13 per cent that has increased to 29 per cent in 1950. It reached to 49 per cent in 2005. Due to rapid growth in urban population, it is estimated that 60 per cent (about 4.6 billion) of the world total population will be living in cities by 2030 (World Urbanization Prospects, 2005).

The first consequence of the urbanization is to deliberate more energy consumption in the cities. The second consequence is to degrade human quality of life and health. Recently, a major part of the energy consumed in the world is produced from combustion of fossil fuels. The burning of fossil fuels in combustion reactions results in emission of number of pollutants and greenhouse gases in the atmosphere (Vedal, 1997; Oke, 1997). Some of the pollutants harm the human health and ecosystems in general. The concentration of greenhouse gases (GHGs) contributes to change the climate and causes to increase the global temperatures. The global average surface temperature is increasing and since 1950s, the rate of increase is faster than the previous decades. During last 100 years (1906–2005), global temperature increased to 0.74°C; and the rate of global warming averaged over the last 50 years (1956–2005) was 0.13°C per decade that is nearly twice that for the last 100 years (Trenberth et al., 2007).

The imprint of urban areas on climate is also widely increasing (Grimmond, 2006). The pace of urbanization poses massive challenges for the whole world generally and for less developed world especially. Removals of vegetation cover for settlement of new towns and extension of existing cities not only enlarged the anthropogenic activities but also spoils the natural land cover and local environment. The loss of green areas as a result of urbanization is also a serious threat to the overall biodiversity of urban areas (Qureshi and Breuste, 2009). The key anthropogenic activities in the cities are mainly concern to use of energy. The cities consume a great majority – between 60 to 80% – of energy production worldwide and account for a roughly equivalent share of global CO₂ emissions. The growing urbanisation is expected to lead

to a significant increase in energy use and CO₂ emissions, particularly in non-OECD¹ countries in Asia and Africa (OECD, 2010). The studies also show that the vacillations in annual gross domestic product (GDP) have effect on energy consumption (Lee, 2006) that is observed during global economic recession in 2009, when the decrease in world GDP of 0.6% caused to drop - 1.1% or 130 Mtoe (Megaton oil equivalent) of the world energy consumption (ENERDATA, 2010). However, about 1% increases in per capita gross national product (GNP) leads to increase 1.03% of energy consumption and conversely, 1% increase in urban population leads to increase 2.2% of energy consumption (Jones and Kandel, 1992). In less developed regions, the fast expansion of cities is leading to higher demand of house hold energy (Dzioubinski and Chipman, 1999; Sajjad et al. 2010).

The increase in temperature of cities all over the world does not have a direct impact upon global warming. However, the cities indirectly have an effect to cause global warming because they are the most important source of greenhouse gases (Alcoforado and Andrade, 2008). The study of Parker (2004) “*Large scale warming is not urban*” shows that urbanization has not systematically exaggerated the observed global warming trends in minimum temperature, and his analysis (264 stations worldwide covering more than 27% of global land area) demonstrates that urban warming has not introduced significant biases into estimates of recent global warming. Easterling et al. (1997) also highlights in his work that the urban areas effect on global and hemispheric temperature trends are negligible. Although at some extent the global changes influence the urban climates, these changes, however, are not only the cause to affect the local climate. The recent study published in ‘*nature climate change*’ by Zhang et al. (2013) gives a new type viewpoint that energy use from multiple urban areas collectively can warm the atmosphere remotely, thousands of miles away from the energy consumption regions. It is because the significant amount of the heat is lifted into the jet stream, causing the fast-moving current of air to widen. When the heat is taken up into the system, it disrupts the normal flow of energy and can cause surface temperatures to change in distant locales affected by the same air circulation pattern. Further Zhang et al. (2013) elaborate that the inclusion of energy use at 86 model grid points (using global climate model) where it exceeds 0.4Wm^{-2} can lead to remote

¹ Countries which are not member of Organisation for Economic Co-operation and Development (OECD)

surface temperature changes by as much as 1 K in mid-and high latitudes in winter and autumn over North America and Eurasia.

The impacts of global warming (including its impacts upon human well-being and health, various ecosystems, and on levels of energy and water consumption) may be exacerbated in urban areas. Depending both on their latitude and on their regional climate, cities will either be losers or winners from global warming (Oke, 1997). In warmer regions, if global warming causes increased air conditioning in cities, then more anthropogenic heat will be released and the UHI will increase further (Auliciems, 1997). Conversely, in colder areas there will be a reduction in energy use for heating, but “. . . early snowmelt will increase the thickness of the thawed layer in summer and threaten the structural stability of roads, buildings and pipelines” (Hinkel et al., 2003; as cited by Alcoforado and Andrade, 2008). Global warming may not necessarily bring about an increase in UHI intensity: urban-rural temperature differences may remain constant even in an overall warmer world (Oke, 1997).

The important internal and external factors of the city influence the local climate, including urban morphology, size of the city, building density, land-use distribution, topography, meteorological conditions, season, water bodies, time of day, increased release of anthropogenic heat associated with rises in energy consumption (Oke, 1982; Magee et al., 1999; Montavez et al., 2000; Martilli, 2002; Kalnay and Cai, 2003; Kim and Baik, 2005, Alcoforado and Andrade, 2008; Zhang et al., 2010; Salamanca et al., 2010; Salamanca and Martilli, 2010). However, the magnitude of the urban effect may also be closely associated with the level of energy consumption (e.g., cal/person/year), which depends on other socio-economic factors such as is seen in studies conducted on Prague (Brázdil and Budíková, 1999) and Shanghai (Chen et al., 2003). In principal, the urban growth incorporates two trends: income growth and spatial growth or sprawl (Kahn, 2006). Income growth cause to equally increase the energy consumption (Lee, 2006; Jones and Kandel, 1992) and urban sprawl has led to worsening environmental problems, as more area is sealed over (i.e., becomes impermeable through paving or building construction), less green area remains and water and energy consumption increase (Oke, 1997; Hassid et al., 2000; Kahn, 2006; Alcoforado and Andrade, 2008). The effects of a large number of buildings in close proximity, as in a city, are greater than the sum of the effects of the individual buildings due to the complex interactions between them (Erell and Williamson, 2007; cited by Petralli et al., 2011). Consequently urban areas experience higher temperature than their surrounding rural

areas, and this phenomenon is widely known as urban heat island (Quattrochi and Rid, 1994; Grimmond et al., 2002; Shepherd and Burian, 2003; Martilli, 2003; Martilli et al., 2003; Bounoua et al., 2009).

The modified land surface in cities affects the storage, radiative and turbulent transfers of heat and its partition into sensible and latent components. Urbanization generally results in modification of all elements of the surface energy balance – net radiant exchange (Q^*), subsurface storage (ΔQ_S) and the channeling of the available heat into sensible (Q_H) and latent (Q_E) fluxes as a result of the presence of moisture together with anthropogenic heat (Q_F) release. In this way, urban areas could be given as the surface energy balance equation: $Q^* + Q_F = Q_H + Q_E + \Delta Q_S + \Delta Q_A$ (Oke, 1987; Oke, 1988; Erell and Williamson, 2007; Rizwan et al., 2008). The relative warmth of a city compared with surrounding rural areas, arises from these changes and may also be affected by changes in water runoff, pollution and aerosols (Oke, 1987; Trenberth, et al. 2007).

The ability of a town or city to generate an urban heat island and the magnitude of urban warming also greatly vary over both time and space. (Oke, 1973; Oke, 1987; Bacci and Maugeri, 1992; Aniello et al., 1995; Grimmond et al., 2002; Shepherd and Burian, 2003; Chung et al., 2004; Liu et al., 2007; Yin et al., 2007; Bounoua et al., 2009). Individual cities show a large heat-island effect, measuring up to $5^\circ\text{C} \sim 11^\circ\text{C}$ warmer than their surrounding rural areas (Aniello et al., 1995). The urban heat island (UHI) intensity varies with urban size and population growth (Bacci and Maugeri, 1992; Chung et al., 2004; Liu et al., 2007; Yin et al., 2007), urban surface characteristics and anthropogenic heat release (Landsberg, 1981). The UHI also vary according to different types of atmospheric circulation pattern or air masses e.g. in Madrid, Spain (Yagüe et al., 1991).

Large cities differ from the surrounding rural areas by virtue of having larger buildings that exert a stronger drag on the wind; less ground moisture and vegetation, resulting in reduced evaporation; different albedo characteristics that are strongly dependent on the relationship between sun position and alignment of the urban street canyons; different heat capacity; and greater emissions of pollutants and anthropogenic heat production. All of these effects usually cause the city center to be warmer than the surroundings (Wallace and Hobbs, 2006). As the major proportion of the world's population is centering towards urban areas, their environmental

issues are getting worse and such areas have gotten significant attention of research communities all around the world. In this context, the cities are more and more concerned by climate change: first by concentrating dense population, they become more and more vulnerable to climate change risks; secondly by concentrating human activities and energy consumption, their responsibilities in climate change are increasing. In order to reduce the vulnerability and the energy consumption of such cities and improve inhabitants comfort, urban planners and decision makers may try to find best sustainable urban strategies

The researchers adopted different approaches to study the urban climate at different scales. The recent advancements in numerical models have made it easier to simply simulate the effect of urban areas on local climate either by using a model or by coupling the different models as Advanced Regional Prediction System (Baik et al., 2007); Linear statistical model (Bottyan et al., 2005); Simple Biosphere Model (Bounoua et al., 2009); State-of-science meteorological models (MetMs) and chemistry-transport models (CTMs) (Chemel et al., 2008); MODIS approach for satellite data (Cheval and Dumitrescu, 2009); Regional Atmospheric Modelling System and the Town Energy Budget model (Freitas et al., 2007); Tree-structured regression model (Hart and Sailor, 2009) Surface heat island model (Oke et al., 1991); WRF (Kusaka et al., 2005; Shrestha et al., 2009, Miao et al., 2009; Salamanca et al., 2012).

1.2 Urbanization in Pakistan

Unlike most of the rest of the world, South Asia has been marked by low levels of urbanization despite being one of the most urbanized pre-colonial regions of the eighteenth century (Revi et al., 2002). However, Pakistan is on top among the South Asian countries by having the highest percentage of urban population (Figure 1.1). Currently 39% of total population is living in urban areas and in 2050, it is estimated that almost 60% of the country's population will be living in urban areas (UNDESA, 2011). Karachi, Lahore and Faisalabad are three large cities of the country with a population of 18, 10 and 4.1 million, respectively by having population density over 10,000 persons/km² (Demographia, 2011; Wikipedia, 2012).

Figure 1.2 shows the growth of urban population in Pakistan. Share of urban population increased from 17.5% in 1950 to 33.1% in year 2000. It is further guesstimate that in 2050, 59.4% of total population of the country will be living in urban areas (UNDESA, 2011). It is

important here that many of the Pakistani cities are densely populated with huge population size. According to recent population estimates, major cities of Pakistan like Karachi, Lahore, Rawalpindi, Hyderabad, Faisalabad, Multan, Peshawar, Islamabad and Quetta have population of 18.0, 10.0, 3.25, 3.0, 2.88, 1.6, 1.43, 1.33 and 0.89 million, respectively. Population density of these cities is over 10,000 persons/km² (Demographia, 2011). The mega cities such as Karachi are highly dense where about 17,325 persons live in per square kilometre (Qureshi, 2010). Although we could not find data of spatial extent of all cities however the available data of Karachi shows that this city has grown nearly 25 times since 1947 and is growing at the rate of about 5.4% per annum (Qureshi, 2010). If Karachi is considered as a reference city, it can be imagined that the Pakistan is facing higher urbanization.

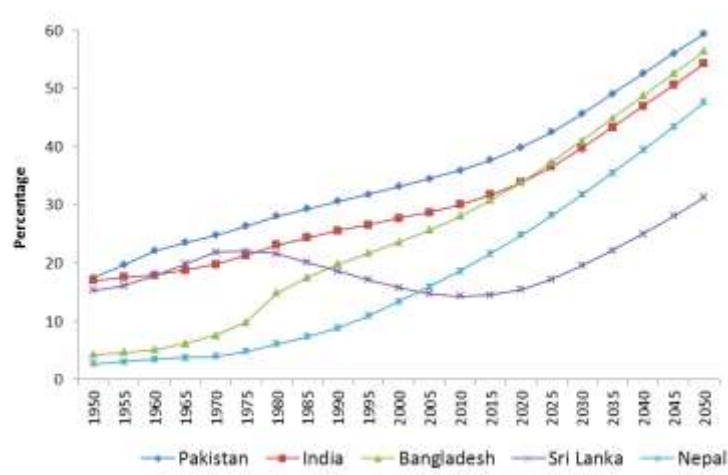


Figure 1.1: Percentage of urban population of major countries of South Asian region. Data source: United Nations, Department of Economic and Social Affairs, Population Division (2011): World Population Prospects, 2011.

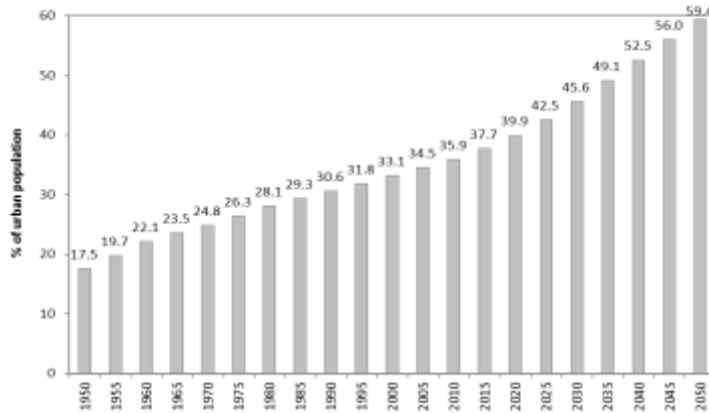


Figure 1.2: Percentage of Pakistan’s urban population during 1950 – 2050. Data source: United Nations, Department of Economic and Social Affairs, Population Division (2011): World Population Prospects, 2011.

As it is discussed earlier, there are many factors that can be the cause of higher increase in temperature of urban areas. Rapid urbanization causes the expansion or densification of the cities and causes the replacement of the natural land cover (green spaces) by urban built areas (buildings, roads). The increasing urban population causes the densification of urban areas and the cities are growing horizontally and vertically. The expansion of cities causes the modification of the urban energy balance as more the artificial surfaces urban areas will have; there will be more absorption of solar energy and less emission of infrared radiation. Moreover, as the cities are growing, the anthropogenic activities are enhancing. Most of the human activities in urban areas are concerned to the use of energy (in buildings and for vehicles). Higher rate of consumption of energy in urban areas significantly causes the emission of heat into atmosphere that ultimately causes to warm-up the urban atmosphere as compare to its surrounding rural areas.

1.3 Objectives of the study

The objective of this work is to address a series of questions, such as:

- Is the temperature of urban areas of Pakistan increasing or not?
- If increasing, at which rate (more or less than the evolution of temperature at global and regional scale)?
- Which temperature parameter is being affected more by urban areas (minimum or maximum temperature)?
- Which are the important factors that cause the higher change in evolution of temperature of urban areas such as:
 - is it changing because of the size of the city?
 - is it changing because of the increasing urban fraction?
 - or is it because of the densification of the city with increasing building's height?
- And what is the contribution of each of the factor in evolution of urban areas temperature?

In this study, the efforts is to made to answers of the above mentioned questions by using observational and modelling approaches.

The first aim is to see the urban areas effect on local temperature trends, by evaluating the annual averages of daily mean, minimum and maximum temperatures data from 1950 to 2004 at several locations of urban, town and rural areas of Pakistan. The second aim is to assess the effect of major urban factors such as city size, landuse change and building height effects on minimum and maximum temperature trends of urban area and to identify the factors that cause the minimum temperature to increase faster than the maximum temperature.

To fulfill the first objective, the temperature data of 37 meteorological stations of Pakistan will be analyzed for the temperature trends at urban, town and rural areas. A comparative quantification of the change in temperature on urban areas of Pakistan will be calculated and will be compared with global trends for the periods 1950-2004 and 1980 to 2004. The meteorological

stations are located in all parts of the country so they are classified into urban, town and rural stations².

To accomplish the second objective, Finite Volume Mesoscale model (FVM) will be used to run the several scenarios on theoretical round cities by changing their building's height (meters), city size (radius in km) and urban fraction (in percentage). FVM is a mesoscale model that is able to simulate the interaction between cities and the atmosphere.

This work has been decided in order to evaluate on which contribution part decision makers can directly act to reduce local temperatures and make their cities more livable and become the part of global efforts to mitigate the climate changes at local and global scales.

1.4 Structure of the thesis

For better understanding and reviewing urban-atmospheric energy balance and UHI cause, effects measuring and studying approaches, chapter 2 presents a complete review that will help to easily understand the UHI and its mechanism linked to urban energy balance. In chapter 3, observed data of 37 meteorological stations (17 urban, 7 town and 13 rural) of Pakistan is homogenized first and then statistically analyzed. The results of this chapter are useful to comparatively quantify the evolution of minimum and maximum temperature at urban areas of Pakistan and then compare them with global evolution of temperature trends. In Chapter 4, Finite Volume Mesoscale (FVM) is used to run monthly simulations for 48 different scenarios based on urban size (4 scenarios), urban fraction (4 scenarios) and buildings height (3 scenarios). In this chapter all the scenarios are run in a combination where all are run with each other ($4*4*3=48$ scenarios per month). The procedure to use the Finite Volume Mesoscale (FVM) model, inputs, initializing time and urban parameterization is also discussed in this study. Chapter 5 is concluding all the study and giving the future perspectives for further study.

² Urban stations refer to the major cities declared as metropolitan areas by the local governments and the cities with population density more than 5000 persons/km². The town stations refer to the cities with population density between 1000 to 5000 persons/km². The rural stations refer to the stations with population density less than 1000 persons/km². As there is no metadata available about all the meteorological stations considered in this study, some urban stations may not necessary be located in centre of the city.

CHAPTER 2

ENERGY BALANCE, URBAN HEAT ISLAND AND ITS MEASURING TECHNIQUES

2.1 Introduction

Radiation is the most important factor of energy exchange. It is the source of power that drives the atmospheric circulation, the oceanic circulation, and the hydrological cycle, and is the only means of energy exchange between the earth and the rest of the universe (Geiger et al., 1995). Energy of importance to climatology exists in the Earth-Atmosphere (E-A) system in four different forms (*radiant, thermal, kinetic and potential*) and is continually being transformed from one to another. The exchange of energy within the E-A system is possible in three modes (*conduction, convection and radiation*). Inside the atmospheric system, the energy is likely to be

channelled into different subsystems, and converted into different combinations of energy forms and modes of transport. Some will lead to energy storage change and others to energy output from the system. This partitioning is not haphazard; it is a function of the system's physical properties. In the case of energy these properties include the ability of the system to absorb, transmit, reflect and emit radiation, its ability to conduct and convect heat, and its capacity to store energy (Oke, 1987).

There are essentially four types of energy fluxes at an ideal surface (surface relatively smooth, horizontal, homogeneous, extensive and opaque to radiation), namely, the net radiation to or from the surface, the sensible (direct) and latent (indirect) heat fluxes to or from the atmosphere, and the heat flux into or out of the submedium (soil or water). The net radiative flux is a result of the radiation balance at the surface. During the daytime, it is usually dominated by the solar radiation and is almost always directed towards the surface, while at night the net radiation is much weaker and directed away from the surface. As a result the surface warms up during the daytime, while it cools during the evening and night hours, especially under clear sky and undistributed weather conditions (Arya, 2001).

A short description of atmospheric boundary layer is given in section 2.2, E-A and urban energy balance is given in section 2.3, urban heat island, its causes and consequences are given in section 2.4, and UHI studying approaches such as field measurements, GIS and remote sensing and modelling approaches are given in section 2.5.

2.2 The Atmospheric Boundary Layer

The vertical distribution of temperature for typical conditions in the Earth's atmosphere provides a basis for dividing the atmosphere into four distinct layers: troposphere, stratosphere, mesosphere, and thermosphere (Wallace and Hobbs, 2006) (see figure 2.1a). Almost major part of all the weather processes and human activities takes place in troposphere that is the lowest layer of the atmosphere and is characterized by decreasing temperature with height, rapid vertical mixing, contains almost all of the atmosphere's water vapor and holds about 80% of atmosphere's total mass. Troposphere is divided into several layers mainly atmospheric boundary layer (ABL) or simply boundary layer, free atmosphere, turbulent surface layer, and roughness layer (Oke, 1987; Arya 2001, see Fig. 2.1b). *Free atmosphere* extends from about 1 km to the tropopause

(Seinfeld and Pandis, 2006). The ABL is directly influenced by the presence of the earth's surface and may be characterized by well developed mixing (turbulence) generated by frictional drag as the atmosphere moves across the rough and rigid surface of the earth, and by the 'bubbling-up' of air parcels from the heated surface (Stull, 1988; Jacobson, 2005). The boundary layer receives much of its heat and all of its water through this process of turbulence (Oke, 1987). The thickness of the boundary layer is quite variable in space and time. Normally ~1 or 2 km thick (i.e., occupying the bottom 10 to 20% of the troposphere), it can range from tens of meters to 4 km or more (Wallace and Hobbs, 2006). The *turbulent surface layer* is characterized by intense small scale turbulence generated by the surface roughness and convection; by day it may extend to a height of about 50 m, but at night when the boundary layer shrinks it may be only a few metres in depth. The *roughness layer* extends above the tops of the elements to at least 1 to 3 times of their height or spacing. In this zone the flow is highly irregular being strongly affected by the nature of the individual roughness features (e.g. blades of grass, trees, buildings, etc.). The *laminar boundary layer* is in direct contact with the surface(s). It is the non-turbulent layer, at most a few millimetres thick that adheres to all surfaces and establishes a buffer between the surface and the more freely diffusive environment above (Oke, 1987).

The urban boundary layer (UBL), above roof level, in contrast, is that part of the boundary layer whose characteristics are affected by the presence of the urban surface (or its land-use zones) below and is a local to meso-scale phenomenon controlled by processes operating at larger spatial and temporal scales (Fig. 2.2). Characteristics of urban boundary-layer regions are presented by Roth (2000) in Table 2.1 in which the regions identified are based on a simple classification first proposed by Oke (1976) that recognizes the urban canopy layer (UCL) and UBL, respectively (as cited by Roth, 2000).

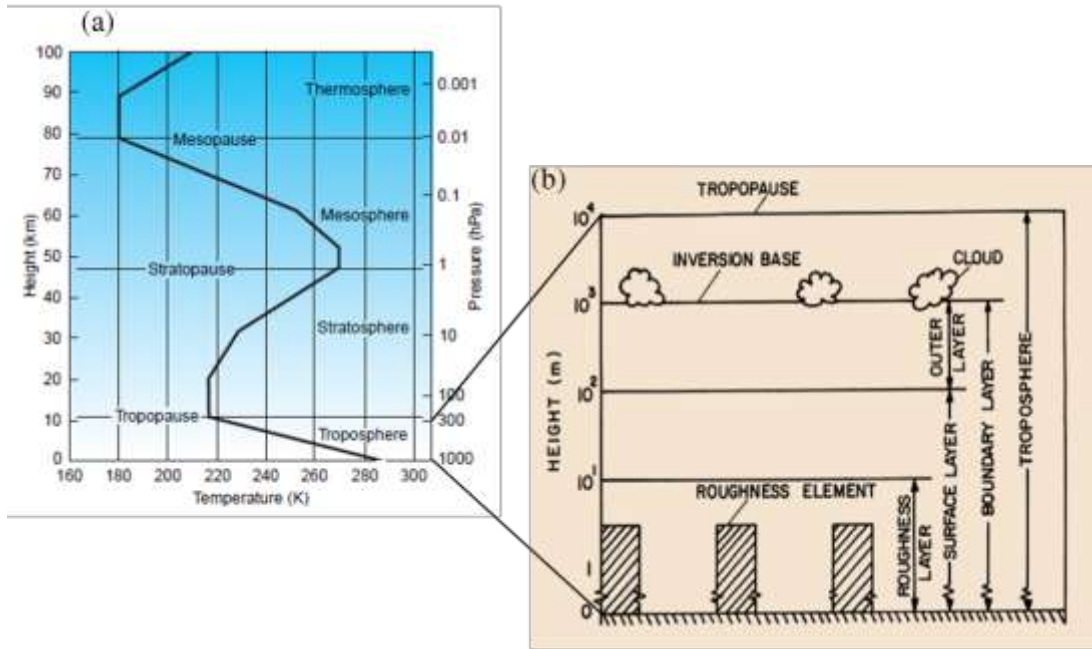


Figure 2.1: (a) A typical mid-latitude vertical temperature profile, as represented by the U.S. Standard Atmosphere (After: Wallace and Hobbs, 2006); (b) Schematic of the planetary boundary layer as the lower part of the troposphere (After: Arya, 2001).

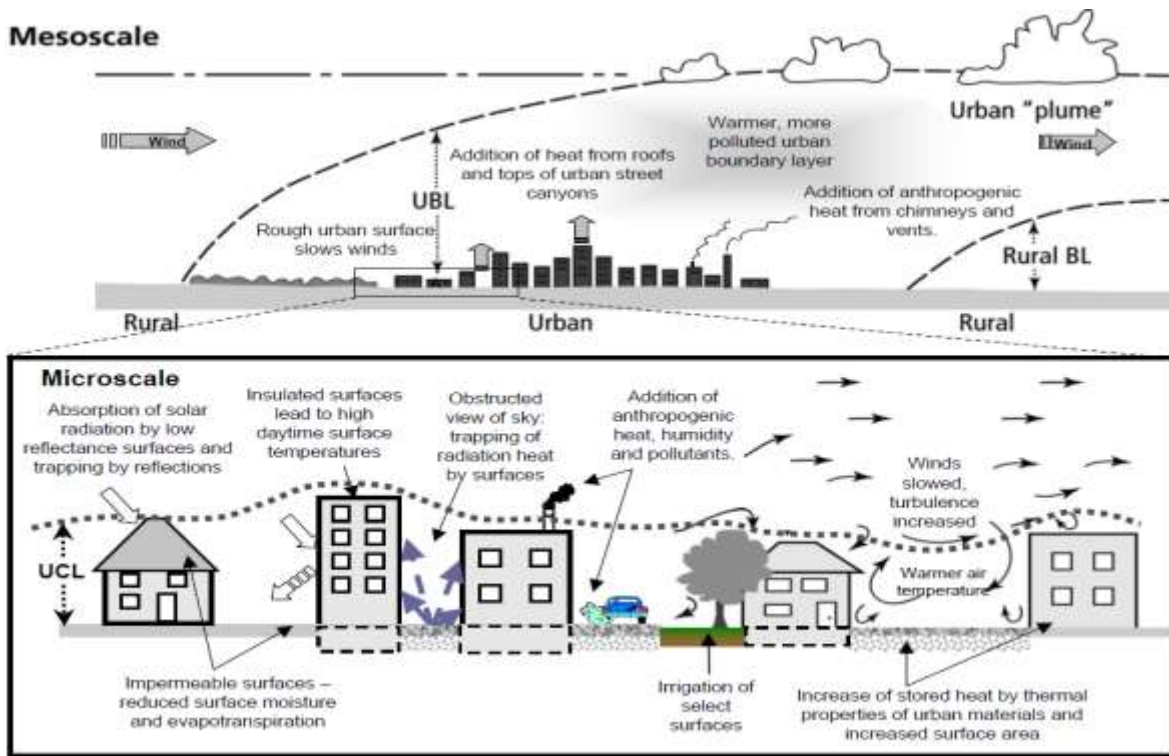


Figure 2.2: Urban heat island processes at mesoscale and microscale (After Voogt, 2007).

Table 2.1: Characteristics of urban boundary-layer regions (After Roth, 2000). Here z_* presents the depth of the Roughness sub-layer (RSL), $0.1z_*$ denotes up to 10% of z_* and z_i denotes the top of mixed layer (often defined as the average base of the overlying stable layer).

Region	Characteristics
Urban boundary layer (UBL) Ground to top of boundary layer	Portion of planetary boundary layer whose characteristics are affected by the presence of the urban area. Local to mesoscale phenomenon. Includes all other layers.
Urban canopy layer (UCL) Ground level to about roof level	Produced by microscale effects of site characteristics. Dynamic and thermal processes are dominated by the immediate surroundings. Flow and scalar structure are generally very complex. Most clearly pronounced in areas of high building density, but may be discontinuous in less developed suburban areas.
Roughness sub-layer (RSL) Ground to z .	Also called the transition layer, interfacial layer or wake layer; includes UCL. Mechanically and thermally influenced by length-scales associated with the roughness. Because of wake diffusion and differential source/sinks of momentum and scalars, momentum and heat transfers are dissimilar, and therefore Reynold's analogy may not be valid (Roth and Oke 1995). As a result of local-scale advection, the turbulence field is often not horizontally uniform, even in a time average, and must be considered three-dimensional (e.g. Ching 1985; Schmid et al. 1991).
Constant-flux layer (CFL) z to $\sim 0.1z_i$.	Also called the inertial sub-layer. Mean profiles obey semi-logarithmic laws or their diabatic extensions and Monin-Obukhov similarity (MOS) applies. Very little is known about it in urban areas, in part due to the height restrictions of measurement towers which, due to the existence of a RSL with dimensions of tens of metres, often do not extend into the CFL. The vertical extent of the urban CFL is also determined by the development of an internal boundary layer which responds to mesoscale land-use changes in upwind surface characteristics. It is possible that under unstable conditions the depth of the RSL exceeds the potential depth of the CFL and no such layer exists (Oke et al. 1989).
Mixed layer (ML) $\sim 0.1z_i$ to z_i	Little is known about urban MLs, but turbulence properties are probably independent of the surface roughness. It is topped by an entrainment layer which may be substantial because of enhanced coupling between the rough and warm urban surface and the ML (Roth and Oke 1995) and the relatively larger availability of turbulent kinetic energy (TKE) (e.g. Eaton and Dirks 1977).

As explained by Oke (1987) the wind field in the boundary layer is largely controlled by the frictional drag imposed on the air flow by the underlying rigid surface (Fig. 2.3). The drag retards motion close to the ground and gives rise to a sharp decrease of mean horizontal wind speed (\bar{u}) as the surface is approached. The force exerted on the surface by the air being dragged over it is called the surface shearing stress (τ) and is expressed as a pressure (Pa, force per unit surface area). The increased drag and turbulence results in a deeper zone of frictional influence within which wind speeds are reduced in comparison with those at the same height in the country. This local slowing of the air flow causes it to 'pile-up' (i.e. converge) over the city, and this is relieved by uplift. The vertical motion induced is in addition to that brought about by the heat island effect, and may be sufficient to cause the urban boundary layer to 'dome' up over the city by about 250 m in the daytime. Downwind of the city the return to less rough rural surfaces results in subsidence but an elevated 'plume' of rising air may persist for tens of kilometres.

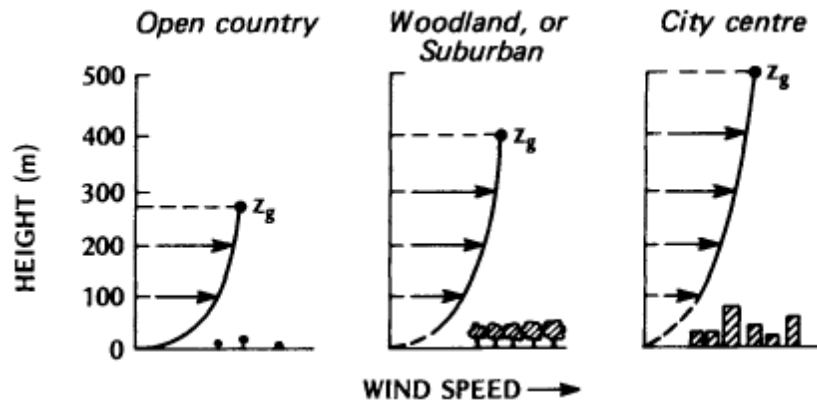


Figure 2.3: The effect of terrain roughness on vertical profile of wind speed (After Oke, 1987).

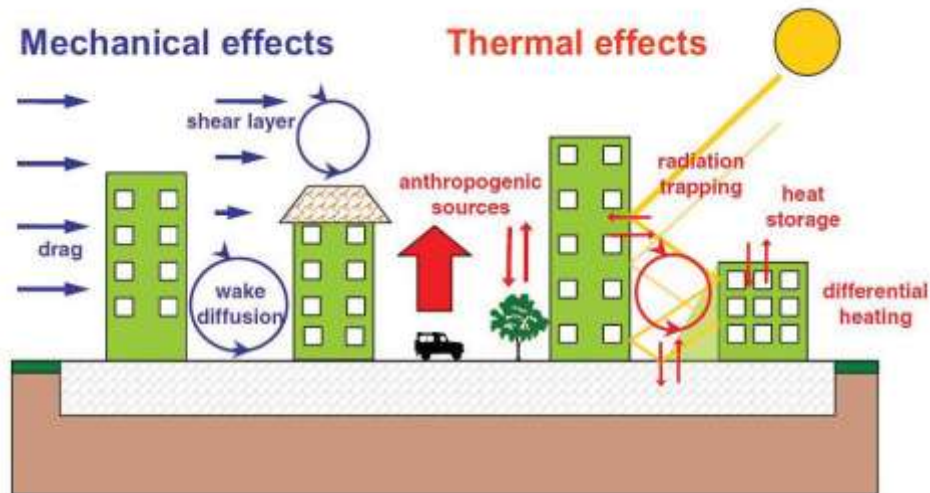


Figure 2.4: A scheme of mechanical and thermal effect due to presence of buildings in urban areas. Source: Air and Soil Pollution Laboratory, École Polytechnique Fédérale de Lausanne (EPFL), Switzerland.

The boundary layer is said to be unstable whenever the potential temperature of the air is warmer than the above air, such as during a sunny day with light winds over land, or when cold air is advected over a warmer water surface. This boundary layer is in a state of free convection, with vigorous thermal updrafts and downdrafts. The boundary layer is said to be stable when the surface potential temperature of air is colder than the air, such as during a clear night over land, or when warm air is advected over colder water. Neutral boundary layers form during windy and

overcast conditions, and are in a state of forced convection (Wallace and Hobbs, 2006). Figure 2.4 presents the mechanical and thermal effects and resulting of the interaction between the urban surface and the boundary layer of the atmosphere. Large cities differ from the surrounding rural areas by virtue of having larger buildings that exert a stronger drag on the wind; less ground moisture and vegetation, resulting in reduced evaporation; different albedo characteristics that are strongly dependent on the relationship between sun position and alignment of the urban street canyons; different heat capacity; and greater emissions of pollutants and anthropogenic heat production. All of these effects usually cause the city center to be warmer than the surroundings – a phenomenon called the urban heat island. The largest cities generate and store so much heat that they can create convective mixed layers over them both day and night during fair-weather conditions. This urban heat source is often associated with enhanced thermals and updrafts over the city, with weak return-circulation downdrafts over the adjacent countryside. One detrimental effect is that pollutants are continually recirculated into the city. Also, the enhanced convection over a city can cause measurable increases in convective clouds and thunderstorm rain (Wallace and Hobbs, 2006).

2.3 Radiation budget

Knowledge of the surface energy balance is fundamental to an understanding of the boundary layer meteorology and climatology of any site. In conjunction with the synoptic wind, it provides the energetic driving forces for the vertical fluxes of heat, mass and momentum (Oke, 1988). Basically all the energy that reaches the Earth comes from the Sun. The absorption and loss of radiant energy by the Earth and the atmosphere are almost totally responsible for the Earth's weather on both global and local scales. The average temperature on the Earth remains fairly constant, indicating that the Earth and the atmosphere on the whole lose as much energy by reradiation back into space as is received by radiation from the Sun. The accounting for the incoming and outgoing radiant energy constitutes the Earth's energy balance. The atmosphere, although it may appear to be transparent to radiation, plays a very important role in the energy balance of the Earth. In fact, the atmosphere controls the amount of solar radiation that actually reaches the surface of the Earth and, at the same time, controls the amount of outgoing terrestrial

radiation that escapes into space (Seinfeld and Pandis, 2006). A brief description of E-A and urban radiation budget are given in section 2.3.1 and 2.3.2.

2.3.1 Earth-Atmospheric radiation budget

Schemes of global-mean energy budget (in W m^{-2} and in %) are presented and described by Rotty and Mitchell (1974), Wehrli (1985), Oke (1987), Ramanathan (1987; 1989), Salby (1996) and other researchers. Such schemes recognize the Earth, the Atmosphere and Space as separate sub-systems and places magnitudes on the energy exchanges between them (Oke 1987; Ramanathan, 1989). Incoming solar energy is distributed across the earth. Therefore, the global-mean short-wave (SW) flux $\overline{F_s}$ incident on the top of the atmosphere is given by $\overline{F_s} = F_s/4 = 343 \text{ W m}^{-2}$, where F_s the global solar flux and the factor 4 represents the ratio of the surface area of the earth to the cross-sectional area of the intercepted beam of SW radiation. Figure 2.5 represents the global-mean energy budget (W m^{-2}). Of the incident 343 W m^{-2} , a total of 106 W m^{-2} (approximately 30%) is reflected back to space (21 W m^{-2} by air, 69 W m^{-2} by clouds, and 16 W m^{-2} by the surface) and does not participate further in the E-A system energy balance. The remaining 237 W m^{-2} is absorbed in the Earth-Atmosphere System. Of this, 68 W m^{-2} (about 20% of the incident SW flux) is absorbed by the atmosphere (48 W m^{-2} by atmospheric water vapor, ozone, and aerosols and 20 W m^{-2} by clouds). This leaves 169 W m^{-2} to be absorbed by the surface – nearly 50% of that incident on the top of the atmosphere (Salby, 1996).

At a global-mean the surface temperature reaches to 288 K. As any warm body, the surface emits longwave (LW) radiation. 390 W m^{-2} is emitted far more than it absorbs as short-wave (SW) radiation. Excess LW emission must be balanced by transfer of energy from other sources. Owing to the greenhouse effect, the surface also receives LW radiation that is emitted downward by the atmosphere in the amount of 327 W m^{-2} . Collectively, these contributions result in a net transfer of radiative energy to the surface:

SW absorption (K^*_e)	+	LW absorption from atmosphere (L^*_{gc})	-	LW emitted by Surface ($L\uparrow_e$)	=	Net radiative forcing of surface (ΔK_s)
169 W m^{-2}	+	327 W m^{-2}	-	390 W m^{-2}	=	$+106 \text{ W m}^{-2}$

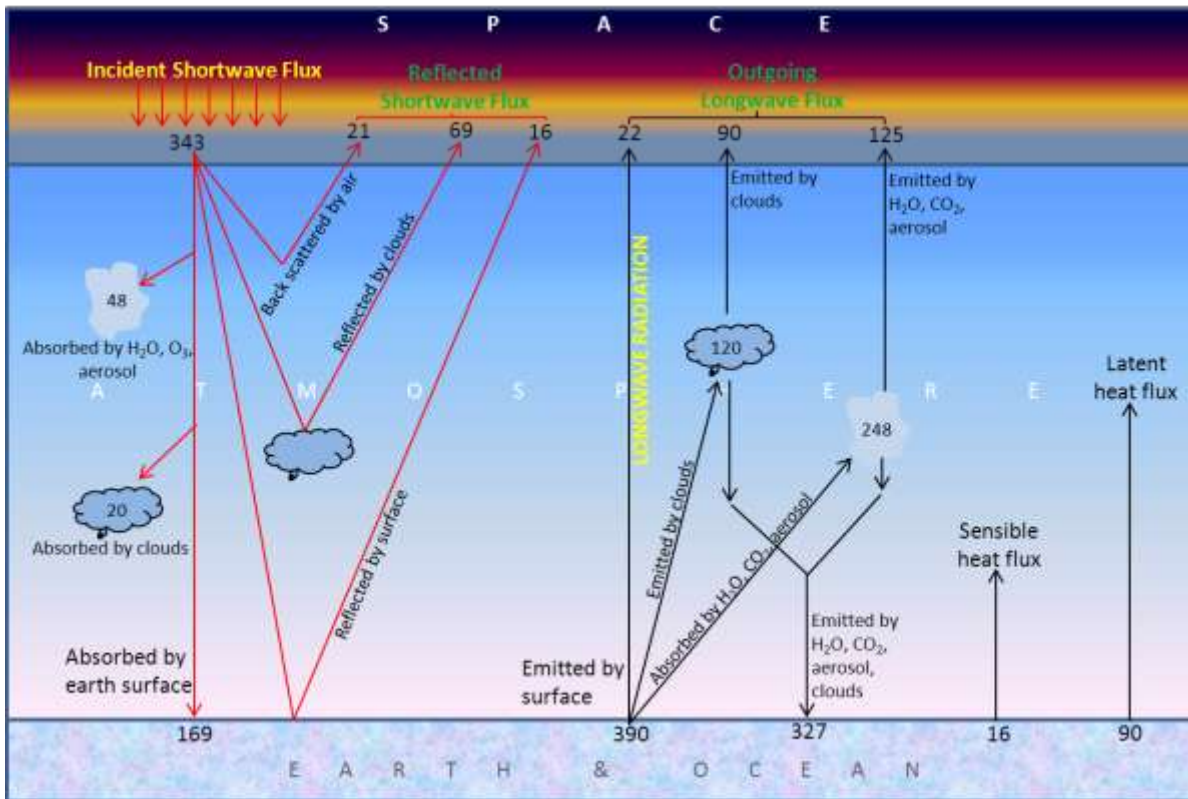


Figure 2.5: Schematic representation of global-mean energy budget (W m^{-2}) (After Salby, 1996).

The surplus of 106 W m^{-2} represents net “radiative heating of the surface.” For equilibrium, this must be balanced by transfers of sensible and latent heat for the atmosphere. Were it not for these supplemental forms of energy transfer, the earth’s surface would have to be some 50 K warmer to balance the net absorption of radiant energy. The energy budget of the atmosphere must also balance to zero to maintain thermal equilibrium. The atmosphere receives 60 W m^{-2} directly through absorption of SW radiation. Of the 390 W m^{-2} of LW radiation emitted by earth’s surface, only 22 W m^{-2} passes freely through the atmosphere and is rejected to space. The remaining 368 W m^{-2} is absorbed by the atmosphere: 120 W m^{-2} by clouds and 248 W m^{-2} by water vapor, CO₂ and aerosol. The atmosphere loses 327 W m^{-2} through LW emission to the earth’s surface. Another 215 W m^{-2} is rejected to space: 90 W m^{-2} emitted by clouds and 125 W m^{-2} emitted by water vapor, CO₂, and other minor constituents. Collecting these contributions gives the next flux of radiative energy to the atmosphere:

SW absorption ($K_g^* + K_c^*$)	+	LW absorption from surface ($L_g^* + L_c^*$)	-	LW re-emission to surface (L_{gc}^*)	-	LW emission to surface ($L_{\uparrow g} + L_{\uparrow c}$)	=	Net radiative forcing of atmosphere (ΔK_a)
68 W m ⁻²	+	368 W m ⁻²	-	327 W m ⁻²	-	215 W m ⁻²	=	-106 W m ⁻²

The deficit of 106 W m⁻² represents net “radiatives cooling of the atmosphere,” cooling that is balanced by the transfer of sensible and latent heat from the earth’s surface (Salby, 1996).

2.3.2 The urban energy budget

The urban climates differ from those of rural areas and that the magnitudes of the differences can be quite large at times depending on weather conditions, urban thermophysical and geometrical characteristics, and anthropogenic moisture and heat sources present in the area. The fluxes of heat, moisture, and momentum are significantly altered by the urban landscape and the contrast between the urban and ‘undisturbed’ climates is further enhanced by the input of anthropogenic heat, moisture, and pollutants into the atmosphere (Taha, 1997).

The energy balance determines the energy fluxes exchanged between the surface and the atmosphere. An individual building, for example, consists of walls and roof facets, has a differing time-varying exposure to solar radiation, net longwave radiation exchange and ventilation (e.g. Arnfield, 1984; Arnfield, 2000; Paterson and Apelt, 1989; Verseghy and Munro, 1989a, 1989b). Horizontal ground-level surfaces are a patchwork of elements, such as irrigated gardens and lawns (Oke, 1979; Suckling, 1980), non-irrigated green space, and paved areas (Doll et al., 1985; Asaeda et al., 1996; Anandakumar, 1999) with contrasting radiative, thermal, aerodynamic and moisture properties, frequently including trees (Oke, 1989; Grimmond et al., 1996; Kjelgren and Montague, 1998).

These different surface elements possess diverse energy budgets that generate contrasts in surface characteristics, and lead to mutual interactions by radiative exchange and small-scale advection (Arnfield, 2003). Building walls and the elements lying between buildings, for example, define the urban canyon (UC). UCs and the roofs of adjacent buildings define city blocks, which in turn scale up to neighbourhoods, land-use zones and, ultimately the entire city. At each scale, units will possess distinctive energy balances that, in general, represent more than the area-weighted average of the budgets of individual elements but also incorporate the distinctive interactions among their constituent units. Moreover, each unit interacts with adjacent ones in the same scale category by advection (Ching et al., 1983; as cited by Arnfield, 2003).

The capacity of the materials to store the daytime heat input is large and this storage, plus the extra heat release from the combustion of fuels, creates a huge heat reserve. At night, within the deep street canyons which screen off much of the cold sky and restrict air flow, the heat store can only be released slowly. The contrast between this cooling environment, and that of the usually more open colder rural areas, is what creates the nocturnal warmth of cities that has been dubbed the ‘heat island’ (Oke, 1982; 1995; 1997).

This phenomenon, the urban heat island, has been recognized since the turn of this century and has been well documented (Chandler, 1960; Oke, 1987; Oke, 1988; Karl and Jones, 1989). A heat island can occur at a range of scales; it can manifest itself around a single building (Charles, 1983), a small vegetative canopy (Taha et al., 1989; Taha et al., 1991), or a large portion of a city (Oke, 1973; Camilloni and Barros, 1997; Bottyan and Unger, 2003; Chen et al., 2003; Grimmond, 2007; Cheval et al., 2009; Hart and Sailor, 2009, as cited by Taha, 1997). The UHI effect clearly must be the result of urban/rural energy balance differences (Oke, 1982) which is mainly caused by surface textures. The different material properties of urban areas (Table 2.2) have significant effect on temperature fields because of different characteristics of surface albedo, latent heat flux/evapotranspiration, and anthropogenic heating (Taha, 1997).

Table 2.2: Radiative properties of typical urban materials and areas (After Oke, 1987).

Surface	α Albedo	ϵ Emissivity	Surface	α Albedo	ϵ Emissivity
<i>1. Roads</i>			<i>4. Windows</i>		
Asphalt	0.05–0.20	0.95	Clear glass		
			zenith angle		
<i>2. Walls</i>			less than 40°	0.08	0.87–0.94
Concrete	0.10–0.35	0.71–0.90	zenith angle		
Brick	0.20–0.40	0.90–0.92	40 to 80°	0.09–0.52	0.87–0.92
Stone	0.20–0.35	0.85–0.95	<i>5. Paints</i>		
Wood		0.90	White, whitewash	0.50–0.90	0.85–0.95
<i>3. Roofs</i>			Red, brown, green	0.20–0.35	0.85–0.95
Tar and gravel	0.08–0.18	0.92	Black	0.02–0.15	0.90–0.98
Tile	0.10–0.35	0.90	<i>6. Urban areas</i> [†]		
Slate	0.10	0.90	Range	0.10–0.27	0.85–0.96
Thatch	0.15–0.20		Average	0.15	~0.95
Corrugated iron	0.10–0.16	0.13–0.28			

[†] Based on mid-latitude cities in snow-free conditions.

The process of urbanization involves the transformation of the radiative, thermal, moisture and aerodynamic characteristics and thereby dislocates the natural energy and hydrologic balances. The urban energy budget was first proposed by Nunez and Oke (1977). The complexity of the urban surface means that the First Law of Thermodynamics (conservation of energy) cannot realistically be solved for every point on the urban surface and therefore requires approximation (Harman, 2003). So the researcher use approximations by considering the energy balance of the different building facets (e.g. Masson, 2000) or considering the energy balance of a volume incorporating buildings, intervening air and the underlying substrate (e.g. Oke, 1987; Grimmond *et al.*, 1991).

As discussed by Arnfield (2003), Oke (1988) suggests that, at larger scales, for total urban landscapes, a useful approach is to evaluate the equivalent energy fluxes through the top of an imaginary volume, extending from a depth in the substrate below which energy exchanges are negligible at the time scale of consideration to a level roughly at roof level, at the upper margins of the UCL (Figure 2.6). In order to compare these approximations it is useful to consider the balance of energy through a horizontal plane just above roof level (plane ABCD in Figure 2.6). This is denoted the *urban energy balance* or *bulk energy balance* and fluxes per unit planar area across this plane are denoted *bulk fluxes*. This is the balance of energy required in numerical weather prediction models. Relating the energy balance of the individual facets to the bulk energy balance requires additional assumptions, most commonly that the intervening air does not absorb or release energy. The urban energy balance is then the sum of the energy balances of the individual urban surfaces suitably weighted by surface area (Harman, 2003).

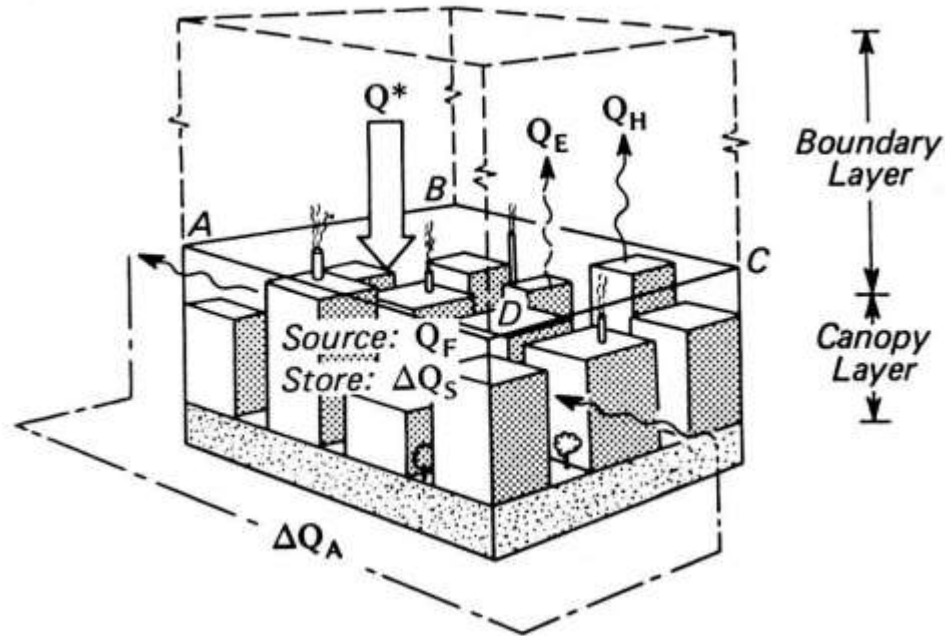


Figure 2.6: Schematic of the volumetric averaging approach to urban energy balance - depiction of the fluxes involved in the energy balance of an urban building-air volume (after Oke, 1987). Q^* is the net radiation; Q_H the sensible heat flux; Q_E the latent heat flux; ΔQ_S storage; ΔQ_A the advective flux; and Q_F the anthropogenic heat flux.

The energy budget of building-air volume such as that illustrated in figure 2.6 is given by a relation similar to that for a single building and this relation of such type of volume can be written as:

$$Q^* + Q_F = Q_H + Q_E + \Delta Q_S + \Delta Q_A \quad (2.1)$$

where Q^* is the net radiation, Q_H and Q_E are the fluxes of the sensible and latent heat, respectively. ΔQ_S is the storage heat flux and represents all energy storage mechanisms within elements of the control volume, including air, trees, building fabrics, and soil, and ΔQ_A is the net advection through the lateral sides of the control volume. Q_F refers to anthropogenic heat sources within the control volume in the city that are associated with combustion. The release of heat, due to combustion of fuels, is a heat source for the city not found in the countryside. Not unreasonably, therefore, this term is often cited as being responsible for the *urban heat island* effect. The magnitude of Q_F in a city depends on its per capita energy use and its population density. The population density depends on many factors including the climate (due to the demand for space heating or cooling), the degree and type of industrial activity, the site of electricity generation (e.g. thermal power plants in the city or imported from afar), the urban

transportation system, etc. Spatial variability of Q_F within cities is considerable and of importance where the central business areas appear as the primary heat source, but there may be localized 'hot spots' in industrial areas (Oke, 1987).

2.4 Urban Heat Island (UHI)

A new surface geometry as a result of removal of vegetation upsets the radiation budget, and albedo (Oke, 1987). Currently, the cities are the foci for the planetary flows of energy and materials, which are used to construct the physical city and sustain its functions (Decker et al., 2000; Mills, 2007). Land-use modifications due to urbanization can modify the energy balance in cities; this in turn affects the urban thermal environment, resulting in the urban heat island (UHI) effect, whereby urban areas often experience different temperatures than surrounding rural areas. An urban heat island can have human health and thermal comfort consequences (Voogt, 2002; Huang et al., 2005), alter the city's photochemistry and thus affect urban air pollution (Saitoh et al., 1996; Taha, 1996; Sarrat et al., 2006), initiate or affect the formation of convective storms (Jauregui and Romales, 1996; Bornstein and Lin 2000). It also affects the energy consumption needs of a city depending upon the demand of heating and cooling requirements (Akbari et al., 2001; Assimakopoulos et al., 2007; Kolokotroni et al., 2007, as cited by Hart and Sailor, 2009).

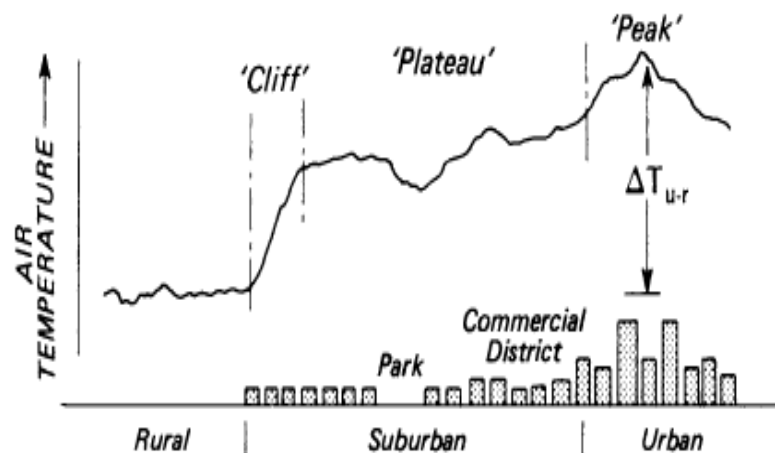


Figure 2.7: Generalized cross-section of a typical urban heat island (After Oke, 1978).

Figure 2.7 highlights that the most obvious phenomena associated to urban climate is UHI in which the air temperature of an urban area is higher than surrounding rural area (Oke, 1987; Kuttler et al., 1996; Kim and Baik, 2004; Unger et al., 2000; Bottyan et al., 2005). In 1868, Emilien Renou (1815 – 1902), a French Meteorologist reported that the Paris was about 1°C warmer than country side (Landsberg, 1981). It was Luke Howard (1833), the first who conducted purposeful study to recognize the effect that urban areas have on local climate and introduced the term of “*UHI*”. Based on the averages of monthly mean temperature during 1807 – 1816, he found that London was 1.48°C warmer than the temperature in the country side. Later, Manley (1958) established his hypothesis that UHI will have greater effect on winter snow fall as most of the snow in London is likely to fall on windy days when the 'heat island' effect will be diminished. Arnfield (2003) summarizes that: UHI intensity decreases with increasing wind speed; UHI intensity decreases with increasing cloud cover; UHI intensity is more severe during summer or warm half of the year; UHI intensity tends to increase with increasing city size and population; and UHI intensity is greatest at night. However, the above conclusions have contradicted by other studies. For example, maximum UHI intensities were found for sunny days in Saskatoon under clear and calm condition (Ripley et al., 1996). Also, negative heat island intensity (rural area warmer than urban area) was reported in Reykjavik (Steinecke, 1999).

2.4.1 Causes of UHI

Depending on the functionality and location of a city, the UHI also greatly vary from city to city al around the world. There are several factors that may affect the UHI. Voogt (2007) suggested the scheme of number of factors that affect the UHI and also highlighted some of the factors for whom the mitigation measures can be adopted to reduce the UHI (Appendix 2.1).

Urban material: Urban areas are made of paved surfaces; high rise buildings and blacktop asphalted roads, streets and concreted paths. The thermal properties (heat capacity and thermal conductivity) and surface radiative properties (albedo and emissivity) of such urban areas are significantly different than the surrounding rural areas. Presence of a single building complex will show a different microclimate than an equal piece of land in its natural state (Landsberg, 1981). As the materials used in urban areas (concrete and asphalts) have higher heat capacity and lower albedo; they absorb a huge amount of heat at day times through solar

radiations which later emit into urban canopy at nights. As a result, the boundary layer's temperature goes higher than nearby rural areas.

Removal of vegetation: Expansion of cities in their spatial size and population growth, cause the elimination of natural lands. The natural lands (vegetation) play a great role to lower the surface temperatures through the process of evapotranspiration. Absence or scarcity of vegetation cover in urban areas minimizes this process and there the surface air temperature remains higher than country sides.

Urban morphology: Due to variety of land utilization (mainly for buildings) urban areas are considered as the areas of high rugosity compared to flat rural areas. The complex urban geometry in presence of buildings not only calms down the urban environment by trapping the flow of wind over urban canopy.

Radiation balance: Urban areas also absorb solar radiation (short-wave) and cause to trap the long-wave radiation in canopy layer. During the day when the surface of the urban canyon receives direct solar radiation, it reflects and emits long-wave energy to the atmosphere. However, the presence of the buildings on both sides of the canyon, traps the reflected energy within the canyon and also with the same process, a huge amount of the long-wave energy is emitted and absorbed. At night, the absorbed heat by the buildings and other objects release into urban atmosphere.

Sources of anthropogenic heat: The anthropogenic heat refers to the heat generated by cars, air conditioners, industrial facilities, and a variety of other manmade sources, which contributes to the urban energy budget (Akbari et al., 2010). Cities consume a great majority – between 60 to 80% – of energy production (OECD, 2010) and emit huge amount of heat into urban atmosphere.

Regional weather conditions and city's geographical location: The regional weather conditions influence the urban climate. The large water bodies (oceans, rivers or huge lakes) cause to temperate the urban temperature. The wind blowing from water bodies toward urban areas also blow away the urban heat and help to keep the urban temperature moderate. The blockage of wind by adjacent mountain ranges can cause to increase the intensity of UHI and conversely, the creation of wind patterns along the mountain valleys can cause to decrease the intensity of UHI by blowing away the heat from nearby urban area.

Greenhouse gases and pollutants: The local increased emission of greenhouse gases (i.e. CO₂) and pollutants (i.e. SO₂, NO_x, PM, CO, H_g) affect the long-wave radiation balance. The presence of pollutants near the urban canopy traps the long-wave radiations to pass through them to the atmosphere and thus cause to warm the urban areas than nearby rural areas.

All these factors depend on the functionality and location of a city that's why the UHI also greatly vary from city to city all around the world.

2.4.2 Consequences of UHI

Energy demand: Urban areas have typically darker surfaces and less vegetation than their surroundings (HIG, 2005). At the building scale, dark roofs heat up more and thus raise the summertime cooling demands of buildings. Every degree increase adds about 500 megawatts (MW) to the air conditioning load in the Los Angeles Basin (Akbari et al. 2001). Similar increases are taxing the ability of developing countries to meet urban electricity demand, while increasing global GHG emissions. The demand of energy for cooling or heating purposes depends upon the intensity of UHI of a city. In general, the peak urban electric demand rises by 2 to 4% for 1 K rise in daily maximum temperature above a threshold of 15–20°C. The additional air-conditioning use caused by this urban air temperature increase causes for 5–10% of urban peak electric demand (Akbari, 2005). Conversely, in temperate and cold climates heat islands may provide some benefits, especially in the cold season because of reduced heating loads, thereby reducing energy use. In these cases impacts of the UHI may be mostly beneficial in the winter, and undesirable in the summer (Voogt, 2003).

Air quality and formation of ground-level ozone: The primary air pollutants, such as carbon monoxide (CO), carbon dioxide (CO₂), sulfuric dioxide (SO₂), nitrous oxide (NO), suspended particulate matter, and hydrocarbons (volatile organic compounds), are substances released directly into the atmosphere. Secondary air pollutants, such as nitrogen dioxide (NO₂) and ozone (O₃), are formed as a result of reactions between primary pollutants and other naturally occurring constituents present in air. The primary active pollutants in the creation of photochemical smog are nitrogen oxides (NO_x) and volatile organic compounds (VOCs). In the presence of sunlight, these reactants are rapidly converted to secondary pollutants, most of which is ozone, but organic nitrates, oxidized hydrocarbons, and

photochemical aerosols are also part of the mix (Gray et al., 1999). If all other variables are equal such as the level of precursor emissions or wind speed and direction ground-level ozone emissions will be higher in sunnier and hotter weather (Akbari, 2005; Akbari et al., 2008). As a result, the summer heat islands often accelerate the formation of harmful smog. Moreover, due to UHI effect, the convergence zone persists over the urbanized area (Fujibe, 2003; Lemonsu and Masson, 2002), resulting in high concentrations of pollutants (Youshikado and Tsuchida, 1996), thus causes to increase the health issue especially the respiratory problems in the warm center of an urban area (Lai and Cheng, 2010).

Human health: In urban regions, the urban heat island has the potential to negatively influence the health and welfare of urban residents. The extensive urban heat island effect, causes additional hot days and heat waves in urban regions compared to rural locales. An examination of summer mortality rates in and around Shanghai yields heightened heat-related mortality in urban regions, and UHI is considered directly responsible, that acted to worsen the adverse health effects from exposure to extreme thermal conditions (Tan et al., 2010). These pollutants are harmful for living things on the earth.

Effect on precipitation: UHI can have a significant influence on mesoscale circulations and resulting convection (Shepherd, 2005). Early investigations (Changnon, 1968; Landsberg, 1970; Huff and Changnon, 1972) found evidence of warm seasonal rainfall increases of 9% to 17% over and downwind of major cities. Jauregui and Romales (1996) observed that the daytime heat island seemed to be correlated with intensification of rain showers during the wet season (May–October) in Mexico City, Mexico (as cited by Shepherd, 2005). During the monsoon season, locations in northeastern suburbs and exurbs of the Phoenix metropolitan area have experienced statistically significant increases in mean precipitation of 12–14% from a pre-urban (1895–1949) to post-urban (1950–2003) period (Shepherd, 2006). However, the formation of a high concentration of small cloud droplets leads to an increased cloud albedo and the suppression of precipitation (Collier, 2006).

2.5 UHI studying approaches and measuring techniques

The study of UHI backs to 1833 when Luke Howard (1833) elaborated that London city is comparatively warmer than its country sides. Many general observations have been made in accordance to the geographic scope used in heat island studies and numerical tools have been developed in recent years.

2.5.1 Field measurements

For measurement of UHI, its intensity and spatial extension, several approaches are being practiced by the researchers. A scheme of UHI measuring approaches at different atmospheric scales is presented in Figure 2.8. The meteorological data can be recorded by using fixed towers or automatic weather stations in which temperature sensors are normally placed in an appropriate manner in urban and rural regions so that the data should not be affected by non-climatic factors (Jauregui, 1997; Kim and Baik, 2005; Lee and Baik, 2010). The temperatures can also be measured by using Tethered Balloons and Radiosondes (Storvold et al., 1998). Sometimes researchers use the Traverse approach (aircraft or automobile) depending upon the atmospheric layer by which the temperature data is collected through aircraft-mounted temperature sensors flown across an urban area (Oke, 1973) or fixed on automobiles at a specific height from the surface (Bottyan and Unger, 2003; Bottyan et al., 2005). Some pre-cautions and post-cautions are required in this method to be sure that the data is homogeneous.

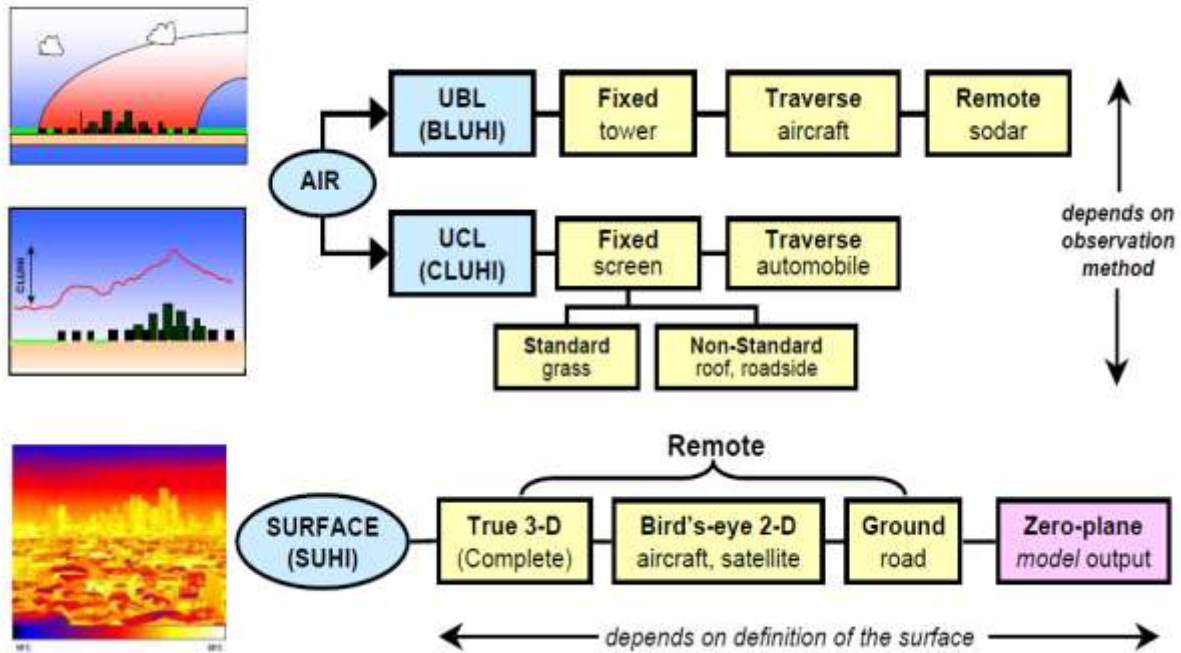


Figure 2.8: The UHI types and their measuring approaches (Adopted from Voogt, 2007).

The data collected through the automobile traverse requires the corrections for temperature changes during the time of the traverse – at least the start and end-points must be common. In this method it is also important that the instrument must be protected from vehicle exhaust/engine heat and should have proper shaded/ventilated sensor (Voogt, 2007). Meteorological observations are also measured by using SOUNd Detection And Ranging (SODAR) units to study UHI (Childs and Raman, 2005). Through advancement in GIS and Remote Sensing, many researchers use non-contact instruments that sense longwave or thermal infrared radiation to estimate surface temperature. For this technique it is important that there should be clear weather conditions and spatial view of the urban surface (Aniello et al., 1995; Hung et al., 2006; Jiang et al., 2006; Cheval and Dumitrescu, 2009; Cheval et al., 2009). To study UHI by using the field measurements of several locations, the near surface temperature of urban stations is generally compared with rural stations. The number of stations to compare may range from one urban and one rural, one urban and an average of set of rural stations or an average of set of several urban and rural stations (Hinkel et al., 2003). Statistical analysis are used to measure urban–rural temperature difference (ΔT_{u-r}) and normally its output results are used to find the spatial distribution and intensity of the heat island inside the city (Yagüe et al., 1991;

Jauregui, 1997; Brunetti et al., 2000; Kim and Baik, 2002; Liu et al., 2007; Hart and Sailor, 2009).

2.5.2 GIS and Remote Sensing

Through advancement in GIS and Remote Sensing, many researchers use non-contact instruments that sense longwave or thermal infrared radiation to estimate surface temperature. For this technique it is important that there should be clear weather conditions and spatial view of the urban surface (Aniello et al., 1995; Hung et al., 2006; Jiang et al., 2006; Cheval and Dumitrescu, 2009; Cheval et al., 2009). The period after 1970s is considered as an era of advancements in Geographical Information System (GIS) and remote sensing. The use of LANDSAT TM satellite data, properly processed by using GIS software are widely practiced to study the change in natural landscape, deforestation, natural hazards studies and urban heat island (Aniello et al., 1995; Adinna et al., 2009). In such type of approach, the primary data sources for the researchers include: Landsat Thematic Mapper (TM), Enhanced Thematic Mapper Plus (ETM+), SPOT, QuickBird, Road vector map and thermal remote sensing (Voogt and Oke, 2003; Kato and Yamaguchi, 2005; Jiang et al., 2006; Hung, et al., 2006; Ouyang et al., 2008; Bounoua et al., 2009). Thermal remote sensing uses non-contact instruments that sense longwave or thermal infrared radiation to estimate the surface temperature. For this approach, it is important that there should be clear weather (cloudless) and spatial view of the urban surface. The moderate resolution imaging spectro-radiometer (MODIS) approach is also being used as well to generate land-surface temperature (LST) maps to study UHI (Hung et al., 2006; Cheval and Dumitrescu, 2009; Cheval et al., 2009; Mohan et al., 2012). Hung et al., 2006 developed three types of methods to estimate LST from space: the single infrared channel method, the split window method and a new day–night MODIS LST method, which is designed to take advantage of the unique capability of the MODIS instrument (Wan, 1999). The first method requires surface emissivity and an accurate radiative transfer model and atmospheric profiles, which must be given by either satellite soundings or conventional radiosonde data (Schmugge et al., 1998). The second method makes corrections for the atmospheric and surface emissivity effects with surface emissivity as an input based on the differential absorption in a split window (Wan and Dozier, 1996). The third method uses day–night pairs of TIR data in seven MODIS bands for

simultaneously retrieving surface temperatures and band-averaged emissivities without knowing atmospheric temperature and water vapor profiles to high accuracy (Wan and Li, 1997. as cited by Hung et al., 2006). Some case studies deal with computation of land surface temperature (LST) and normalized difference vegetation index (NDVI) based on landuse/land cover (LULC) types (Weng and Yang, 2004; Xiao and Weng, 2007).

2.5.3 UHI modelling approaches

Since the advent of atmospheric computer modeling in 1948, models have been applied to study weather, climate, and air pollution on urban, regional, and global scales. Historically, meteorological models have been used to simulate weather, climate, and climate change. Photochemical models have been used to study urban, regional, and global air-pollution emission, chemistry, aerosol processes, and transport of pollutants. Only recently have meteorological models merged with photochemical models to tackle these problems together (Jacobson, 2005). During the past century, weather forecasting also has evolved from an art that relied solely on experience and intuition into a science that relies on numerical models based on the conservation of mass, momentum, and energy. The increasing sophistication of the models has led to dramatic improvements in forecast skill (Wallace and Hobbs, 2006).

Table 2.3 summarizes atmospheric scales and motions or phenomena occurring on each scale. Atmospheric problems can be simulated over a variety of spatial scales. *Molecularscale* motions occur over distances much smaller than 2 mm. Molecular diffusion is an example of a molecular-scale motion. *Microscale* motions occur over distances of 2 mm to 2 km. Eddies, or swirling motions of air, are microscale events. *Mesoscale* motions, such as thunderstorms, occur over distances of 2– 2000 km. The *synoptic scale* covers motions or events on a scale of 500–10 000 km. High- and low-pressure systems and the Antarctic ozone hole occur over the synoptic scale. *Planetary-scale* events are those larger than synoptic-scale events. Global wind systems are planetary-scale motions. Some phenomena occur on more than one scale. Acid deposition is a mesoscale and synoptic-scale phenomenon (Jacobson, 2005).

Table 2.3: Scales of atmospheric motion (Jacobson, 2005).

Scale Name	Scale Dimension	Examples
Molecular scale	<<2 mm	Molecular diffusion, molecular viscosity
Microscale	2 mm – 2 km	Eddies, small plumes, car exhaust, cumulus clouds
Mesoscale	2-2000 km	Gravity waves, thunderstorms, tornados, cloud clusters, local winds, urban air pollution
Synoptic Scale	500-10000 km	High- and low- pressure systems, weather fronts, tropical storms, hurricanes, Antarctic ozone hole
Planetary Scale	>10000 km	Global wind systems, Rossby (Planetary) waves, stratospheric ozone reduction, global warming

During 1950s and 1960s, the use of computer machines to run general circulation models based on the theory developed by Bjerknes was the real start of an era of atmospheric modelling. It was only in the 1970s that mesoscale (scale of circulation like sea/land breezes, slope winds and mountain-valley flows) models started to be developed (Bornstein, 1975; Pielke, 1974, as cited by Martilli, 2001). Due to constraints in computer power, these first models made assumptions to simplify the equations (e. g. hydrostaticity, incompressibility) which limit possible applications. In the 1980s and 1990s the increase in computer power allowed the adoption of less restrictive approximations enlarging the domain of model applicability of the models. Moreover, due also to the improvements in the knowledge of atmospheric phenomena, new physical mechanisms were considered as cloud microphysics, surface energy exchanges in urban areas (Martilli, 2001).

To compute and forecast the atmospheric conditions close to the reality, modelling approaches are being adopted by the researchers. The development of numerical tools has made it possible to simulate the UHI conditions over different types of cities and to compare them with real observed data. The modelling approach is now one of the reliable methods to study the UHI by using plots and run the simulations (Arnfield, 2003; Fan and Sailor, 2005). Table 2.3 explains the scales of atmospheric motion and there are different models developed and used according to these scales.

Small-scale modelling can help to study the interactions of buildings with atmosphere over the small region of a city (Cermak, 1996; Poreh, 1996; Mirzaei and Haghghat, 2010). Accuracy of a small-scale model in the problem depends on the ability to identify the most significant dimensionless numbers, to reduce the number of unmatched dimensionless numbers, and to develop criteria that reduce their impact (Poreh, 1996). Mirzaei and Haghghat (2010) explained in his article ‘*Approaches to study urban heat island – abilities and limitations*’ that meso-scale models are smaller than synoptic-scale and larger than micro-scale systems. The horizontal resolution of these models is approximately ranged from one to several-hundreds of kilometers. Also, these models vertically vary with depth of Planetary Boundary Layer (PBL) between 200m and 2km. This layer exists between the earth surface and geostrophic wind. In meso-scale models, large-scale interactions under the PBL are resolved, including atmospheric stratification and surface layer treatment. Unlike the meso-scale model, micro-scale computational fluid dynamics (CFD) resolve the conservation equation inside the surface layer. Meaning that the horizontal spatial quantities are assumed with bulk values in meso-scale model, where those are simulated with actual geometry and details with surface layer interactions in micro-scale model. These interactions are generally assumed with Monin-Obukhov similarity inside the PBL in meso-scale models. However, it is not feasible to apply the micro-scale models for an entire city, with all the details and geometries, due to the high computational cost. Therefore, the simulations are horizontally limited to a small domain in magnitude of some blocks of buildings (few hundreds of meter). On the other hand, the treatment of the PBL in micro-scale model is not as comprehensive as meso-scale model. It implies that micro-scale model mostly does not include the atmospheric interactions like atmospheric vertical mixing or Coriolis Effect. Many theories have been proposed to model the turbulence such as Direct Naviere Stokes (DNS), Large Eddy Simulation (LES), and Reynolds Average Navier–Stokes (RANS). Although better accuracy can be achieved using LES and DNS (Mochida and Lun, 2008), the application of these schemes is computationally very expensive. Instead, RANS (e.g. $k-\epsilon$ and $k-l$) is widely used for turbulent modeling in UHI studies due to its lower computational cost (Kondo et al., 2006; Xie et al., 2007). However, this scheme does not physically show good performance in simulation of the building canopies, especially inside the wake region (Tominaga et al., 2008; as cited by Mirzaei and Haghghat, 2010). The urban canopy model (UCM) is derived from the energy balance equation for a control volume which contains two adjacent buildings. The energy balance budget

for a building canyon was first suggested by Oke (1988). This method uses the law of conservation energy for a given control volume, and considers the atmospheric phenomena, turbulence fluctuations and velocity field as heat fluxes. These fluxes are generally defined by analytical or empirical equations. The UCM considers the energy exchanges with surfaces and ambient air in the urban canopy. It predicts the ambient temperature and surfaces temperatures of buildings, pavements, and streets. However, the air flow is decoupled from the temperature field, and has to be defined as a particular input in to the control volume. Logarithmic-law and power-law are widely assumed in the UCMs. Unlike the energy balance models in which velocity and temperature fields are separated, computational fluid dynamics (CFD) simultaneously solves all the governing equations of fluid inside the urban areas; conservation of mass, potential temperature, momentum, and species (water vapor and chemical reaction). As a result, CFD is capable of obtaining more accurate information about UHI distribution within and above the building canopies than UCM (Mirzaei and Haghghat, 2010).

CHAPTER 3

A COMPARATIVE ANALYSIS OF THE CHANGE IN TEMPERATURE ON URBAN, TOWN AND RURAL AREAS

ABSTRACT

The purpose of this work is to study the evolution of temperatures at several locations in Pakistan. A comparative quantification of the change in temperature on urban, town and rural areas of Pakistan has been done. The resulting change has been then compared to global trends. For this purpose, averaged daily annual and seasonal mean (T_{mean}) minimum (T_{min}) and maximum (T_{max}) temperatures data from 1950 to 2004 of 42 stations were obtained from Pakistan Meteorological Department (PMD). First, the data was homogenized by using Standard Normal Homogeneity Test (SNHT) and then the resulting homogenized data was analyzed by using the least square linear regression. The data was analyzed for two different periods: 1950–1979 and

1980–2004. The analyses for the two periods are based on per year change in temperature at urban, town and rural stations. The analysis shows that the annual mean, minimum and maximum temperatures over Pakistan are increasing. The trends of annual mean, minimum and maximum temperature observed over urban, town and rural stations during 1980–2004 are significantly higher than the trends observed during 1950–2004. At urban areas, the increase in minimum temperature is higher than the increase in maximum temperature. However, the trends of minimum and maximum temperatures at urban areas during 1980–2004 are $0.27\text{ }^{\circ}\text{C dec}^{-1}$ and $0.20\text{ }^{\circ}\text{C dec}^{-1}$ greater than the trends observed during 1950–2004. The maximum temperature increases more on town and rural stations whereas the increase in minimum temperature at rural areas is the lowest as compared to the town and urban stations. The higher growth in minimum and maximum temperature at urban and town stations is observed in spring and at rural stations minimum temperature increased more in winter and maximum temperature in spring. The corresponding linear trends of minimum and maximum temperature at urban areas of Pakistan during 1980–2004 are measured $0.14\text{ }^{\circ}\text{C dec}^{-1}$ and $0.04\text{ }^{\circ}\text{C dec}^{-1}$, respectively greater than the trends observed for global minimum and maximum temperatures during the same period.

3.1 Introduction

All countries are vulnerable to climate change and instability in weather patterns, but the poorest countries and the poorest people within them are most vulnerable, being the most exposed and having the least means to adapt (IMF and World Bank, 2006). Pakistan is one of the developing country and its populations has been increasing since her independence in 1947. Pakistan also has experienced higher urbanization in different parts of the country. During last three to four decades, the existing cities such as Karachi, Lahore and Faisalabad spatially expanded because of population pressure and the comparatively smaller towns become the cities. Currently almost 40% of the total population is cities and according to an estimate, in 2050 almost 60% of the total population will be living in urban areas (UNDESA, 2011, see Figure 1.2).

The expansion of the city and the closely linked urban clusters not only cause the UHI phenomenon but also cause to increase the regional temperature trends. According to the study of Yin et al. (2007), in Yangtze River Delta (YRD) the increase rate of annual mean air temperature in city-belt is $0.28\text{--}0.44^{\circ}\text{C/decade}$ from 1991 to 2005, which is far larger than that of non-city-

belt. The UHI effect made the regional annual mean air temperature increased 0.072°C from 1961 to 2005, of which 0.047°C from 1991 to 2005, and the annual maximum air temperature increased 0.162°C , of which 0.083°C from 1991 to 2005, all these indicating that the urban expansion in the YRD from 1991 to 2005 may be regarded as a serious climate signal.

As discussed in chapter 1, the cities are the center of the key anthropogenic activities and these activities in the cities are mainly concern to the use of energy. A major share of global energy (between 60% to 80%) is consumed in cities and the cities account for a roughly equivalent share of global CO_2 emissions. Due to rapid urbanization in Pakistan, the demand of energy in country has increased many folds (Sajjad et al., 2010). Pakistan's total primary energy supply during fiscal year 2007– 2008 was 62.88 MTOE (million tons of oil equivalents). More than 99% of this energy was supplied through conventional energy sources such as oil, gas, hydel and nuclear.

The major part of the electricity is consumed in buildings (domestic or commercial) (Sheikh, 2010). In 2002-2003, industrial sector consumed 36% of total energy consumption while 33% is consumed by transportation. Even though total energy consumption is declined to 29% in 2008-2009, but the consumption by industrial sector has increased to 43% over the period (Economic Survey of Pakistan, 2008). In 2005, 0.4% of the world total CO_2 emissions were produced by Pakistan and this “contribution” is worsening day by day. While the income per capita has increased from 32,599 Pakistani rupees in 2006 to 36,305 Pakistani rupees in 2009, the usage of energy per capita was increased from 489.36 (kg of oil equivalent) in 2006 to 522.66 (kg of oil equivalent) in 2009. This led to raise the per capita emission of CO_2 from 0.7657 metric tons in 2006 to 1.026 metric tons in 2009 (Shahbaz et al., 2010). The consumption of electricity in 1980 was just 10.15 billion kilowatt-hours which reached to 68.54 billion kilowatt-hours in 2008 (U.S. Energy Information Administration, 2008). It is to be noted that most of the industrial sites which were established during early 1960s and 1980s, are now surrounded by densely populated areas such as Manghopir, Landhi, FB Area, Northern Karachi and Korangi industrial estates in Karachi, Kot Lakhpat industrial estate in Lahore and Model Town and I-9 industrial estates in Islamabad. In these industrial estates, thousands of industrial units are in operation which may not only have effect on human health but may cause to modify the local climate.

Pakistan is among one of the countries which have complex terrain with all kind of physical features and have four seasons. The highlands in north comprising the highest peaks

located in Karakoram, Himalaya, Nanga Parbat and Hindu Kush such as K2/Godwin Austen (8611 meter), Nanga Parbat (8126 meter), Gasherbrum I/K5 (8080 meter), Broad Peak (8051 meter) to Indus Plain (the land of five rivers) and to the coastal area, the country has highest mountains, plateaus, fertile plain areas, vast deserts lands and long coastal belt (Figure 3.1). Due to diversity of physical features in the country, the surface temperature of Pakistan shows a variety of climate that is greatly modified by the altitude and location (Figure 3.2).

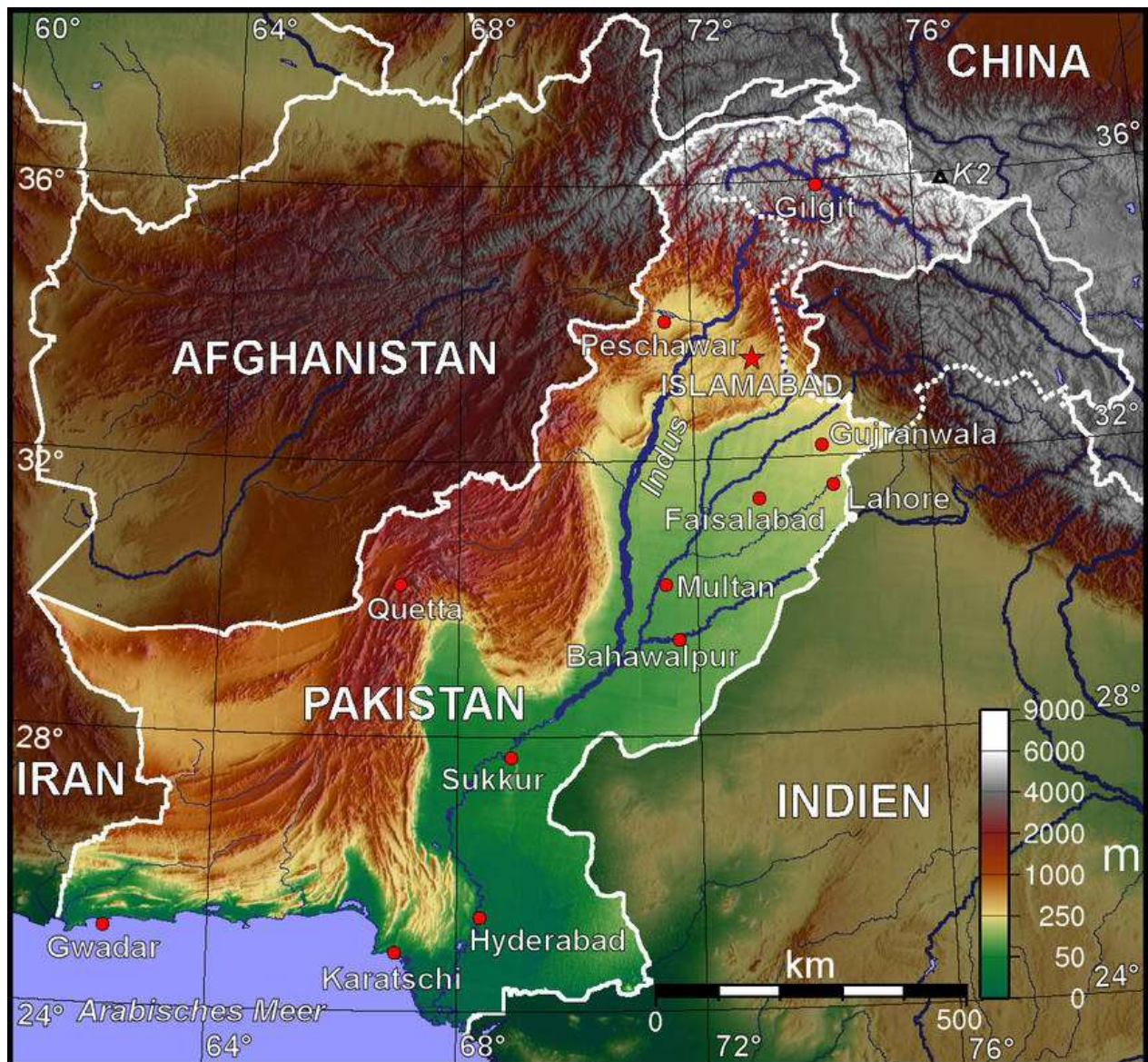


Figure 3.1: Topographic Map of Pakistan. Source: World of Maps, 2013

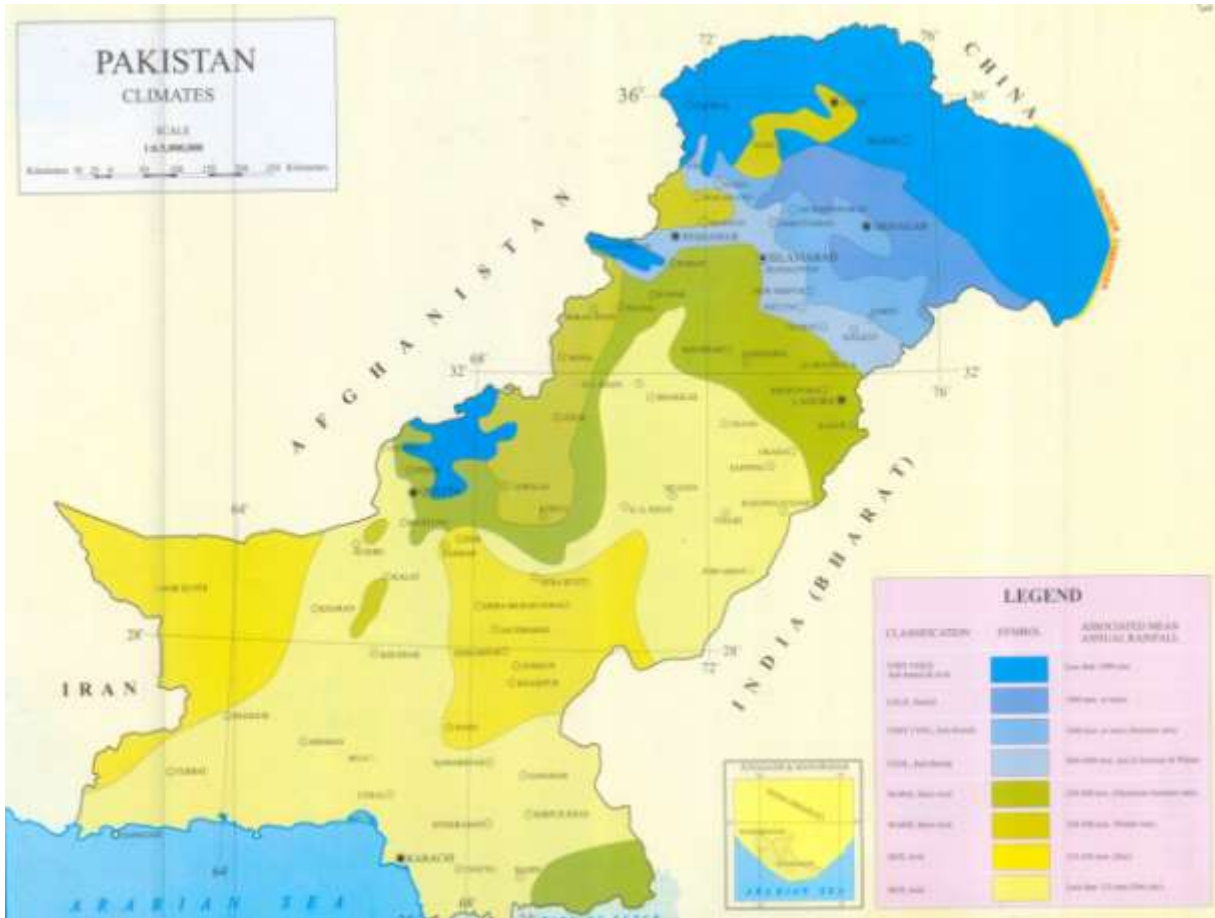


Figure 3.2: Pakistan climates classification and associated mean annual rainfall. Source: Global Security (2011).

The meteorological variables such as air temperature, relative humidity, solar radiation and wind speed greatly affect the daily life of human beings. The extreme weather conditions of hot climate regions sensitively affect the human thermal comfort. The higher temperatures at a place make it difficult to survive without cooling systems. Thom’s discomfort index assesses the levels of human discomfort related to meteorological variables. Thom’s discomfort index is given in Table 3.1.

Table 3.1: Values of Thom's Discomfort Index calculated for Celsius temperature scales.

Discomfort Index (°C)	Interpretation
< 21	No discomfort
21-24	Under 50% population feels discomfort
24-27	Over 50% population feels discomfort
27-29	Most of population suffers discomfort
29-32	Everyone feels severe stress
>32	State of medical emergency

Pakistan is located in the temperate zone. It has arid type climate characterized by hot summers and cool or cold winters with wide variations between extremes of temperature at given locations. Main part of the plane area (comprising over Punjab and Sindh provinces) located in east and south east of Pakistan has dry climate. Several cities of Pakistan are located in plane areas that have warm to hot climate where temperature during summer reaches to 45°C. It is hard to survive in this type of environment without using the cooling appliances. So for human comfort, people frequently use the Air Conditioner Systems (ACS). Such cooling systems for human comfort are the major anthropogenic sources of emission of heat into the urban atmosphere. This extra heat emitted into the urban atmosphere causes further warming of the cities and this process of use of energy and heating up of cities will keep on continuing until the measures and methods are not adopted to reduce the energy consumption especially in urban areas.

The outpouring population in urban areas of the country is not only causing the social unrest but is becoming the major threat for the sustainable urban environment. The absence of measures for mitigation or even adaptation against climate risks is making the cities more vulnerable to live. Pakistan is one of the members of United Nations Framework Convention on Climate Change and signatory of Kyoto Protocol that emphasis the member countries to adopt efficient energy resources to combat global warming. Of course, the effective participation and proper actions of Pakistan in global campaign to combating climate change are need worthy to minimize its contribution in climate change and its impacts at national as well as global scales.

Under these contexts, the purpose of this work is to study the evolution of temperatures at several locations in Pakistan; comparatively quantify the change in temperature on urban, town and rural areas of Pakistan and then compare the resulting change in minimum and maximum temperature at urban stations of Pakistan with global minimum and maximum temperature trends.

The data source, data length, and analyzing method of data are given in section 3.2. Results and their discussion are given in section 3.3 and section 3.4 concludes the findings of the whole chapter.

3.2 Data and methodology

3.2.1 Meteorological data

Daily averaged annual and seasonal temperatures data of mean (T_m), minimum (T_n) and maximum (T_x) temperature data of 42 meteorological stations of Pakistan for the period of 1950–2004 was collected from Pakistan Meteorological Department (PMD). Figure 3.3 shows the locations of the observatories located in Pakistan. Red circles marked on the map show the stations located in plain areas and blue triangles to stations located in mountain areas. This classification of plain and mountain station is made by PMD and is used the same at national level. Table 3.2 gives characteristics of the meteorological stations including station's international codes, complete name, latitude, longitude, elevation, classification in terms of urban, town and rural station.

For classification of monitoring stations into urban, town and rural areas, there are some studies that use night lights observations through satellite (Imhoff et al., 1997; Hansen et al., 2001). This interesting method to classify the monitoring stations may be highly useful for major cities and smaller towns located in the advance countries where there is no shortage of electricity. However, this method can't be homogeneously used for the cities located in developing countries like in Pakistan. It is because many of the developing countries or the countries facing energy crisis, this method can't be used for classification. In this work, the classification of monitoring stations into urban, town and rural stations is done by using the traditional method based on population size (Easterling et al., 1997; Hansen et al., 1999). The classification of the stations here in this study into urban, town and rural stations is based on population density and local

government administrative status of the area where observatory is located. Here the urban stations refer to the major cities declared as metropolitan by the government and the cities with population density more than 5000 persons/ sq.km (except Kakul). The town stations refer to the cities with population density between 1000 to 5000 persons/ sq.km and the rural stations refer to the areas with population density less than 1000 persons/sq.km.

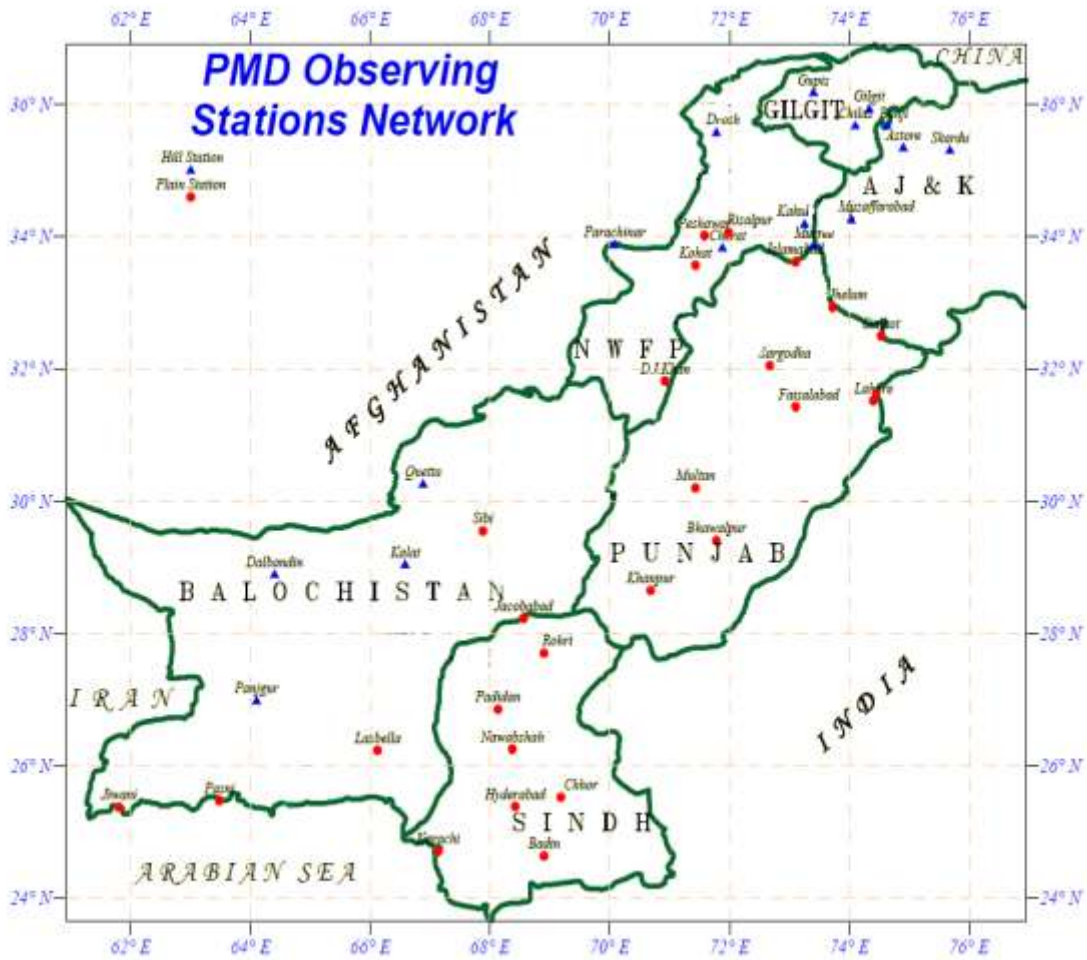


Figure 3.3: Location of meteorological stations on the map of Pakistan (After Pakistan Meteorological Department <http://www.pmd.gov.pk>).

Table 3.2: Geographical descriptions of meteorological stations of Pakistan.

No.	Code	Name	Station location		Elevation (m)	Station type
			Latitude	Longitude		
1	41516	Gilgit	35.55	74.20	1460	Urban
2	41530	Peshawar	34.10	71.35	360	Urban
3	41532	Muzaffarabad	34.22	73.29	2300.9	Urban
4	41535	Kakul	34.11	73.15	1307.9	Urban
5	41571	Islamabad	33.37	73.60	508.1	Urban
6	41594	Sargodha	32.30	72.40	188.1	Urban
7	41598	Jhelum	32.56	73.44	287.1	Urban
8	41600	Sialkot	32.31	74.32	255.1	Urban
09	41624	D.I.Khan	31.49	70.56	171.2	Urban
10	41630	Faisalabad	31.26	73.80	185.6	Urban
11	41640	Lahore-urb	31.33	74.20	214	Urban
12	41641	Lahore-ap	31.35	74.24	216.1	Urban
13	41660	Quetta	30.15	66.53	1588.9	Urban
14	41675	Multan	30.12	71.26	122	Urban
15	41700	Bahawalpur	29.20	71.47	110	Urban
16	41764	Hyderabad	25.23	68.25	28	Urban
17	41780	Karachi-ap	24.54	67.80	21.9	Urban
18	41697	Sibbi	29.33	67.53	132.9	Town
19	41739	Panjour	26.58	64.60	968	Town
20	41785	Badin	24.38	68.54	9	Town
21	41533	Risalpur	34.40	71.59	317	Town
22	41564	Kohat	33.34	71.26	513	Town
23	41715	Jacobabad	28.18	68.28	54.9	Town
24	41749	Nawabshah	26.15	68.22	37	Town
25	41504	Gupis	36.10	73.24	2155.9	Rural
26	41517	Skardu	35.18	75.41	2317	Rural
27	41518	Bunji	35.40	74.38	1372	Rural
28	41519	Chilas	35.25	74.60	1249.1	Rural
29	41520	Astore	35.20	74.54	2168	Rural
30	41565	Cherat	33.49	71.33	1372	Rural
31	41685	Chhor	29.53	69.43	4.9	Rural
32	41696	Kalat	29.20	66.35	2015	Rural
33	41712	Dalbandin	28.53	64.24	848	Rural
34	41742	Lasbella	26.14	66.10	87	Rural
35	41746	Padidan	26.51	68.80	46	Rural
36	41756	Jiwani	25.40	61.48	56	Rural
37	41759	Pasni	25.16	63.29	9	Rural

Following the objectives of the study, the data is limited to mean, minimum and maximum temperature data mainly because of its availability. The data of wind speed, direction, humidity and other parameters were not available to use them to study their relation with evolution of temperature at urban areas.

3.2.2 Homogenization of data

A homogeneous data series is where the variations in data are caused only by variations in climate and inhomogeneous data series is where the variations in data are caused by non-climatic factors. A time series can be homogenous only if the measurements have been consistently performed by the same method, with the same undamaged instrumentation, at the same time and place and in the same environment. This is seldom the case for long time series (Hanssen-Bauer and Forland, 1994). In many ways, the long time series climatic data are altered by non-climatic factors such as stations relocations, changes in instruments, screens of the instrument, observation timings, surrounding areas, observational procedure, calculation procedures, and instrumental inaccuracies, observer capability, attentiveness and observing regulations. Such non-climatic factors hide the real signal of climate change during one specific period (Heino, 1994; Vincent, 1998; Aguilar et al., 2003; Caussinus and Mestre, 2004; Costa and Soares, 2009).

The time series data of a weather observatory from a hill top to relatively lower altitude and installed on flat valley in the surroundings will show an abrupt warming at that station that is actually due to the relocation of the observatory. In some cases, it becomes difficult to differentiate the real change due to climate change and inhomogeneity due to non-climatic factors. For example, consider a station located in the garden of a competent and conscientious observer for 50 years. The instruments are maintained in good repair and the observer accurately records the temperature in his or her garden. But what if 50 years ago the observer planted a tree west of the garden? This tree slowly grows up and shades the observing site during the late afternoon when the daily maximum temperature is observed. While the data accurately represent the temperature in the garden, the tree has caused maximum temperatures in the garden to have cooled relative to the climate of the region. Detecting gradual homogeneity problems such as this is very difficult (Aguilar et al., 2003).

There are a number of non-climatic factors that affect the most of the long-term climatological time series. The affected data by non-climatic factors causes to hide the actual climate variation occurring over time and leads to misinterpretations in the results of the studied climate. So, it is very important to remove the inhomogeneities from the time series data that is being taken into account for the climate studies and is being analyzed. The researchers and the

scientists follow the certain procedures to remove the inhomogeneities from time series data such as a given scheme in Figure 3.4 by Aguilar et al., 2003.

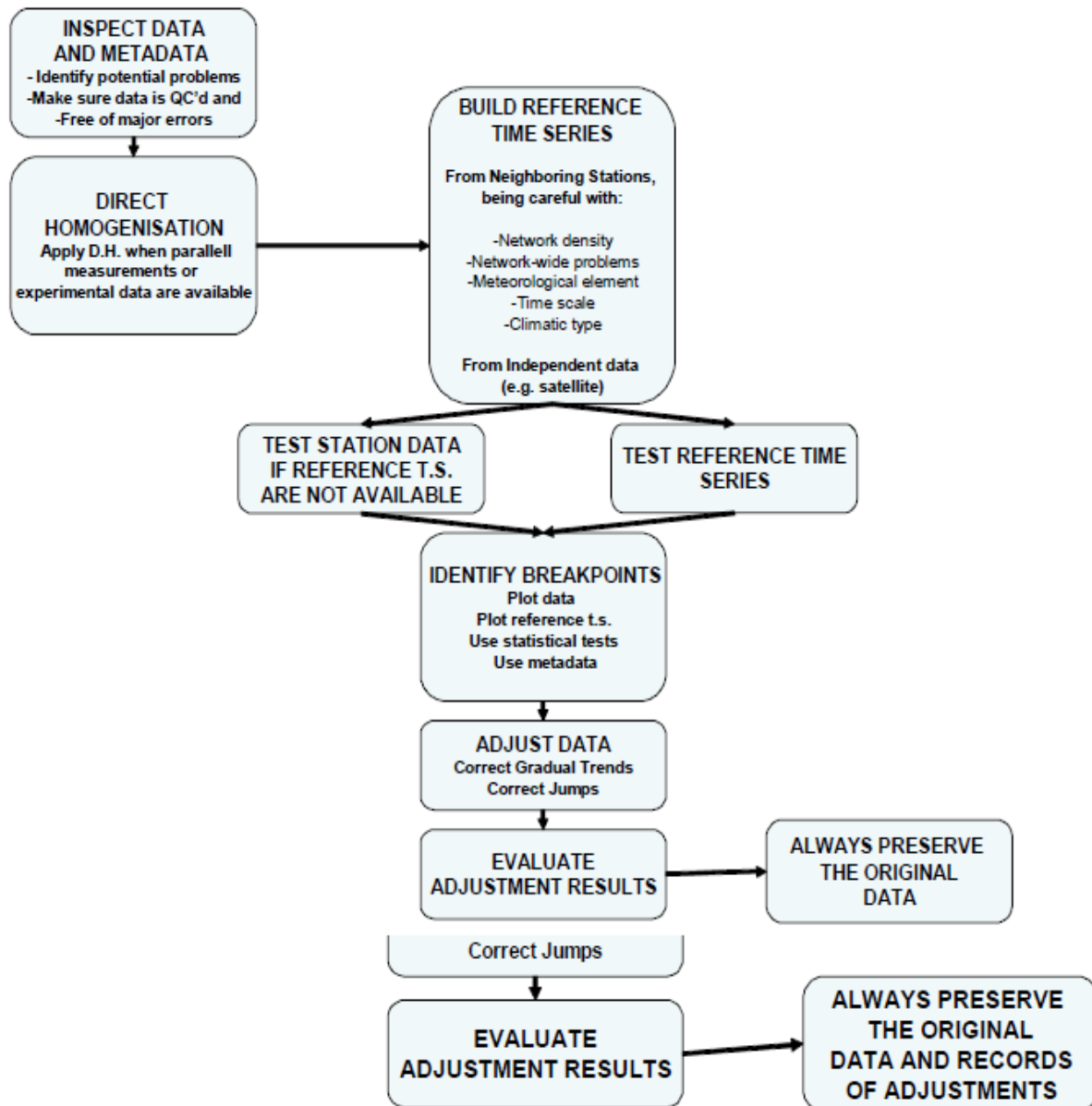


Figure 3.4: Schematic representation of homogenization procedures for monthly to annual climate records (After Aguilar et al., 2003).

3.2.3 Metadata

The meteorological data all around the world is not measured consistently and are highly influenced by a wide variety of observational practices. As stated above, there are many factors that can influence the observational data. The proper record about a meteorological station since its installation is therefore very necessary. Comprehensive metadata about a station describes its history since its establishment to the present and hopefully onwards to the future to make the best possible use of the data of that station. The maintain and keep updating the comprehensive documentation of a newly established station is recommended by the scientists as most of the metadata have to be derived from the documentation of that station and can be found from the data themselves by using homogenization techniques (Aguilar et al., 2003).

As recommended in World Meteorological Organization (WMO) Report WMO/TD No. 1186 (Aguilar et al., 2003), WMO has a strong interest in encouraging metadata recording, in supporting metadata recovery efforts and encourages National Meteorological and Hydrological Services (NMHSs) to not only accomplish the minimum requirements, but also try to meet the best practices. Good metadata ensure the final data user about the accuracy or doubts in the data. Metadata highlights the way in which the data was recorded, gathered and transferred. Metadata also provide the information about when and how the data measuring instruments were replaced, relocated, washed or removed along with the reasons and characteristics about an action performed. So metadata of any sort of data or station is very important as it helps to eliminate the non-climatic fingerprints of certain abrupt changes in the meteorological data record especially in temperature data.

3.2.4 Homogeneity assessment

Although many researchers are succeeded to develop the techniques to identify the non-climatic inhomogeneities and then to adjust the inhomogeneous data to use it for further analysis, since the homogenization of meteorological data is not considered as the perfect way. However, many researchers believe that homogenization techniques improve the quality of the data and homogeneous data can be trusted for the analysis of climate studies. Homogenization techniques address a variety of factors that impact climate data homogenization such as the type of element (temperature versus precipitation), spatial and temporal variability depending on the part of the

world where the stations are located, length and completeness of the data, availability of metadata, and station density (Aguilar et al., 2003).

World Meteorological Organization (WMO) Report WMO/TD No. 1186 (Aguilar et al., 2003) describes that it is almost impossible to be 100% sure about the quality of past data. Several techniques can be used to check the quality of the data and remove the inhomogeneities from the data caused by the non-climatic factors. However, for homogenization of time series data, the steps listed below are commonly followed (Aguilar et al., 2003):

- Metadata Analysis and Quality Control
- Creation of a reference time series
- Breakpoint detection
- Data adjustment

There are many techniques to quality control and homogenize the time series data. There are several studies which has used different methods of homogenization such as Buishand Range Test (Busishand, 1982; Wijngaard et al., 2003), Caussinus-Mestre Technique (Caussinus and Mestre, 1996; Caussinus and Lyazrhi, 1997; Mestre and Caussinus, 2001; Caussinus and Mestre, 2004), Craddock Test (Craddock, 1979; Auer, 1992), Expert Judgement Methods (Jones et al., 1986; Rhoades and Salinger, 1993), Instruments Comparisons (Forland et al., 1996; Nichols et al., 1996; Quayle et al., 1991), Multiple Analysis of Series for Homogenization (MASH) (Szentimrey, 1996; Szentimrey, 1999; Szentimrey, 2000), Multiple Linear Regression (Gullett et al., 1991; Vincent, 1998), Pettit Test (Pettit, 1979; Wijngaard et al., 2003), Potter's Method (Plummer et al., 1995; Potter, 1981), Radiosonde Data (Free et al., 2001), Rank-Order Change Point Test (Siegel and Castellán, 1988; Lanzante, 1996), Standard Normal Homogeneity Test (Alexandersson and Moberg, 1997; Alexandersson, 1986; Hanssen-Bauer and Forland, 1994; Khaliq and Ouarda, 2007; Toreti et al., 2011; Esteban et al., 2010; Brunet, 2012), Stop-Trend Method (Kobysheva and Naumova, 1979) and Two-Phase Regression (Solow, 1987; Easterling and Peterson, 1995a; Easterling and Peterson, 1995b, as cited by Aguilar et al., 2003).

The initial check of the quality of raw data of several meteorological stations of Pakistan shows significant inhomogeneities in the data. It was not trustworthy to use it for the analysis as it was showing irregularities and breaks in time series data sets. For example, Figure 3.5 highlights the quality of raw data of monthly mean minimum temperature of Bunji and Rohri. To ensure the quality of data and to check the inhomogeneity in time series data used in this study,

Standard Normal Homogeneity Test (SNHT), proposed and developed by Aguilar (personally working with him in December 2010), is used. However, the time series data homogenized by using SNHT is used for further analysis and trends detection. SNHT is a parametric test using neighbouring station(s) as a reference to identify non-homogeneities in the time series of the station being tested (candidate station). It is used to detect abrupt or linearly developing differences between the candidate and the reference station (Tuomenvirta, 2002).

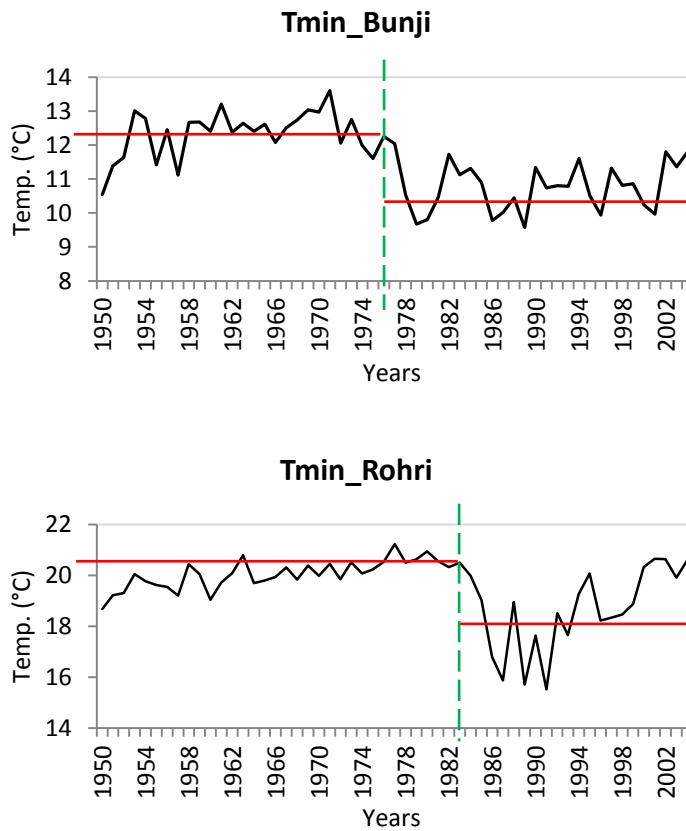


Figure 3.5: Quality of raw data of minimum temperature measured at Bunji and Rohri during 1950 to 2004.

Hawkins (1977) presented a formulation of a testing method that was subsequently developed into SNHT and applied to climatological series by Alexandersson (1984, 1986). The SNHT is related to a curve fitting technique using the least squares principle (Alexandersson and Moberg, 1997), as is explained by Tuomenvirta (2002). The basic assumption behind SNHT is

that the ratio/difference, Q , between e.g. precipitation/temperature at the candidate station and a neighbouring reference station remains fairly constant in time. This requires a sufficient correlation between the test and reference stations. An inhomogeneity will be revealed as a systematic change in this ratio/difference, Q , (Tuomenvirta, 2002).

As described by Tuomenvirta (2002) SNHT uses normalized series of the ratios/differences, Z_i , defined as:

$$Z_i = (Q_i - \bar{Q}) / \sigma_Q$$

where \bar{Q} is the sample mean value and σ_Q the sample standard deviation of the ratio/difference Q_i at time step i (denoted in many climatological applications as one year). In the following discussion, "year" will be used instead of "time step" or "unit time", although the time step is by no means restricted to one year.

After making the assumption that Z_i is described by a Normal distribution, N , the null hypothesis for all variants of SNHT is:

$$H_0: Z_i \in N(0,1) \quad i \in \{1, \dots, n\}$$

i.e. the whole series is homogeneous. All values in the normalized series of ratios/differences are normally distributed with a mean value equal to zero and standard deviation equal to one (Tuomenvirta, 2002).

Table 3.3 and Table 3.4 show the break-points of annual minimum and annual maximum temperature, respectively for different stations. The break-points are detected through procedure of homogenization and then are adjusted to remove inhomogeneity from each station. Figure 3.6 and Figure 3.7 are also representing the breakpoints and adjustment of minimum temperature data of Quetta (airport) and Lahore (city) meteorological observatories, respectively. In both figures, annual and seasonal average of daily minimum temperature from 1950 to 2004 is homogenized. Detection of break points is given on left side and adjustment of data is given on right side in each figure. In right panel, original data for annual and seasonal adjustments is given in red line and adjusted data is given in green line. Figure 3.8 is summarizing the whole homogenization procedure in which the whole data is given in raw and adjusted forms.

Table 3.3: Break-Points detection of T_{min}

Minimum te mpe rature			
Station name	Remark	Year	Month
Sargodha	BREAK	1957	12
Sargodha	BREAK	1969	9
Sargodha	BREAK	1981	9
Jhelum	BREAK	1964	5
Sialkot	BREAK	1957	6
Sialkot	BREAK	1971	1
Sialkot	BREAK	1986	12
Faisalabad	BREAK	1961	12
Faisalabad	BREAK	1974	12
Faisalabad	BREAK	1984	1
Lahore_City	BREAK	1964	9
Lahore_City	BREAK	1983	11
Lahore_City	BREAK	1997	5
Quetta(AP)	BREAK	1959	1
Quetta(AP)	BREAK	1982	9
Quetta(AP)	BREAK	1997	1
Chhor	BREAK	1957	12
Chhor	BREAK	1971	8
Chhor	BREAK	1990	11
Kalat	BREAK	1958	1
Kalat	BREAK	1968	12
Kalat	BREAK	1985	12
Sibbi	BREAK	1969	11
Sibbi	BREAK	1975	12
Dalbandin	BREAK	1971	1
Dalbandin	BREAK	1983	7
Panjgur	BREAK	1960	10
Panjgur	BREAK	1999	12
Lasbella	BREAK	1960	12
Lasbella	BREAK	1971	11
Lasbella	BREAK	1982	6
Lasbella	BREAK	1990	5
Lasbella	BREAK	1998	1
Jiwani	BREAK	1978	3
Jiwani	BREAK	1988	5
Jiwani	BREAK	1997	6
Pasni	BREAK	1959	6
Pasni	BREAK	1978	1
Karachi(AP)	BREAK	1957	9
Karachi(AP)	BREAK	1964	1
Karachi(AP)	BREAK	1981	1
Karachi(AP)	BREAK	1995	1
Badin	BREAK	1974	9
Badin	BREAK	1987	1

Table 3.4: Break-Points detection of T_{max}

Maximum temperature			
Station name	Remark	Year	Month
Sargodha	BREAK	1957	12
Sargodha	BREAK	1969	9
Sargodha	BREAK	1981	9
Jhelum	BREAK	1964	5
Sialkot	BREAK	1957	6
Sialkot	BREAK	1971	1
Sialkot	BREAK	1986	12
Faisalabad	BREAK	1961	12
Faisalabad	BREAK	1974	12
Faisalabad	BREAK	1984	1
Quetta(AP)	BREAK	1959	1
Quetta(AP)	BREAK	1982	9
Quetta(AP)	BREAK	1997	1
Chhor	BREAK	1957	12
Chhor	BREAK	1971	8
Chhor	BREAK	1990	11
Kalat	BREAK	1958	1
Kalat	BREAK	1968	12
Kalat	BREAK	1985	12
Sibbi	BREAK	1969	11
Sibbi	BREAK	1975	12
Dalbandin	BREAK	1971	1
Dalbandin	BREAK	1983	7
Panjgur	BREAK	1960	10
Panjgur	BREAK	1999	12
Lasbella	BREAK	1960	12
Lasbella	BREAK	1971	11
Lasbella	BREAK	1982	6
Lasbella	BREAK	1990	5
Lasbella	BREAK	1998	1
Jiwani	BREAK	1978	3
Jiwani	BREAK	1988	5
Jiwani	BREAK	1997	6
Pasni	BREAK	1959	6
Pasni	BREAK	1978	1
Karachi(AP)	BREAK	1957	9
Karachi(AP)	BREAK	1964	1
Karachi(AP)	BREAK	1981	1
Karachi(AP)	BREAK	1995	1
Badin	BREAK	1974	9
Badin	BREAK	1987	1

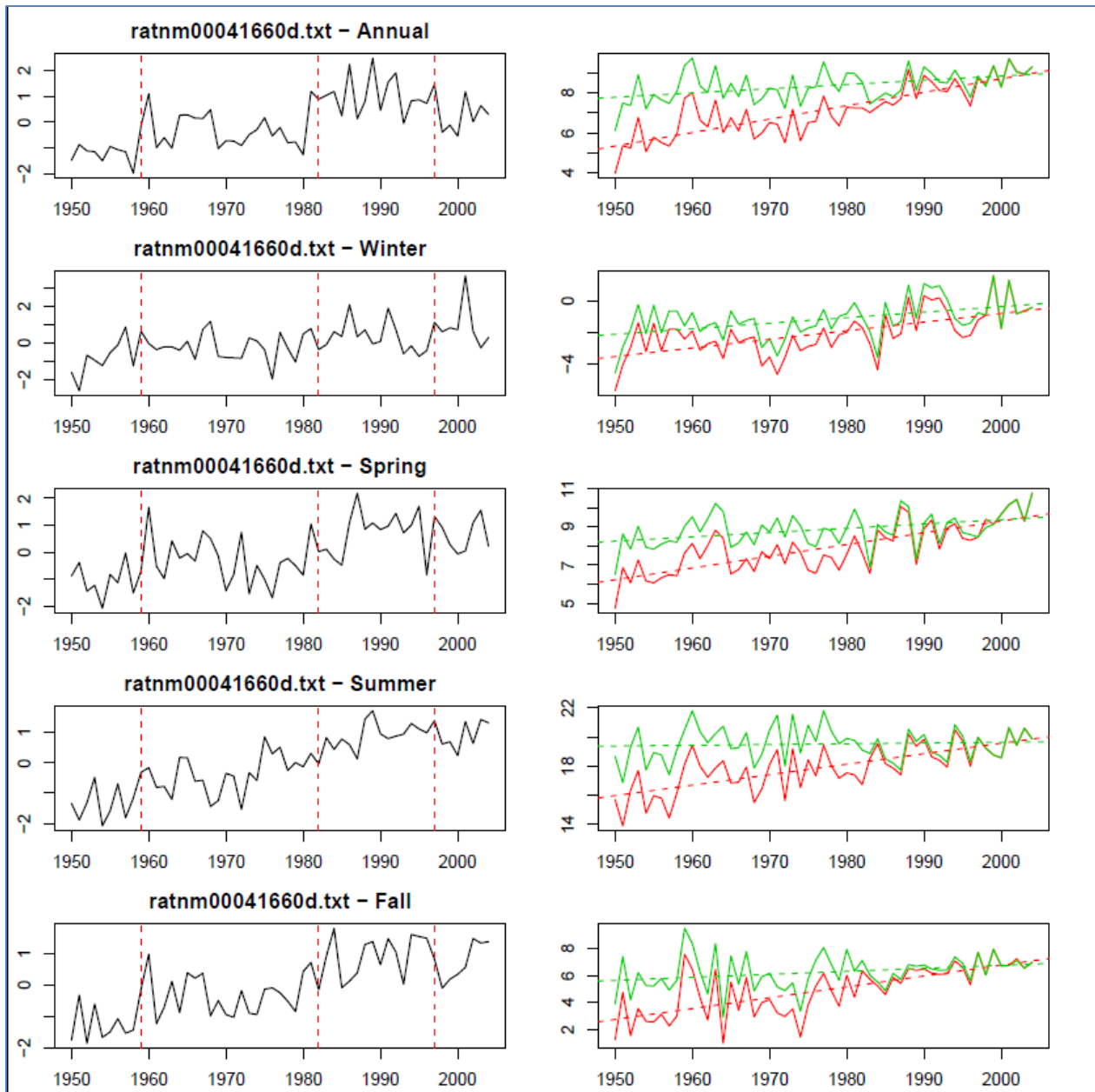


Figure 3.6: Annual and seasonal average of daily minimum temperature of Quetta airport for 1950 to 2004. Detection of break points (on left) and adjustment of data (on right). In right panel, original data for annual and seasonal adjustments is given in red line and adjusted data is given in green line. Data is given in °C.

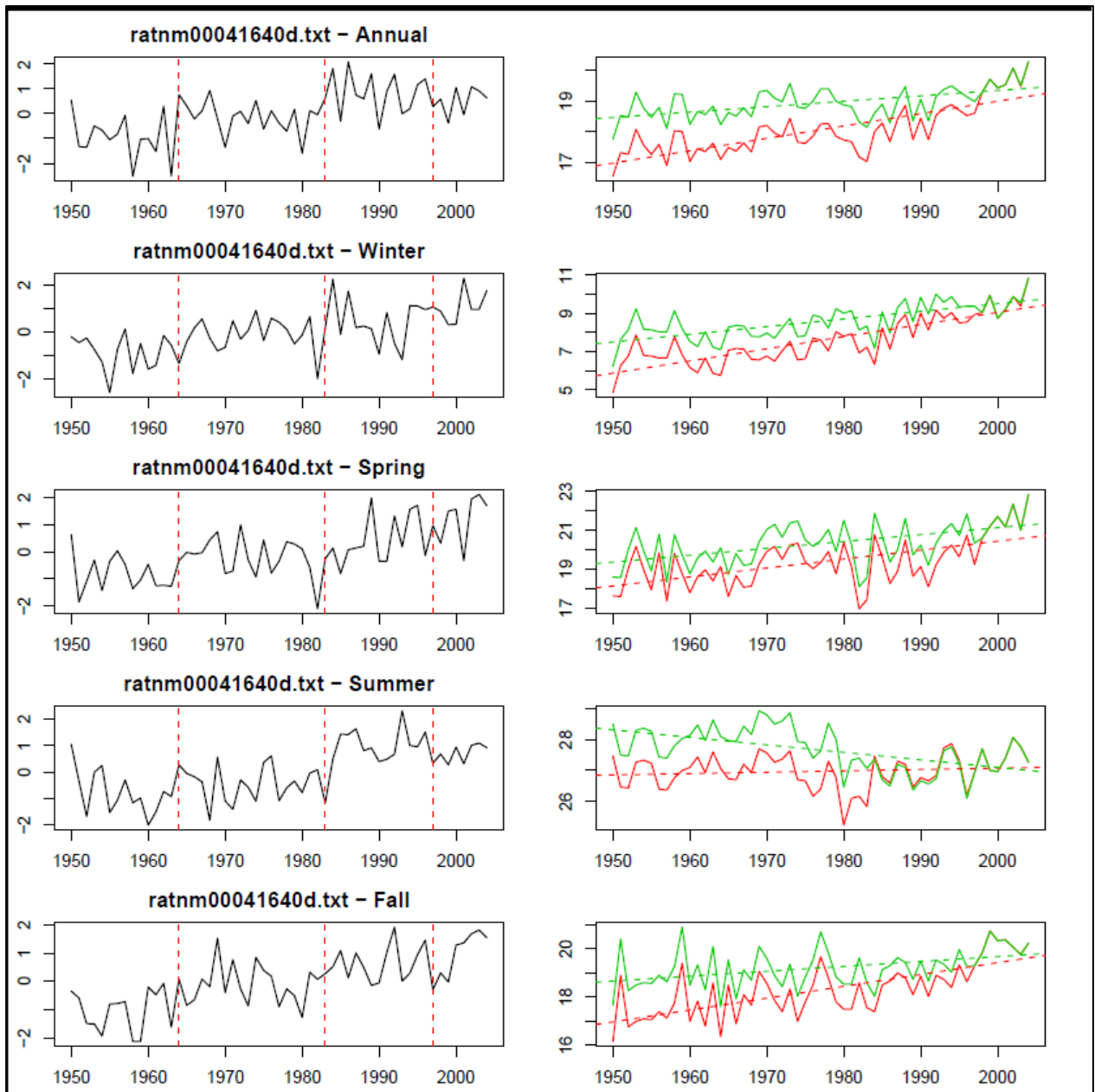


Figure 3.7: Annual and seasonal average of daily minimum temperature of Lahore city for 1950 to 2004. Detection of break points (on left) and adjustment of data (on right). In right panel, original data for annual and seasonal adjustments is given in red line and adjusted data is given in green line. Data in is given in °C.



Figure 3.8: A presentation of data points of annual average of daily minimum temperature of a reference and a candidate series representing the trends before and after homogenization. On x axis are data points and on y axis σ .

3.2.5 Mann-Kendall test

The Mann-Kendall test is a non-parametric test that is normally used to identify the trends in time series data. All the given data values are evaluated in an order of time series in which each data value is compared to all subsequent data values. The Mann–Kendall test can be used only when all the observations in a time series are serially independent. It defines whether the observations in the data tend to increase or decrease with time (Mohsin and Gough, 2010). The initial value of the Mann-Kendall statistic S is assumed to be 0 (no trend). If a data value from a later time period is higher than a data value from an earlier time period is incremented by 1. On the other hand, if the data value from a later time period is lower than a data value sampled earlier, S is decremented by 1. The net result of all such increments and decrements yields the final value of S (Khambhammettu, 2005).

To identify the urbanization effect on times series data of different types of the stations located in Pakistan, we used the sequential Mann–Kendall test to find any abrupt change in time series data sets of minimum and maximum temperature. For example, figure 3.9 shows the sequential Mann–Kendall trend analysis for the monthly minimum and maximum temperature for Lahore (urban) stations for 1950 to 2004, in which only the statistics for the forward series, $u(t)$, is plotted against the time. The test significantly detects an abrupt change in minimum temperature starting from February 1984. This technique is applied one by one on all the stations. In most of the cases, at urban and town stations, the abrupt change was found around 1980 (± 4). Based on the results of this test, the whole data series was divided into two periods: period 1 (1950-1979) and period 2 (1980-2004) for better analysis to significantly identify the evolution in temperature during less urbanized period (1950-1979) and highly urbanized period (1980-2004).

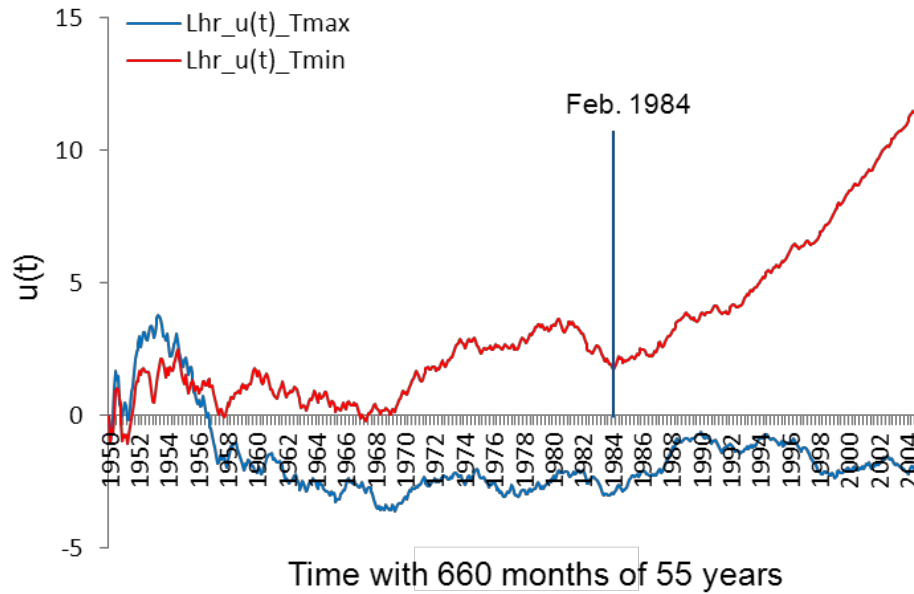


Figure 3.9: Abrupt changes in time series of monthly averaged minimum and maximum temperature of Lahore (urban) by using the sequential Mann–Kendall test for statistics of forward time series.

3.2.6 Principal Component Analysis

Principal component analysis was performed in order to discover hidden sub-structure in the dataset and meteorological stations group with homogenised behaviour. The temperature data includes annual mean of T_n , T_x , and T_m , and means reduced to the four seasons: autumn, winter, spring and summer. Latitude and Altitudes were added as supplementary variables to help to give sense to the dimensions. Averaged trends of all urban, town and rural stations for seasonal and annual T_n , T_x , and T_m were computed and considered for performing the PCA as supplementary individuals to qualify the behaviour of each group (urban, town and rural).

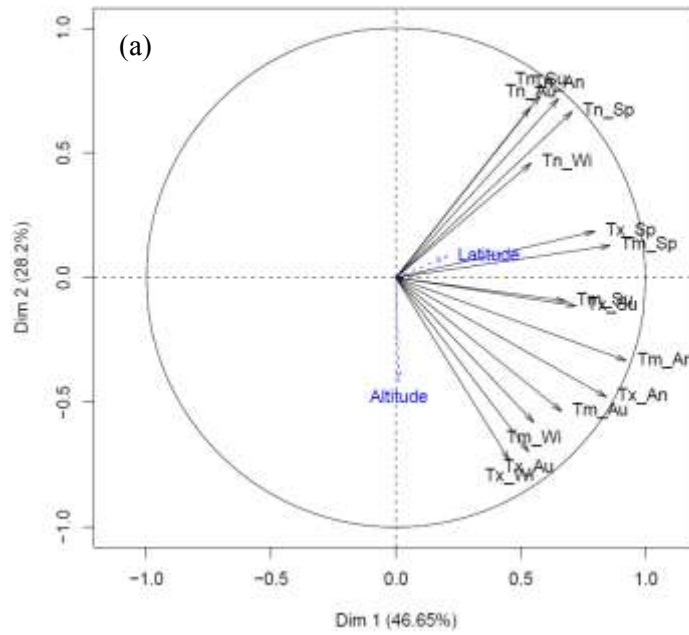
After application of PCA on whole considered period (1950–2004), it came out that over the large period analysis, no clear signal was found and it was difficult to properly distinguish between monitoring stations. By using the Mann-Kendall test on urban stations to identify the signal of change in temperature due to urban effect, the data was divided into two periods 1950–1979 and 1980–2004. PCA was then run for the two periods one by one and the for the trends difference of the two periods. As the two first dimensions summarize 74.85% of the total

variances of the cloud of dataset, so we considered only these two dimensions for the further interpretation.

Variable (Fig. 3.10a): The whole set of variables are well correlated to the first axis. It is a positive correlation. T_{m_an} (annual temperature) shows the maximum correlation with a R of Pearson of 0.92, following with T_{m_spring} , T_x annual, spring and summer. Variables are less correlated with the second factor. Some of them show negative correlation like T_{x_autumn} and T_{x_winter} . T_{n_summer} , T_{n_annual} , T_{n_autumn} and T_{n_spring} show stronger positive correlation with the second factor.

Individus (Fig. 3.10b): To distinguish which group is opposite to another one, we consider stations which have coordinates superior of 2 or inferior of -2 . The first component (dim 1) opposes stations with highest and lowest temperature trends while second factor opposes urban and rural stations. Kakul (Kak) station is the one which contribute the most to the construction of the first factor. Then Chilas (Chil), Hyderabad (Hdb) and Kohat (Kht) follows with a contribution of about 10% and Jiwani (Jiw and Padidan (Pidn) with a contribution of about 5.9% for the explanation of the axis 1. For the axis 2, there is no strong atypical behaviour. Cherat (Chrt), Jiwani (Jiw), Kohat (Kht), Dalbandin (Dbn), Faisalabad (Fdb), Islamabad (Isb) Sargodha (Sgd), Multan (Mln) are the most typical stations which influenced the most of the construction of the second factor with a contribution of about 4–6% to the variance explanation of the factor 2.

Plot variables graph of slope differences (Phase 2 – Phase 1) of 37 station



Plot individuals graph of slope differences (Phase 2 – Phase 1) of 37 stations

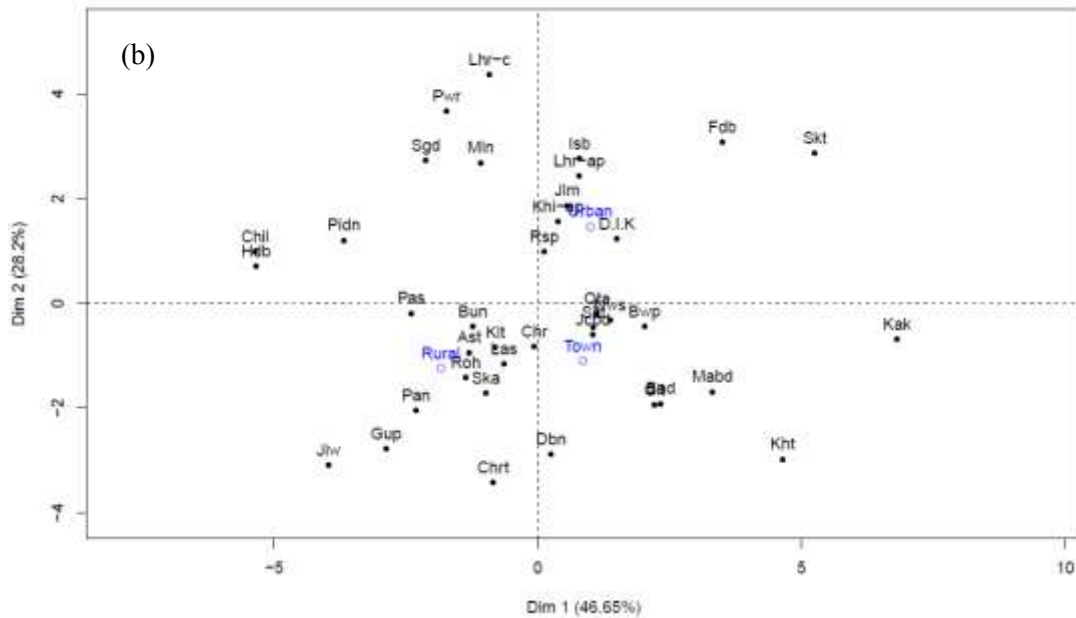


Figure 3.10: Principal Component Analysis results on the differences of temperatures trends between the period 180–2004 and 1950–1979 (a) Variables graph, (b) individuals graph

3.2.7 Calculation of temperature trends

The focus of this study is to analyse the change in annual and seasonal minimum (dT_n) and maximum (dT_x) temperatures at urban, town and rural stations. Initially 42 stations were taken into account for homogenization and trend analysis (18 urban, 9 town and 15 rural stations). Out of 42 stations, 5 stations [Murree (urban), Khanpur and Rohri (town) and Drosh and Parachinar (rural)] had noncontinuous data series and had several outliers and extreme values especially in minimum temperature series. To avoid any biasness of these stations on average trend values of other urban, town and rural stations, they were not taken into account for further analysis. For final examination and results given in this study, 37 meteorological stations (17 urban, 7 town and 13 rural) comprising the reliable and quality controlled data were used (Table 3.2). As the mean temperature (T_m) derives from minimum and maximum temperature series, so it is not used for further study in this work. By using the least square linear regression, only homogenized data of minimum and maximum temperature was used for trends analysis for two different periods: 1950–1979 and 1980–2004 (i.e., Chung et al., 2004). To detect seasonal behaviour, the trends for minimum and maximum temperature for each season (winter, spring, autumn and summer) have also been computed. The trend differences in both minimum and maximum temperature for two period (1980–2004 - 1950–1979) and the average trends of minimum and maximum temperature of all urban, town and rural stations are also computed.

3.3 Results and discussion

3.3.1 *Analysis of variation in minimum and maximum temperature*

Table 3.5 represents the annual and seasonal minimum and maximum temperature trends computed for the periods 1950–1979 and 1980–2004. It also presents the trend differences between these two periods (1980–2004 - 1950–1979). The values for the trends given in Table 3.5 are computed by using least square linear regression and represent per year change in temperature.

During 1950–1979, the annual average per decade change in minimum temperature (dT_{n-An}) at urban, town and rural stations is observed -0.11°C , 0.12°C and 0.16°C , respectively. Out of the total urban, town and rural stations, 35% of urban, 57% of town and 77% of rural

stations showed an increase in annual minimum temperature 1950–1979. In general, the behaviour of growth in minimum temperature during different seasons at urban, town and rural stations is not different from the behaviour seen in dT_{n_An} (see Table 3.5 and Table 3.6). Per decade change in annual average maximum temperature at urban and rural stations is homogeneous to the trends of minimum temperature during the same period however, maximum temperature also decreased at town stations. During 1950–1979, the per decade change in annual maximum temperature (dT_{x_An}) at urban, town and rural stations is computed -0.046°C , -0.18°C and 0.021°C , respectively where 35% of urban, 29% of town and 62% of rural stations showed an increasing trend in annual maximum temperature. The seasonal behaviour of change in maximum temperature also correspond to the annual trends except spring and autumn at town stations where they showed positive trends and winter and autumn at rural stations where they showed negative trends. Further investigations reveal that during 1950–1979, among all the seasons, the increase in minimum and maximum temperature at urban, town and rural stations is calculated the highest in spring than other seasons (Appendix 3.3).

During 1980–2004, per decade change in annual minimum temperature (dT_{n_An}) at urban, town and rural stations is observed 0.43°C , 0.26°C and -0.046°C , respectively. During this period, the increase in minimum temperature is observed greater than it the period 1950–1979. During 1980–2004 at 94% of urban, 86% of town and 62% of rural stations minimum temperature increased (see Table 3.5 and Table 3.6). The seasonal trends show that during 1980–2004 at urban and town stations the higher increase in minimum temperature is computed during spring and at rural stations during winter. However, it is also detected that during 1980–2004, in ‘*winter*’ at maximum number of urban, town and rural stations (94%, 86% and 62%, respectively) minimum temperature increased and in ‘*summer*’ at minimum number of urban, town and rural stations (82%, 57% and 23%, respectively) minimum temperature increased.

Table 3.5: Annual and seasonal temperature trends computed for the periods 1950–1979, 1980–2004 and for the difference between the two periods. dT_n and dT_x correspond to change in minimum and maximum temperatures, whereas An, Wi, Sp, Su, Au correspond to the Annual, Winter, Spring, Summer and Autumn.

Period and Settlement type		Minimum temperature					Maximum temperature				
Period	Type	dTn_An	dTn_Wi	dTn_Sp	dTn_Su	dTn_Au	dTx_An	dTx_Wi	dTx_Sp	dTx_Su	dTx_Au
1950 - 1979	Urban	-0.0111	-0.0248	-0.0030	-0.0150	-0.0106	-0.0046	-0.0162	0.0076	-0.0241	0.0045
	Town	0.0117	-0.0122	0.0243	0.0093	0.0164	-0.0179	-0.0388	-0.0036	-0.0230	-0.0160
	Rural	0.0157	-0.0066	0.0244	0.0250	0.0112	0.0021	-0.0122	0.0168	0.0006	-0.0051
1980 - 2004	Urban	0.0427	0.0395	0.0597	0.0221	0.0427	0.0336	0.0325	0.0968	-0.0042	0.0081
	Town	0.0266	0.0237	0.0411	0.0097	0.0256	0.0487	0.0639	0.0929	0.0120	0.0257
	Rural	-0.0046	0.0146	-0.0041	-0.0369	-0.0003	0.0305	0.0524	0.0527	-0.0060	0.0211
Period 2 - Period 1	Urban	0.0538	0.0643	0.0628	0.0371	0.0533	0.0382	0.0487	0.0892	0.0199	0.0037
	Town	0.0149	0.0359	0.0167	0.0004	0.0093	0.0667	0.1027	0.0965	0.0350	0.0417
	Rural	-0.0203	0.0212	-0.0285	-0.0619	-0.0115	0.0283	0.0646	0.0359	-0.0066	0.0262

Table 3.6: Percentage of stations showing positive trends for annual and seasonal minimum and maximum temperature at urban, town and rural stations for the period 1950–1979 and 1980–2004.

Period	URBAN		TOWN		RURAL	
	1950 - 1979	1980-2004	1950 - 1979	1980-2004	1950 - 1979	1980-2004
dTn_An	35%	94%	57%	86%	77%	62%
dTn_Wi	29%	94%	43%	86%	46%	62%
dTn_Sp	59%	88%	57%	71%	100%	54%
dTn_Su	24%	82%	43%	57%	69%	23%
dTn_Au	41%	88%	71%	71%	62%	62%
dTx_An	35%	88%	29%	71%	62%	85%
dTx_Wi	12%	71%	14%	57%	31%	100%
dTx_Sp	53%	100%	43%	86%	77%	100%
dTx_Su	12%	53%	29%	57%	54%	38%
dTx_Au	53%	47%	57%	57%	69%	77%

During 1980–2004, per decade change in annual maximum temperature ($dT_{x_{An}}$) at urban, town and rural stations is observed 0.34°C, 0.49°C and 0.30°C, respectively. This increase in maximum temperature is greater than the change observed during 1950–1979. During 1980–2004, 88% of urban, 71% of town and 85% of rural stations showed an increase in maximum temperature. Maximum temperature is increasing mostly during spring season where 100% of urban, 86% of town and 100% of rural stations have increasing maximum temperature over the period of 1980–2004 (Appendix 3.4). However, the lowest increase in maximum temperature at all the stations is observed in summer.

Figure 3.11 highlights the dT_n trends as a function of dT_x trends observed on 17 urban, 7 town and 13 rural stations for both of the analysed periods. Figure 3.11(a) shows that during 1950-1979, at majority of the urban stations annual dT_n and dT_x are negative, at majority of the town and rural stations dT_n is measured positive and at majority of the town stations, dT_x is negative. However, the behaviour of annual dT_n and dT_x observed during 1980-2004, is seen different than the trends noticed during 1950-1979. During 1980-2004, urban effect is extensively observed on dT_n and dT_x . Figure 3.11(b) elaborates that dT_n and dT_x almost at all the urban stations have positive trends. Like as the urban stations, all the town stations except one station also have shown positive dT_n and dT_x . Contrary of the period 1950-1979, during 1980-2004 many of the rural stations have shown negative dT_n and have observed lower dT_n and dT_x than urban and town stations. Figure 3.11(c) shows per year average dT_n and dT_x of all urban, town and rural stations for 1950-1979 and 1980-2004. It shows clear shift in dT_n and dT_x at urban stations. The average dT_n and dT_x of all urban stations show the significant positive trend than town and rural average however the average dT_n and dT_x of all town stations is close to the urban average. The higher increase in minimum temperature at urban stations than town and rural stations is a result of rapid urbanization in Pakistan.

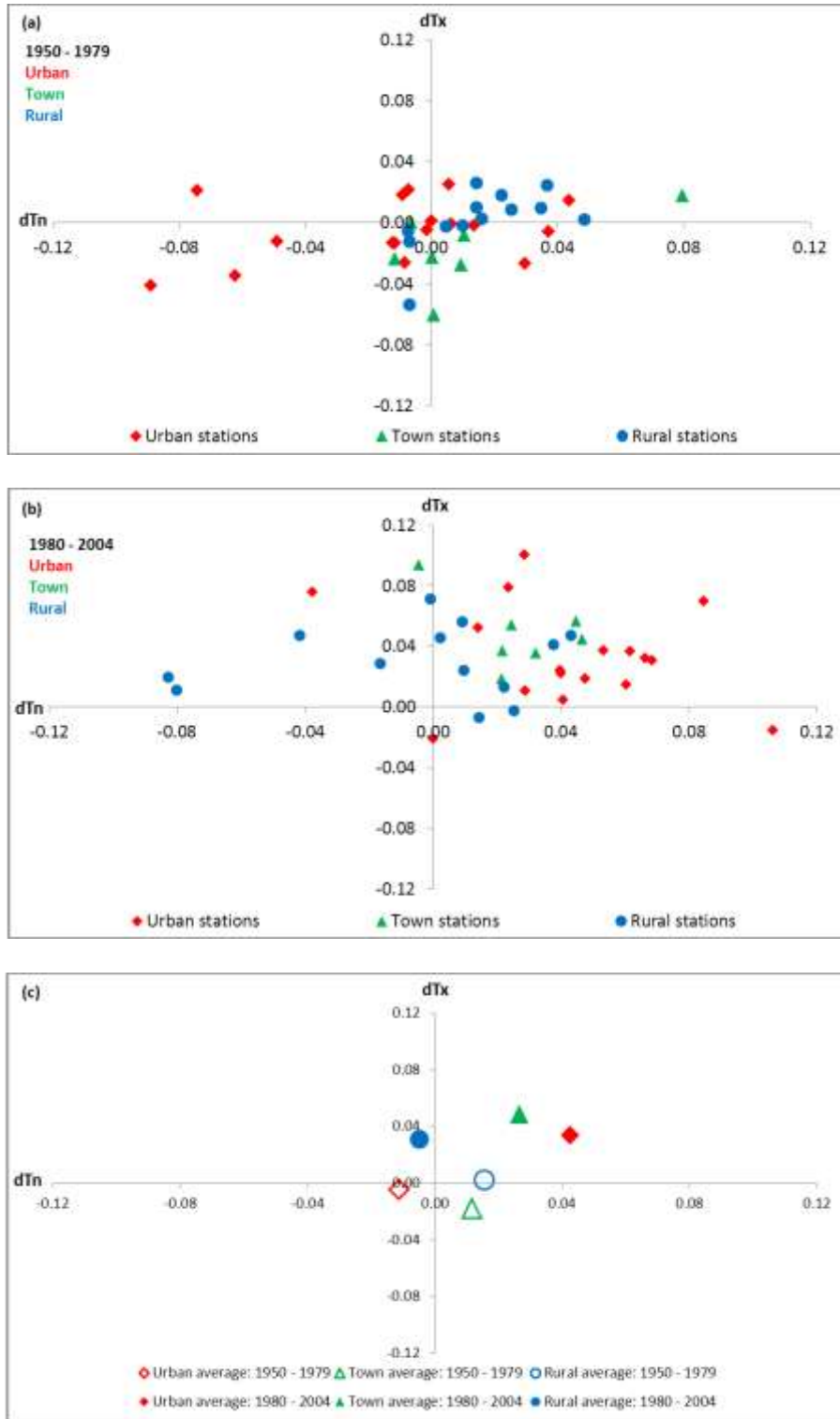
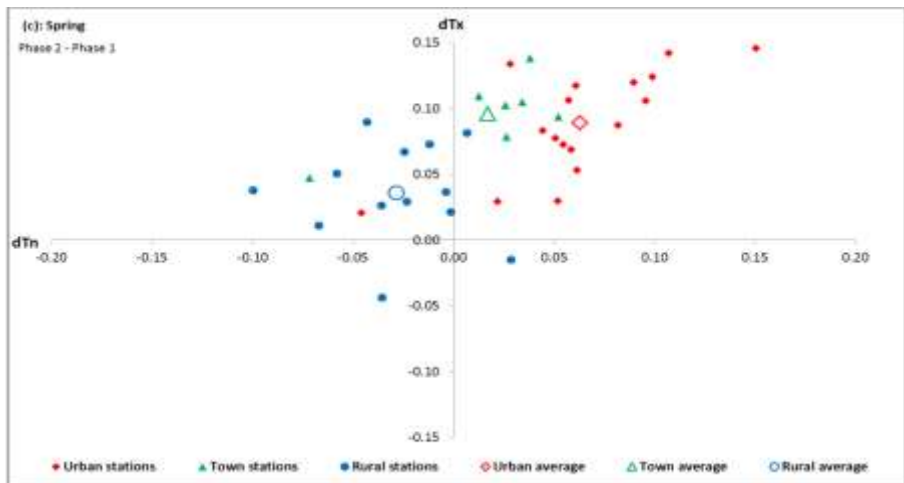
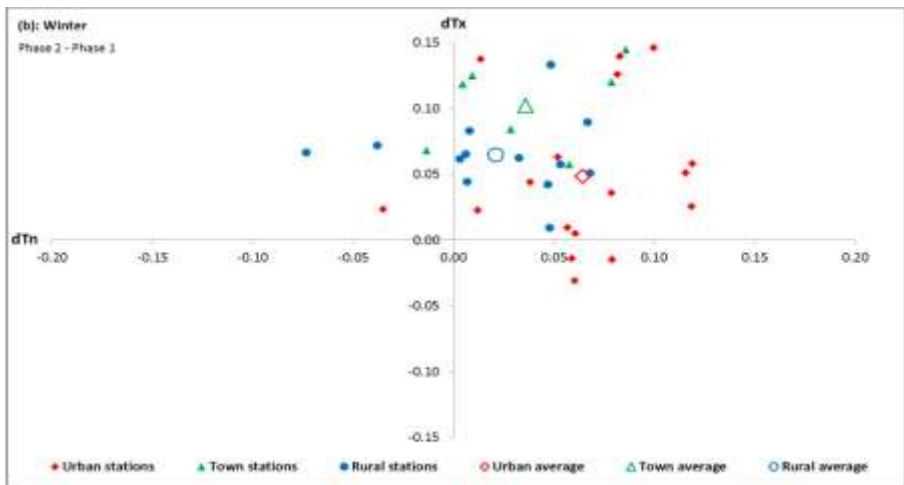
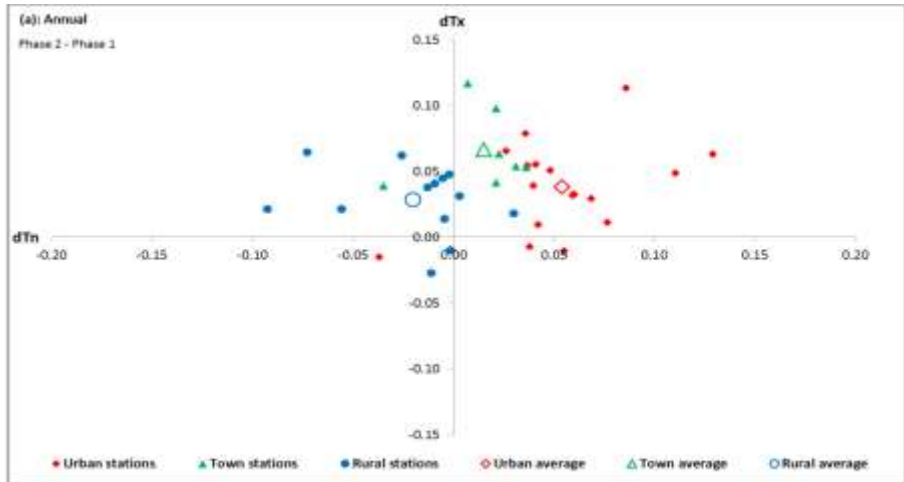


Figure 3.11: dT_n trends as a function of dT_x trends for urban, town and rural stations. Per year trends computed for 1950–1979 (a) ; for 1980–2004 (b); mean trends computed for all urban, town and rural stations for phase 1 and phase 2 (c). The values of dT_n and dT_x are in $^{\circ}\text{C}/\text{year}$.



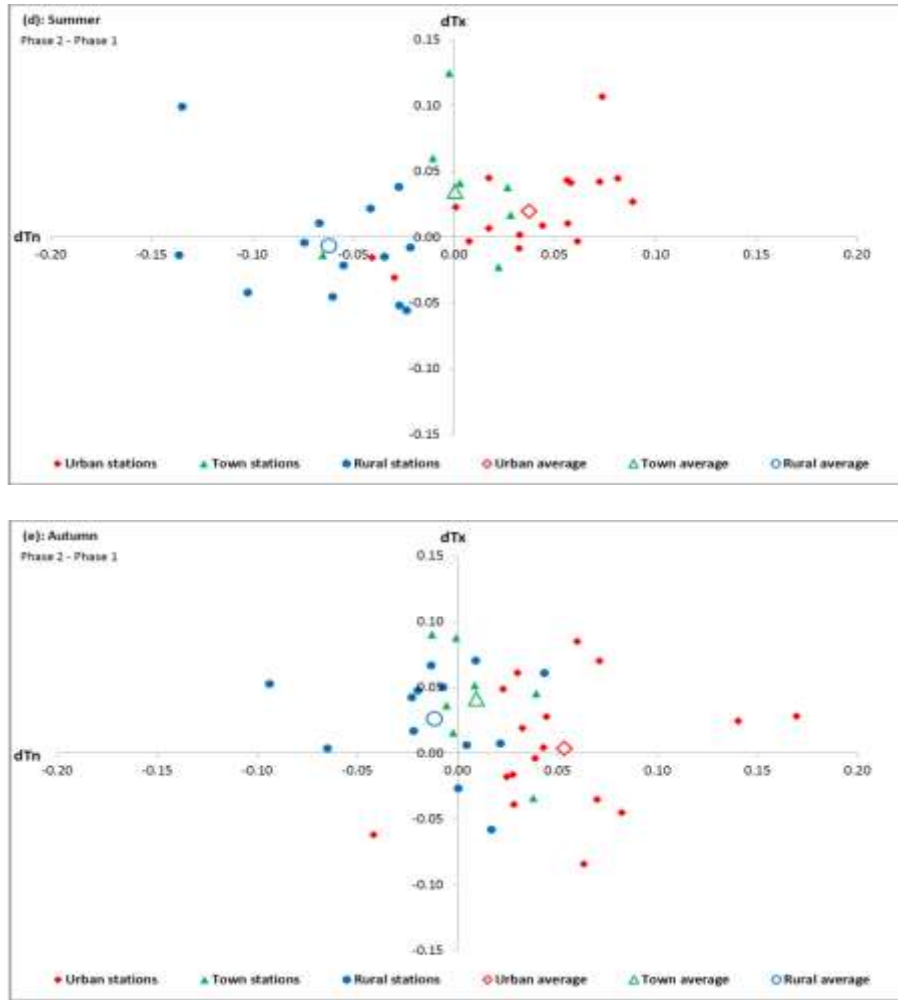


Figure 3.12: Illustration of per year variance in $dT_{n(1980-2004)} - dT_{n(1950-1979)}$ as a function of per year variance in $dT_{x(1980-2004)} - dT_{x(1950-1979)}$ for each station as well as for average of each type of stations for *annual* (a); *winter* (b); *spring* (c); *summer* (d); and *autumn* (e).

Figure 3.12 illustrates per year variance in $dT_{n(1980-2004)} - dT_{n(1950-1979)}$ as a function of per year variance in $dT_{x(1980-2004)} - dT_{x(1950-1979)}$ for each station as well as for average of each type of stations (urban, town and rural stations) for annual and seasonal trends. This type of investigation made us able to clearly understand the effect of recent urbanization on temperature trends as compared to less-urbanized period. Figure 3.12(a) highlights the annual difference for change in minimum and maximum temperature during two periods (1980–2004 - 1950–1979). It is very important to note that positive annual dT_n trends at most of the urban stations highlight that during 1980–2004, minimum temperature at urban stations increased more than the town and

rural stations. Figure 3.12(b-e) highlight that during all the seasons, the minimum temperature at urban stations during 1980–2004 increased more than the town and rural stations (see Table 3.5). Figure 3.12(a-e) also highlight that based on the difference of two periods, annual and seasonal dT_x at smaller cities (towns) during 1980–2004 are higher than the urban and rural stations.

3.4 Discussion

At global scales mean, minimum and maximum temperature trends are increasing (Easterling et al., 1997 (Appendix 3.1); Vose et al., 2005; Trenberth et al., 2007). However, the minimum temperature is increasing at a faster rate than the maximum temperature (Karl et al., 1991; Karl et al., 1993; Easterling et al., 1997; Vose et al., 2005). During last one hundred years (1906–2005), the global mean surface temperatures have risen by 0.74°C . The rate of warming over the last 50 years is almost double that over the last 100 years (0.13°C vs. $0.07^{\circ}\text{C dec}^{-1}$). However an increasing rate of warming has taken place over the last 25 years (1981-2005) and 11 of the 12 warmest years on record have occurred in the past 12 years (1994-2005) (Trenberth et al., 2007). The examination of regional scale data of Pakistan also highlights the same behaviour of change in mean, minimum and maximum temperatures. It is observed that the evolution in temperature at urban, town and rural areas vary in Pakistan. The comparison of global and regional (Pakistan) trends is given in Table 3.7 and Table 3.8 and the comparison of mean, minimum and maximum temperature trends of urban, town and rural areas of Pakistan for the period 1950–2004 and 1980–2004 is presented in Table 3.9.

Many local studies also have demonstrated that the average temperature of many cities of the world is increasing faster than their surrounding rural areas such as Barrow in Alaska (Hinkel et al., 2003); Göteborg in Sweden (Eliasson and Holmer, 1990), Seoul in South Korea (Kim and Baik, 2002) and Mexico city in Mexico (Jauregui, 1997). However, most of the studies highlight that minimum temperature shows the greatest tendency at the urban stations whereas maximum temperature shows the greatest increase at the rural station (Liu et al., 2007). The urban, town and rural areas trends are consistent to the global and other local studies.

Table 3.7: Annual trends ($^{\circ}\text{C dec}^{-1}$) of mean, minimum and maximum temperatures for global and regional (Pakistan) land areas.

Global			Regional		
IPCC, 2007 (1956-2005)	Vose et al., 2005 (1950-2004)		Pakistan (1950-2004)		
Mean	Minimum	Maximum	Mean	Minimum	Maximum
0.13	0.20	0.14	0.15	0.13	0.15

Table 3.8: Annual trends ($^{\circ}\text{C dec}^{-1}$) of mean, minimum and maximum temperatures for global and regional (Pakistan) land areas.

Global			Regional		
IPCC, 2007 (1981-2005)	Vose et al., 2005 (1979-2004)		Pakistan (1980-2004)		
Mean	Minimum	Maximum	Mean	Minimum	Maximum
0.18	0.30	0.29	0.38	0.23	0.35

Table 3.9: Annual trends ($^{\circ}\text{C dec}^{-1}$) of mean, minimum and maximum temperatures for average of urban, town and rural stations of Pakistan.

Pakistan	1950-2004			1980-2004		
	Mean	Minimum	Maximum	Mean	Minimum	Maximum
Urban	0.12	0.16	0.14	0.39	0.43	0.34
Town	0.20	0.19	0.15	0.49	0.27	0.49
Rural	0.17	0.06	0.16	0.30	-0.05	0.30

3.5 Conclusion

The objective of this work was to study the evolution of temperatures at several locations in Pakistan and to comparatively quantify the change in temperature on urban, town and rural areas of Pakistan. In order to highlight the local urban effects, it was also aimed to compare the change in minimum and maximum temperature trends of urban stations of Pakistan with global trends and thus to evaluate on which contribution part the decision makers can directly act to reduce local temperatures and make their cities more livable. The study focused on evolution of temperature in Pakistan especially on urban stations where the rapid urbanization since 1980's is observed. Averaged daily annual and seasonal minimum and maximum temperatures data quality

controlled by using homogenization techniques for two periods 1950–1979 and 1980–2004 of 37 meteorological observatories (17 urban, 7 town and 13 rural) was analyzed.

The variation in change in mean, minimum and maximum temperatures at urban, town and rural areas also greatly vary from one period (1950–1979) to another period (1980–2004). This variation in can be concluded as under:

- The increase in annual T_{min} and T_{max} at urban areas is significantly higher during 1980–2004 than the period 1950–1979.
- The increase in annual T_{min} at urban areas is significantly higher during 1980–2004 than the period 1950–1979 as compare to town and rural stations.
- At town stations, the increase in annual T_{min} and T_{max} is greater during 1980–2004 than the period 1950–1979 and T_{max} is observed higher than urban stations.
- At rural stations, the annual T_{min} decreased and the annual T_{max} increased during 1980–2004 than the period 1950–1979.
- During 1980–2004, the highest growth in T_{min} and T_{max} at urban and town stations is observed in spring season and at rural stations it is observed in winter for T_{min} and in spring for T_{max} .

The comparison of global and regional (Pakistan) annual trends ($^{\circ}\text{C dec}^{-1}$) of T_{mean} , T_{min} and T_{max} for 1950–2004 (Table 3.7) shows that:

- During 1950–2004, the annual T_{mean} , T_{min} and T_{max} increased at global and regional scales.
- The trends of annual T_{mean} and T_{max} of Pakistan for 1950–2004 are closely consistent with global mean and maximum temperatures trends for the same period however over this period, annual T_{min} at global scale increased more than the increase of annual T_{min} of Pakistan.

The comparison of global and regional (Pakistan) annual trends ($^{\circ}\text{C dec}^{-1}$) of T_{mean} , T_{min} and T_{max} for 1979–2004 (Table 3.8) shows that:

- The annual T_{mean} , T_{min} and T_{max} at global and regional scales showed quite higher trends during 1980–2004 than the trends observed over large period i.e. 1950–2004.
- At global and regional scale, per decade change in trends of T_{min} during 1980–2004 is 0.10°C greater than the observed trends during 1950–2004.
- At regional scale, per decade change in trends of annual T_{mean} and T_{max} during 1980–2004 is 0.23°C and 0.20°C , respectively greater than the observed trends during 1950–2004

but at global scale per decade change in trends of T_{mean} and T_{max} during 1980–2004 is 0.15 °C and 0.05°C greater than the observed trends during 1950–2004.

The comparison of annual trends (°C dec⁻¹) of T_{mean} , T_{min} and T_{max} for urban, town and rural areas of Pakistan for the period 1950–2004 and 1980–2004 (Table 3.9) shows that:

- The annual T_{mean} , T_{min} and T_{max} over Pakistan are increasing during the both periods.
- The trends of annual T_{mean} , T_{min} and T_{max} observed over urban, town and rural stations during 1980–2004 are significantly higher than the trends observed during 1950–2004.
- At urban areas, the increase in T_{min} is higher than the increase in T_{max} (i.e., Easterling et al., 1997; Vose et al., 2005). However, the trends of T_{min} and T_{max} at urban areas during 1980–2004 are 0.27 °C dec⁻¹ and 0.20 °C dec⁻¹ greater than the trends observed during 1950–2004.
- The T_{max} increases more on town and rural stations (i.e., Liu et al., 2007) whereas the increase in T_{min} at rural areas is the lowest as compared to the town and urban stations.

The results of this part of study are in agreement with several studies conducted on global scale such as Trenberth et al. (2007), Vose et al. (2005), Easterling et al. (1997) and conducted on local scale such as Hua et al. (2008), Liu et al. (2007) and Brunetti et al. (2000) (Appendix 3.2) in which the increase in minimum temperature at global, regional and urban scale is observed higher than maximum temperature and higher warming after 1980s than the period before 1980s. However the warming over urban areas of Pakistan after 1980s is observed greatly higher than regional and global trends for the same periods. The increase in minimum temperature at urban areas of Pakistan is very distinctive than maximum temperature. The higher increase in minimum temperature than maximum temperature at urban areas is the major concerns of urban climate studies mainly related to urban heat island. But there is no specific source of research which explain that which factors among urban features cause the minimum temperature to increase more than the maximum temperature. To find the suitable explanation about higher increase in minimum temperature in urban areas, in Chapter 4, an effort to evaluate its causes is made by taking into account the different characteristics of urban area such as city size, building height and landuse change.

CHAPTER 4

URBAN SIZE, LANDUSE CHANGE AND BUILDING HEIGHT EFFECT ON URBAN TEMPERATURE

ABSTRACT

In Chapter 3, it was observed that during the recent decade's minimum temperature (T_{min}) at urban areas of Pakistan increases more than the maximum temperature (T_{max}), it increases more than the town and rural stations and more than the increase in global minimum temperature. In this context the major objective of this part of study is to examine the factors that cause the minimum temperature to increase more than the maximum temperature in urban areas. For this purpose, first four city size scenarios (in radius kilometres), four urban fraction scenarios (percentage of occupied land with artificial material) and three building height scenarios (in meters) are designed. To quantify the relative impact of city size (r), urban fraction (u) and building height (h) on minimum and maximum temperature of urban areas Finite Volume Model (FVM) is applied for the simulations of 48 possible combinations (4·4·3) of scenarios of

theoretical cities. By using this model, the interaction between the cities and atmosphere can be well simulated on mesoscale. All the simulations are run for three days of all the months starting at 00:00 (GMT) on 19th day of each month and ending at 00:00 (GMT) on 22nd day of each month. The results show that based on annual average of all 576 simulations), T_{min} and T_{max} increases when city size r and building height h increase and T_{min} increases and T_{max} decreases when h increases. The individual impact of urban parameters shows that the city size r is the main factor that causes to increase the minimum temperature of urban areas more than the maximum temperature. Further investigations confirm that the higher increase in minimum temperature in urban areas is mainly during colder months than the warmer months.

4.1 Introduction

The relationship of heat island intensity (ΔT_{u-r}) and city size (*as measured by its population - P*) is found positive by Oke (1973); Park (1986) and Karl et al. (1988). Oke (1973) found that ΔT_{u-r} is directly proportional to $\log P$; larger the city size, higher the temperature than its surrounding areas (Figure 4.1). Base on the data of a network of 1,219 stations across United States, the stations with populations near 10,000 were shown to average 0.1°C warmer for the mean annual temperature than nearby stations located in rural areas with population less than 2,000 (Karl et al., 1988). Exploring the effect of city size on urban heat island in Asian mega cities (Table 4.1) by considering the population as a surrogate of city “size”, Hung et al. (2006) also found the surface UHI magnitude proportional to the population size of the cities; highly intense during day and less intense during night times (Figure 4.2).

In principal studies regarding the relationship between city size and UHI on wide scales were conducted by Oke (1973). He explored this relationship for several cities of North America and Europe and found more amenable to generalization than that for location is the relationship between heat island intensity and city size (Oke, 1973). Such relationships have been shown to exist in Figure 4.2 in which the data of $\Delta T_{u-r(max)}$ from many North American and European settlements are plotted against their $\log P$. It can be implicit that the population size effect in North American settlements on $\Delta T_{u-r(max)}$ is clearly greater than the settlements located in Europe that shows that ΔT is often inhomogeneous for the settlements located in different climate zones and have different physical and geographical characteristics.

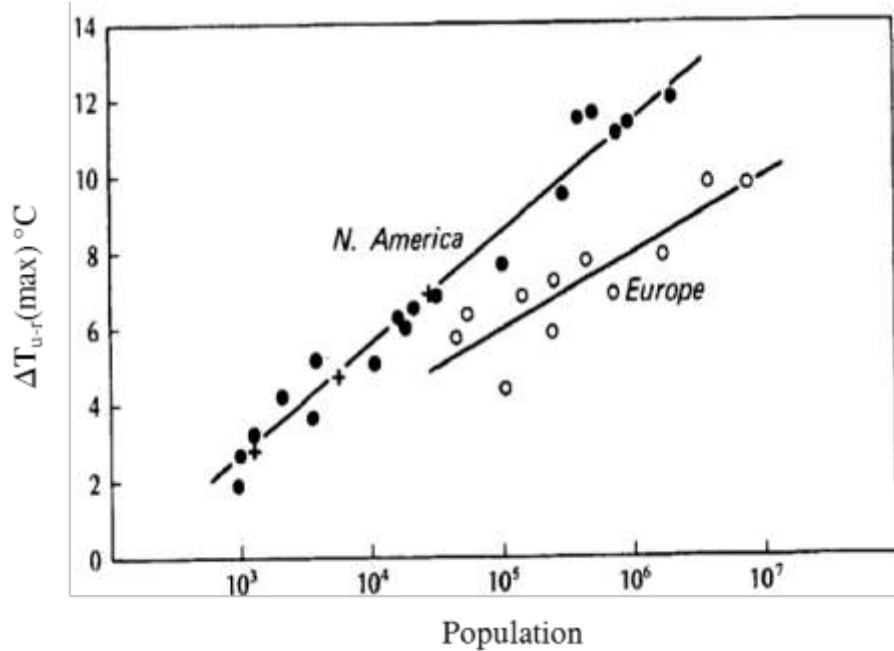


Figure 4.1: Relationship between maximum heat island intensity ($\Delta T_{u-r(max)}$) and population (P) for European and North American settlements (After Oke, 1973).

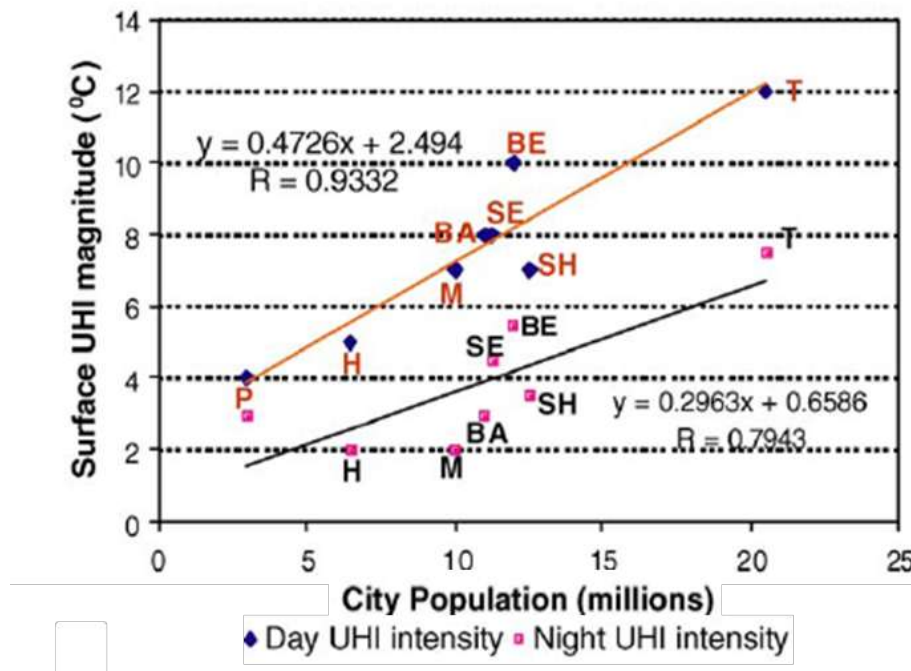


Figure 4.2: Effect of city size (in population) on day and night time surface UHI magnitude. Tokyo (T); Beijing (BE); Shanghai (SH); Seoul (SE); Pyongyang (P); Bangkok (BA); Manila (M); Ho Chi Minh City (H) (After Hung et al., 2006).

Zhao et al. (2006) highlighted in their work that the degree of urbanization with time has significant difference in evolution of temperature from one period to another period. Figure 4.3 illustrates the vivacious substantial urban effect on dT in Shanghai. The difference in MAT between urban and rural areas increased from 0.1 °C in the late 1970s to 0.7°C in the early 2000s, with an increase of 0.24°C per decade (Figure 4.3a). Similarly, MT_{max} and MT_{min} did not show a difference between urban and rural areas in the late 1970s, although the differences increased to 0.7°C and 0.5°C in the early 2000s, respectively, with a decadal increase of 0.26°C and 0.21°C (Figures 4.3b and 4.3c). However, the differences in temperature between urban and rural areas increase substantially as the degree of urbanization expanded (in sq.km), and that this increase is faster for MT_{max} than for MT_{min} (Figure 4.3d).

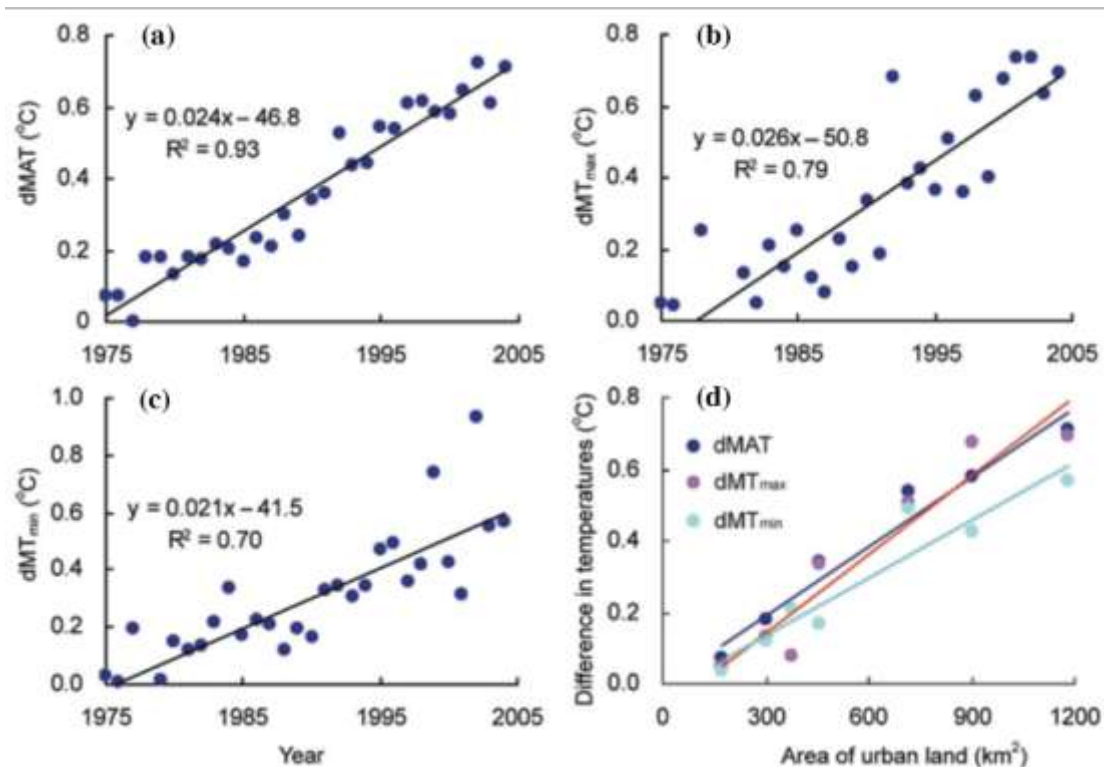


Figure 4.3: Changes in temperature differences between urbanized and rural areas in the years 1975–2004. (a) Difference in mean annual temperature ($dMAT$); (b) difference in monthly mean maximum temperature (dMT_{max}); (c) difference in monthly mean minimum temperature (dMT_{min}); and (d) relationships between the temperature differences and degree of urbanization (After Zhao et al., 2006).

Table 4.1: UHI magnitudes and spatial extensions for the eight selected Asian mega cities (After Hung et al., 2006).

	Time	Pyongy ang	Ho Chi Minh	Manil a	Bang kok	Seo ul	Beiji ng	Shangh ai	Tok yo
UHI magnitude °C	Day	4	5	7	8	8	10	7	12
	Night	3	2	2	3	4.5	5.5	3.5	7.5
Population (million) in 2000		3	6.5	9.93	11	11.3	12	12.55	20.5
Pop. Density/sq.km in 2000		6000	9373	15617	11677	1066 3	5879	8882	6218
Observed month/year		Aug. 2001	Feb. 2002	Nov. 2001	Feb. 2002	Aug. 2001	Aug. 2001	Aug. 2001	Aug. 2001

In fact, the use of population size as a criterion for estimating the urban effect is also subject to controversy. Normally it is seen that the results of dT of a city is not in agreement of dT of other cities with the same population size and the population density. An illustration of this point comes from Portugal where the meteorological stations Sintra/Granja (located on a military base far from the nearest densely urbanized area) and Lisboa/Geofisico (in the Lisbon city center) are both presented in the National Climatic Data Center (NCDC) database as being associated with a population of 1.1 million (i.e., the population of the Lisbon metropolitan area). In addition, the population of numerous cities in “developed” countries has recently tended to stagnate or even decrease (Alcoforado and Andrade, 2008).

In 2000, the population of Beijing and Shanghai was 12 and 12.5 million, respectively and the population density of the both cities was 5,879 and 8,882 persons/km², respectively. Although the total population and density of Beijing is lower than Shanghai, the UHI magnitude of Beijing is 3°C higher at day and 2°C at night than Shanghai (Hung et al., 2006; Table 4.1). The cities located in North America and Europe are less dense than the cities located in Asia. The highest urban population density of Asian cities goes up to 40,000 persons/km² (Dhaka) while in European and North American major cities; it goes maximum up to 7,500 persons/km² (London) and 2,500 persons/km² (Los Angeles), respectively (Appendix 4.1). It is because the cities located in North America and Europe cover larger urban areas (in Kms) than Asian cities. As is shown in Appendix 4.1, among 67 selected cities based on their population density, the top 29

dense cities (except London and Madrid are located in Asia and rest are located in Europe and North America (except Pyongyang). There are limited studies concerning to analyze the relationship between urban size (in kms) versus dT .

Urbanization “the movement of people into cities and to the transformation of ‘natural’ into urban land-cover” (Mills, 2007) has an important impacts on surface air temperatures (Vose et al., 2004). There are two aspects to considering impacts of land use: effects of land use on climate change and the effects of human-induced climate change on land use. The direct ecological effects of the land-use and climate change are dominated by the land-use change effects, at least over the period of a few decades. Because climate-change effects are largely determined by land-cover patterns, land-use practices set the stage on which climate alterations can act (Dale, 1997). Although, an extensive work about land use/land cover change’s effect on surface air temperature at global, regional and local scales has been done and widely debated by researchers and scientists (Mathews, 1983; Dale, 1997; Bonan, 1997; Lean and Rowntree, 1997; Heck et al., 2001; Fu, 2003), the importance of this study has never decrease because of concentration of more and more population in urban areas (Mills, 2007).

Remarkable works to study the land use change effect on surface temperature have been done by research community. In most of the studies, numerical models as surface heat island model (SHIM) by Johnson et al, 1991, Global Climate Model (GCM) by Fan et al. (1998), Atmospheric Global Circulation Model (AGCM) by Wang (1999), NCAR Community Climate Model V3, coupled to the Biosphere Atmosphere Transfer scheme and a mixed layer ocean model by Zhao et al. (2001), a general circulation model (Colorado State University GCM) coupled to a biophysically-based land surface model (SiB2) by Bounoua et al. (2002), RegCM2, by Gao et al. (2003) and Suh and Le (2004), Urban Growth Model [UGM] and the Land Cover Deltatron Model [LCDM] (the part of the SLEUTH program) by Solecki and Oliveri (2004), meso-scale numerical atmospheric model for BUBBLE project by Rotach et al. (2005), Simple Biosphere Model by Bounoua et al. (2009); statistical models and tools by Oke, 1981, 1982; Park, 1986 ; Jones et al., 1990; Kalnay et al., 1996; Kuttler et al., 1996; Unger et al., 2000; Bottyan and Unger, 2003; Kalnay and Cai, 2003; Zhou et al., 2004; Vose et al., 2004; Bottyan et al., 2005; Zhang et al., 2005; Zhao et al., 2006 and GIS, remote sensing and aerial approaches by Aniello et al., 1995; Voogt and Oke, 1998, 2003; Gallo and Owen, 1998, 1999; Lo and Quattrochi, 2003; Weng et al., 2004; Chen et al., 2006a; Hung et al., 2006; Hu and Jia, 2010 are

used for identification of relationship between land use change vs land surface temperature. However, almost all studies depicts that the difference and the magnitude of change in temperature as a results of change in land-cover is often inhomogeneous. The trends of UHI intensity in different land use change regions are spatially correlated with regional land use and are prominent in areas of rapid urbanization (Chen et al., 2006b; He et al., 2007).

Figure 4.4 highlights that urban and rural temperature difference also greatly vary during heating and non-heating seasons (Bottyan et al., 2005) and over warming of cities due to UHI enhanced the air conditioning load (Hassid et al., 2000) depending upon the density of artificial land-cover occupied by urban areas. There is also strong connection between the mean maximum UHI intensity ΔT and the built-up ratio. In Debrecen (Hungary), it is noticed that in the areas near the geometrical centre of the city where the artificial surface cover is the highest (the extreme value is 86%), the mean maximum UHI intensity is the highest (Bottyan et al., 2005). However in some cases where the artificial surface increased and vegetated land decreased, on average minimum temperatures rose by 0.3°C and maximum temperatures by 0.9°C (Pauleit et al. (2005) with letting down the creation of UHI. The park sites inside the cities cause great reduction in temperature than the areas occupied by streets, buildings and other artificial materials. The temperature at urban street of New York measured by Gaffin et al. (2008) was almost 3°C higher than the temperature at park site measured just after 26 minutes of the first measurement.

Regardless of urban population size and land use change as an indicator to measure UHI, other important internal and external factors of the city influence the local climate, including urban morphology, spatial size of the city, building's density, spatial distribution of land-use, topography, street canyon, meteorological conditions, seasons, nearby water bodies and quantity of emission of heat associated with anthropogenic activities (Oke 1982; Magee et al. 1999; Montavez et al. 2000; Martilli, 2002; Kalnay and Cai, 2003; Kim and Baik 2005, Alcoforado and Andrade, 2008; Zhang et al., 2010; Salamanca et al., 2010; Salamanca and Martilli, 2010). The magnitude of the urban effect may also be more closely associated with the level of energy consumption (e.g., cal/person/year), which depends on other socio-economic factors (Brázdil and Budíková 1999 i.e., Prague); Chen et al. 2003 i.e., in Shanghai; cited by Alcoforado and Andrade, 2008).

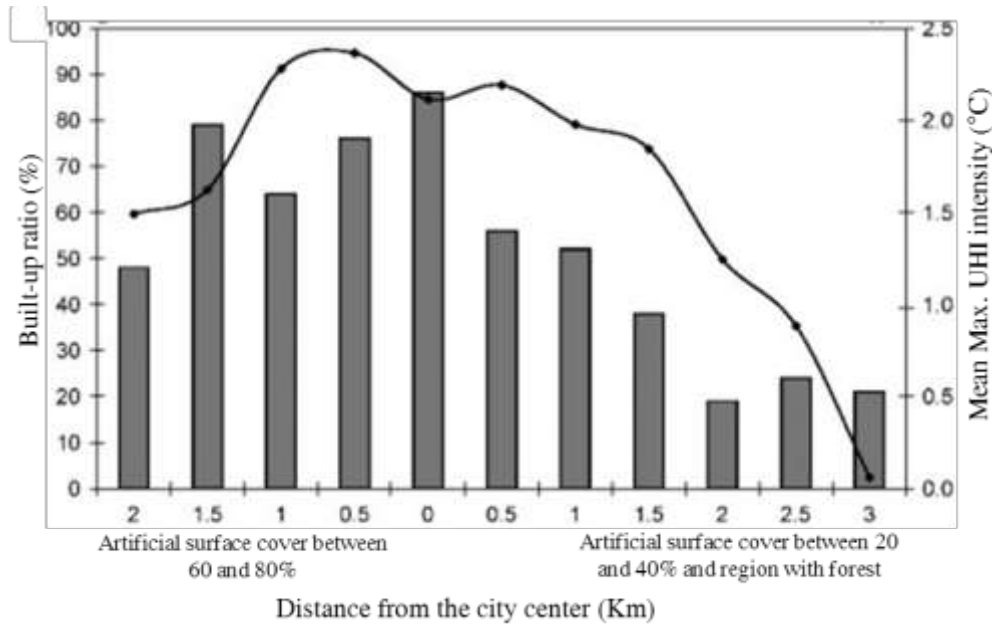


Figure 4.4: Relationship between built-up ratio, distance from the city centre and annual mean maximum UHI intensities along South–North cross-section in Debrecen, Hungary (After Bottyan et al., 2005).

In Chapter 3, it was observed that during the recent decades minimum temperature at urban areas of Pakistan increases more than the maximum temperature. It was also noticed that minimum temperature at urban areas increases more than the town and rural stations. Further comparisons also highlighted that the rate of increase of minimum temperature at urban areas is quite higher than the increase in global minimum temperature. However, the available literature about urban climate studies does not clearly elaborate the reason of higher increase in minimum temperature than the maximum temperature in urban areas. In this context the major objective of this part of study is to examine the factors that are the cause of higher increase of minimum temperature than the maximum temperature in urban areas. For this purpose, in this chapter, an effort is made through model simulations to understand the effect of major urban characteristics such as building height, city size and urban fraction on urban temperature.

In section 2, the description of FVM model is given that is used as a method to simulate different types of scenarios of theoretical cities. In section 3 results are discussed and in section 4 conclusion of the study is given.

4.2 Methodology

4.2.1 Model description

Numerical models are often used to solve the highly non-linear equations that describe atmospheric flows at different scales and especially at mesoscales. A mesoscale model, referred as FVM (Finite Volume Model) developed by Clappier A. et al., (1996) is used for this part of the study to run the simulations for different scenarios. It is a three-dimensional non-hydrostatic model that calculates the main meteorological variables such as wind speed and directions, pressure, air temperature, density and humidity. The basic equations of mass, momentum, humidity, energy and turbulent kinetic energy conservation equations and equation of state are solved using a system of partial differential equations (Mauree, 2011). The description and governing equations solved in the model as given by Mauree (2011) and Martilli (2002) are given in Appendix 4.2. FVM model is already used and validated by Martilli et al. (2003) in which they performed two sets of simulations over the city of Athens (Greece) first by using a mesoscale model with a detailed urban surface exchange parameterisation and second with the traditional approach. Comparison with measurements showed better agreement for the simulation with the detailed parameterisation.

Since a city is probably one of the most complex surfaces, a complete reproduction of all the heterogeneity of a ‘real’ city would be too complex to simulate in a model and hardly realizable in most cases due to the lack of detailed data. The most important effects of the urban surfaces on airflow are: (i) drag induced by buildings with consequent loss of momentum, (ii) enhancement of the transformation of mean kinetic energy into turbulent kinetic energy and (iii) modification of the heat fluxes due to shadowing and radiation trapping effects. A simplification is therefore needed for parameterization of urban areas (Martilli, 2001). The city as a combination of several urban classes is proposed by Martilli, (2002) where each class is characterized by an array of buildings of the same width B located at the same distance from each other (canyon width W), but with different heights h (with a certain probability $\gamma(h)$ to have a building with height h).

By using FVM model, series of simulations are run through developing several scenarios of theoretical round cities by changing their building’s height, city size (in km) and urban fraction

(in percentage). The geographical coordinates of the theoretical cities are fixed over Faisalabad, a real city located in Pakistan. Faisalabad that is located on a fairly flat plain of central Punjab with an average height of 175m from sea level, comparatively far from the higher mountain ranges located in north and west, far from coastal zone of Arabian Sea and eventually has no major water reservoir close to it. The selection of a domain with coordinates over this city was to avoid the effect of such physical factors on simulated. It was also desired to use the realistic and typical Pakistani's meteorological situations to create the meteorological forcings to use in FVM to run the simulation for proposed scenarios of the hypothetical cities. Moreover, it is a plan city that has an appropriate urban physical geometry and allows to easily detecting the urban and vegetation fraction. Such types of flat and non-complex city also allow to properly parameterizing its characteristics to run the model for better results.

4.2.2 Model setup for simulation

The model is based on the method of finite volume in which the atmosphere is divided into boxes of fixed volumes in three dimensions (x, y, z) and the equations of conservation laws of mass, momentum and energy are resolved within each of these volumes. The 3-D mesh of studied area is adjustable according to its resolution. It is also deformable to follow the contours of the land. For the domain, the x and y axis depends upon the selected domain to study.

Initially the larger domain with grid cell dimensions over x and y axis was selected to 30 cells with a resolution of 10x10 km was selected. Then for the case studies of round cities, comparatively smaller domains with 30 cells of resolution of 4x4 km were used. To interpolate the meteorological conditions, the smaller domains were nested with the larger domain. Then for the case studies of round cities, comparatively smaller domain was selected where its horizontal extension is 30 km with a resolution of 4 km. The vertical resolution range from 10 m to 18 m in the first 55 m above the ground and then it keeps on stretching as the distance from the ground increase to its maximum limit of 1000 m at the model top (9347 m). The top of the vertical axis is the tropopause, which means that in this study only troposphere is considered for forcing and simulations. In the city the street canyon width is assumed as 30 m and the horizontal building size is 15 meter.

The time for all the simulations run in this study was homogeneously fixed for all type of scenarios and for all months. All the simulations for all scenarios were run for three days starting at 00:00 (GMT) on 19th day of each month and ending at 00:00 (GMT) on 22nd day of each month.

The major urban parameters considered for this study for ground, wall, window, roof and street are albedo α (0.2 for all), emissivity ϵ (0.9 for all), roughness length of the surface Z_0 (0.01 for all), substrate thermal conductivity of the material K_s ($1.73 \text{ m}^{2\text{s}^{-1}}$ for all), specific heat of the material C_s ($\text{J}^{\text{m}^{-3}\text{K}^{-1}}$). Temperature initial is considered as 293 K for all type of surfaces.

4.2.3 Model input and data acquisition

The model is designed on three major features: topography, landuse and meteorological conditions (temperature, wind speed and direction, humidity, surface and atmospheric pressure). It takes into account all these components around the place and time period, chosen for the simulations. It integrates the data grids in its operations during the pre-processing of raw data taken from the original databases. These operations consist of interpolations of these data to correspond with the spatial and temporal resolution of FVM. The brief description of pre-processors and interpolation is given below.

4.2.3.1 Topographical data input

The topography of a region plays an important role in modification of the meteorological conditions such as changing wind direction, altering isotherms, shifting pressure cycles and causing the instability of the overall climate. As the mesoscale domain can range from few kilometers to few hundred kilometers, the effect of topography also vary according to the physical features (mountains, water bodies and other physical barriers) located in particular domain area. During the simulation process, the FVM model takes into account the topography and its associated effects on meteorological conditions. So topography is one of the important inputs of FVM.

The model use the topography's information downloaded from the GTOPO 30. It is a global Digital Elevation Model (DEM) with a horizontal grid spacing of 30 arc seconds (approximately 1 kilometer). GTOPO30 is derived from several raster and vector sources of

topographic information. For easier distribution, GTOPO30 has been divided into tiles which can be selected, downloaded and used as raw data from the website of GTPPO30 (<http://www1.gsi.go.jp/geowww/globalmap-gsi/gtopo30/gtopo30.html>). Detailed information on the characteristics of GTOPO30 including the data distribution format, the data sources, production methods and accuracy can be found on <http://www1.gsi.go.jp/geowww/globalmap-gsi/gtopo30/README.html>. For the selected domain to study here, the topographical data extracted from GTOPO30 is interpolated to extract the topographical data by using the pre-processors of FVM. The raw topography tile and the processed topography map are given in figure 4.5.

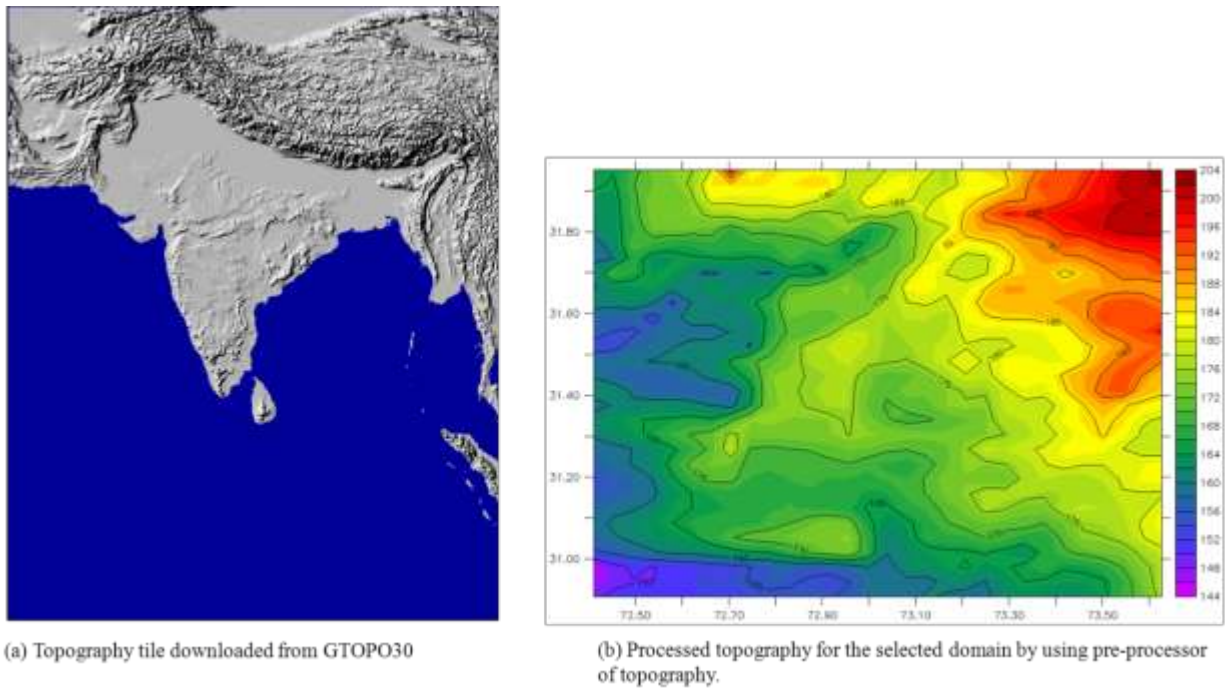


Figure 4.5: Raw topography tile and the processed topography map.

4.2.3.2 Landuse data input

Landuse change has a significant effect on climate (Bonan, 1997; Dale 1997; Bounoua et al., 2002) and its effect becomes more prominent at microscale. The findings of many researchers around the world elaborates that the conversion of green spaces into built-up area is one of the major reason of UHI (Bottyan et al., 2005; He et al., 2001, 2007; Jusuf et al 2007) as is described in Chapter 2. FVM takes into account the landuse data for the simulations and is able to use it as

an input. The landuse data to use in FVM is obtained from Global Environment Monitoring Unit (GEM) of Joint Research Center (JRC) of European Commission which was developed under the project of Global Land Cover (GLC) mapping and monitoring, a project of Global Vegetation Monitoring (GVM) unit (<http://bioval.jrc.ec.europa.eu/products/glc2000/glc2000.php>). As the data used in FVM for this study is extracted from the landuse tile of South Asia, its further description can be read in detail and the data can be downloaded from Joint Research Center of European Commission: http://bioval.jrc.ec.europa.eu/products/glc2000/products/India_paper.pdf.

The data obtained from GLC2000 for the region of South Asia is based on larger scales extending from 1.1°N to 37.5°N latitude to 60°E to 105°E Longitude. To use it at mesoscale for our selected domain, it is processed by using pre-processors of landuse before to use it for the simulations. The actual landuse data tile downloaded from GLC2000 website is given in figure 4.6(a) and processed data for the selected domain that is used in FVM is given in figure 4.6(b). As we used the hypothetical cities, the landuse of different round cities scenarios is not constant.

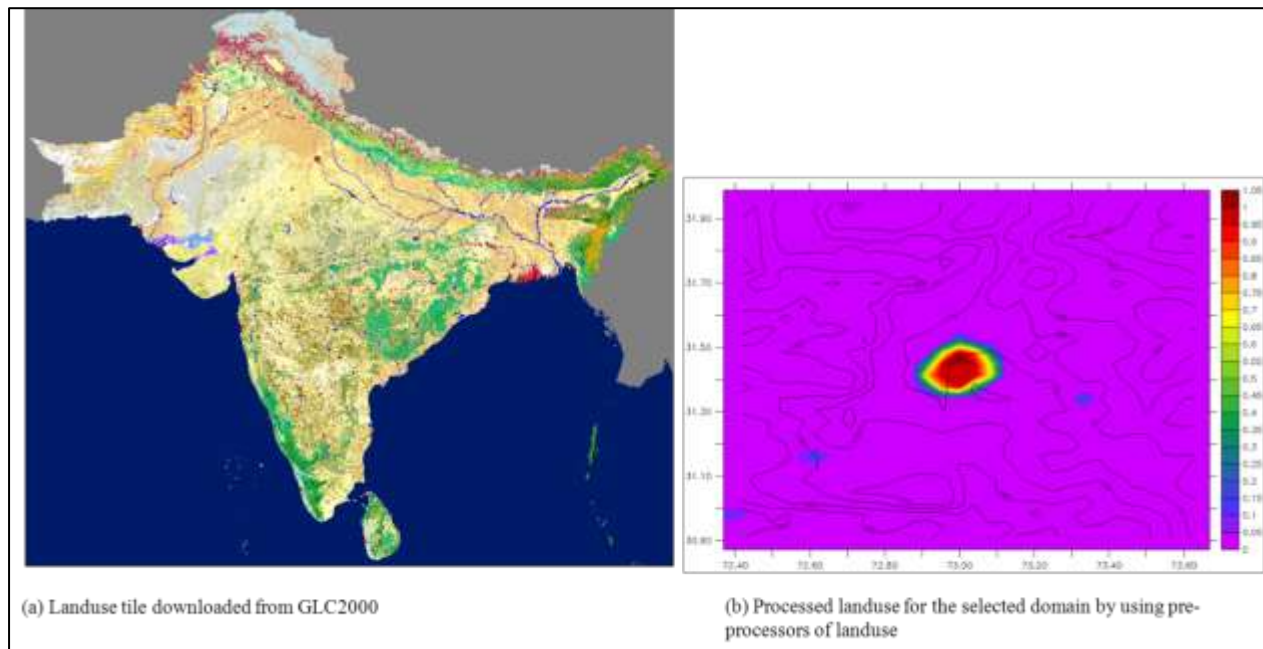


Figure 4.6: (a) Raw landuse tile; and (b) processed landuse map for the selected domain.

4.2.3.3 *Meteorological data*

The meteorological data (wind, temperature, pressure and humidity) for the forcing of boundaries were derived from National Center for Environmental Predictions (NCEP) data base. The global model (NCEP) generating these data has a horizontal resolution of 270km×270km and the vertical resolution is given in terms of 17 different pressure levels. It provides the data for every six hours i.e. four times a day. To use these data to force the mesoscale model having a much finer spatial and temporal resolution these raw data are interpolated over space and time (Roches, 2007; Rasheed, 2009).

For the simulation scenarios on this study, two different grids with two different resolutions are selected. The coarse grid comprises on 30 cells of 10km x 10km and the smaller grid has the same number of cells but with a resolution of 4km x 4km. The coarse grid uses the NCEP interpolated data at the boundaries and the smaller grid uses the interpolated results of the coarse grid at the boundaries.

Figure 4.7(a) shows the interpolated NCEP wind on the coarse grid. Figure 4.7(b) displays the simulated wind obtained by using FVM on the coarse grid. Figure 4.7(c) illustrates the interpolated wind from the coarse grid on the smaller grid. Figure 4.7(d) shows the simulated wind obtained by using FVM on the smaller grid.

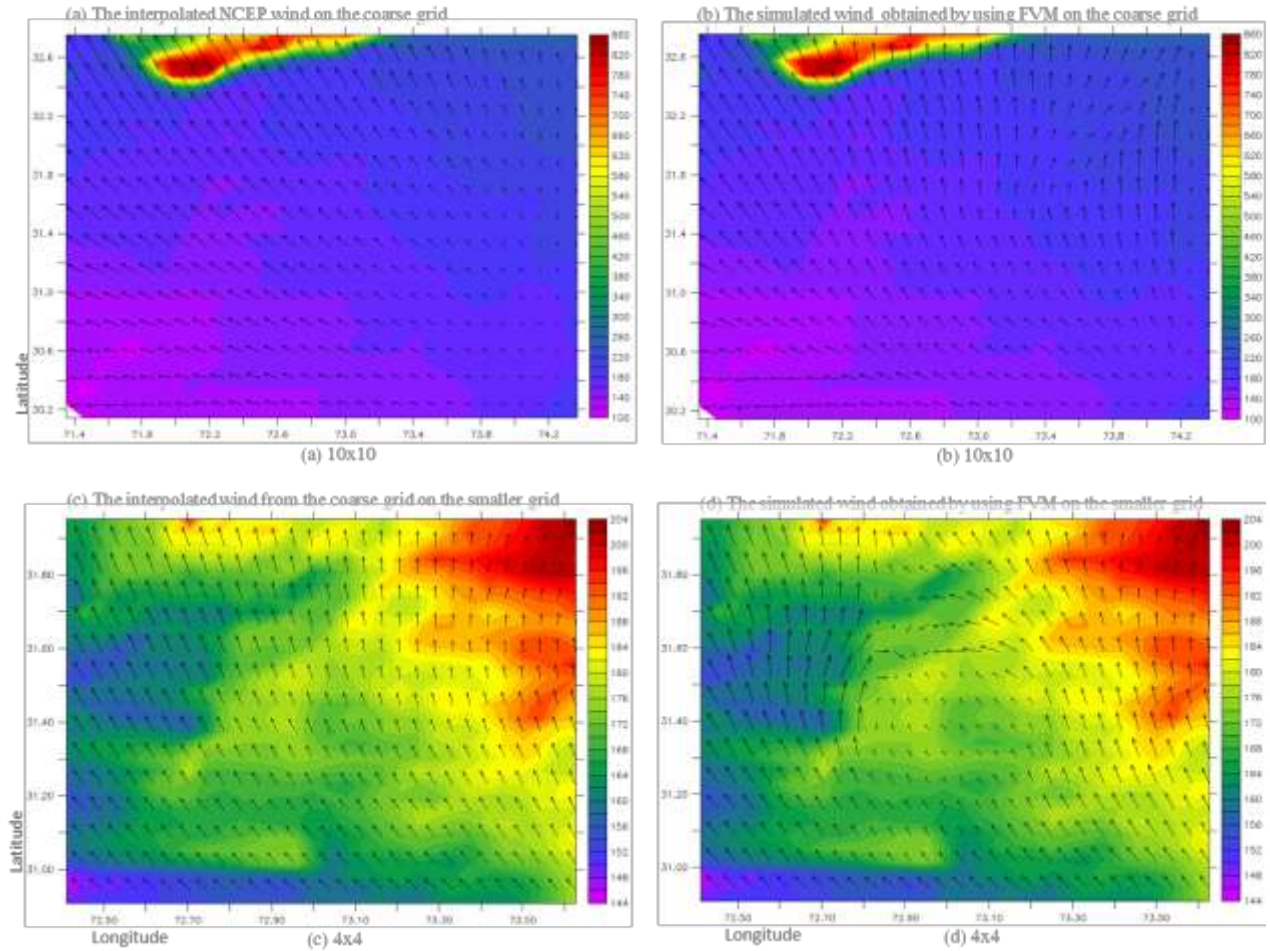


Figure 4.7: Wind at 5 meter above the ground. The color contours represent the topography in meters above sea level.

4.2.4 Preparation of simulation scenarios

To analyse the effect of city size, urban fraction and building height effect on urban temperature, 4 scenarios for city size, 4 scenarios for urban fraction and 3 scenarios for building height are designed. For each month, 48 possible combinations for the developed scenarios are run for the simulation ($4 \times 4 \times 3$) by using model FVM. As we have simulated all these combinations for each month, so there are total 576 simulations (48×12).

4.2.4.1 Preparation of landuse scenarios

The landuse data about urban fraction in the model is acquired from Global Land Cover 2000. For the theoretical cities, 4 urban fraction scenarios are designed. Among all these scenarios, highly densely built city contains the 95% of its soil occupied with artificial material (buildings, roads and other paved surfaces) and only 5% of its area is without the presence of the city. The other 3 scenarios contain the urban fractions of 90%, 80% and 70%, respectively. The urban land surface (buildings, roads, vegetation etc) is parameterized inside the FVM model that takes it into account with all other parameters designed for this work.

4.2.4.2 Preparation of city size scenarios

Figure 4.8 represents four theoretical round cities with a radius of 8km, 12km, 16km and 20km. The difference between the city sizes is kept homogeneous. Each of the city size is simulated in combination with all other scenarios of landuse and building height.

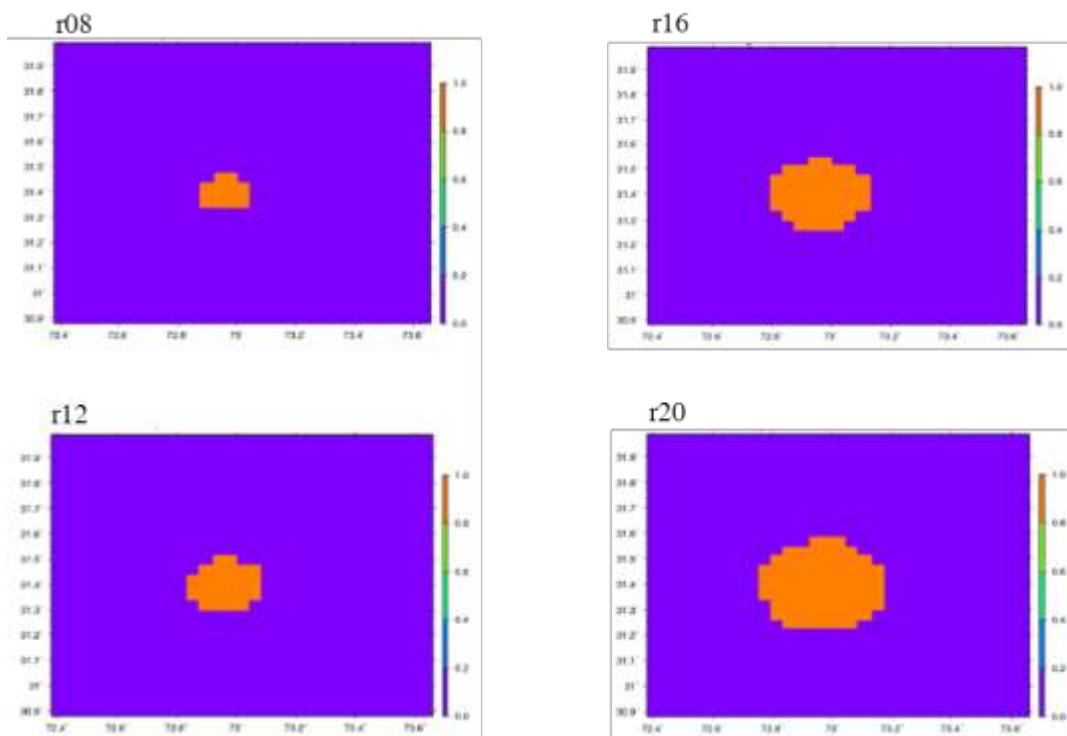


Figure 4.8: Scheme of the city size scenarios. In all 4 city size scenarios, the scale is representing the percentage of urban and rural fraction.

4.2.4.3 *Preparation of building height scenarios*

For the theoretical cities, the real data about probability of buildings height in Pakistan was not available. A conceivable data for urban building's height located in selected domain is used in this study where three types of buildings with height of 20m (4 floors), 25m (5 floors) and 30m (6 floors) are considered for the simulations. Between the two buildings, the street canyon width is assumed as 15 m and the horizontal building size is 30 m. The probabilities of building's height scenarios are fixed to 100% for 20 m, 100% for 25 m and 100% for 30 m. Each building height scenario is simulated with each city size and urban fraction. As we have only used the theoretical round city scenarios, the building height used in this study may be different than the actual height of the building located in cities of Pakistan in general and in the city located within selected domain.

4.2.4.4 *Computation of temperature variations for urban parameters*

By using the results of simulations of all the scenarios; the change in temperature of different hypothetical cities is studied. First, the temperature data is extracted from the resulted simulations for each month and then it is used to find variation in average temperature dT with changing city size dr , urban fraction du , and building's height h . Although, for each month, the simulations are run for three days, to avoid the effect of border conditions during initialization of the simulations, averaged T_{min} and T_{max} data of only last two days (20 and 21 June 2005) is analyzed here. The T_{min} and T_{max} data used here is the average of all cells containing the proportion of urban classes (by following the landuse file as an input of landuse).

Based on the two days average of T_{min} and T_{max} at urban areas for each scenario, the variation in minimum and maximum temperature with varying city size (dT_{min}/dr and dT_{max}/dr), urban fraction (dT_{min}/du and dT_{max}/du), building height (dT_{min}/dh and dT_{max}/dh) are calculated according to the urban parameterization used in the simulations.

For city size scenarios, four different city size with radius of 8, 12, 16 and 20 km are taken into account for the simulations and from its results the dT/dr is computed as under:

$$dT_{r12-r08}/dr = (T_{r12} - T_{r08})/(r12-r08)$$

$$dT_{r16-r12}/dr = (T_{r16} - T_{r12})/(r16-r12)$$

$$dT_{r20-r16}/dr = (T_{r20} - T_{r16})/(r20-r16)$$

here T denotes for *temperature* and r is symbolizing the city size (in radius of kilometers). So in this case, the results are given in K per kilometer. For landuse change, four types of urban fraction scenarios $u95$, $u90$, $u80$ and $u70$ are used for the simulations. For these scenarios, dT/du is calculated as under:

$$dT_{u95-u90}/du = (T_{u95} - T_{u90})/(u95-u90)$$

$$dT_{u90-u80}/du = (T_{u90} - T_{u80})/(u90-u80)$$

$$dT_{u80-u70}/du = (T_{u80} - T_{u70})/(u80-u70)$$

here u is signifying the urban fraction. In these types of scenarios, the results are given in K. As mentioned before, three different scenarios of building heights with 20m, 25m and 30m are used in this study. For building height scenarios, dT/dh is considered as under:

$$dT_{h30-h25}/dh = (T_{h30} - T_{h25})/(h30-h25)$$

$$dT_{h25-h20}/dh = (T_{h25} - T_{h20})/(h25-h20)$$

here h is signifying the building's height in meters. As these scenarios are based on building height in meters (20m = $f4$; 25m = $f5$, 30m = $f6$) the results of these type of scenarios are given in K per meter.

4.2.4.5 *Computation of contribution of urban parameters in temperature variation*

Using the temperature variations caused by different urban parameters, the contribution of temperature of each parameter or the total contribution of temperature of all the parameters induced by a variation in time is possible to calculate. The model to compute the contribution of each parameters or the total contribution of all the parameters is written as follows:

$$\frac{dT}{dt} = \frac{dT}{dr} \cdot \frac{dr}{dt} + \frac{dT}{du} \cdot \frac{du}{dt} + \frac{dT}{dh} \cdot \frac{dh}{dt} \quad (4.1)$$

where dT is for change in temperature, dt for change in time, dr for change in radius, du for change in urban fraction and dh for change in building height. dT/dt finally represents the sum of contribution of the increases of the city size, the urban fraction and the building height.

In order to compare the modeling approach with observed data of Lahore city, the data of city size of Lahore is derived from Khaliq-uz-zaman and Baloch (2010), urban fraction is computed from the data provided by Almas et al. (2005) and through personal communication with Amjad S. Almas (2010). An approximate value about the evolution of building height by a variation of time is used that vary for the two time periods.

4.3 Results and discussion

As it was noticed in the previous chapter that after 1980s, T_{min} and T_{max} at urban stations are increasing but T_{min} increases more than T_{max} , the purpose of this study was to identify the factors that cause the higher increase in minimum temperature than maximum temperature at urban areas. For this purpose, we parameterized several types of theoretical cities and based on the urban parameters, we run 48 simulations for each month of a year with possible combination of all the scenarios of theoretical cities.

Due to the large amount of simulations that have been produced, Figure 4.9(a to d) and Figure 4.10(a to d) are highlighting only one of the example out of the total simulations obtained through using FVM model. In this case, the model is applied to study the effect of urban areas on local temperature by varying the city size r (8 km, 12 km, 16 km and 20 km) for 09:00 GMT and 17:00 GMT, respectively on 20th of April 2005. In all the simulations, urban fraction and building's height are constant (80% for urban fraction and 20 meters for building's height). In order to use the real meteorological conditions over one of the Pakistani city located on flat surface and less affected by nearby physical features, the coordinates (longitudes and latitudes) of all the given figures in Figure 4.9 and 4.10 are fixed over the city of Faisalabad. These figures show the spatial variation of temperature and wind circulation simulated over the selected domain

in the first level. It can be noticed that during day and night times, the temperature over urban areas is higher as compared to non-urban areas and the intensity of higher temperature over urban zones increases with increasing city size. Due to higher temperature and lighter air over urban zones, there are convergence zones over and nearby cities. The same method is applied to study the effect of urban fraction and buildings height on local temperatures. Further results of city size, urban fraction and building's height are given in appendices 4.3 to 4.9, and only summarize in the following sections.

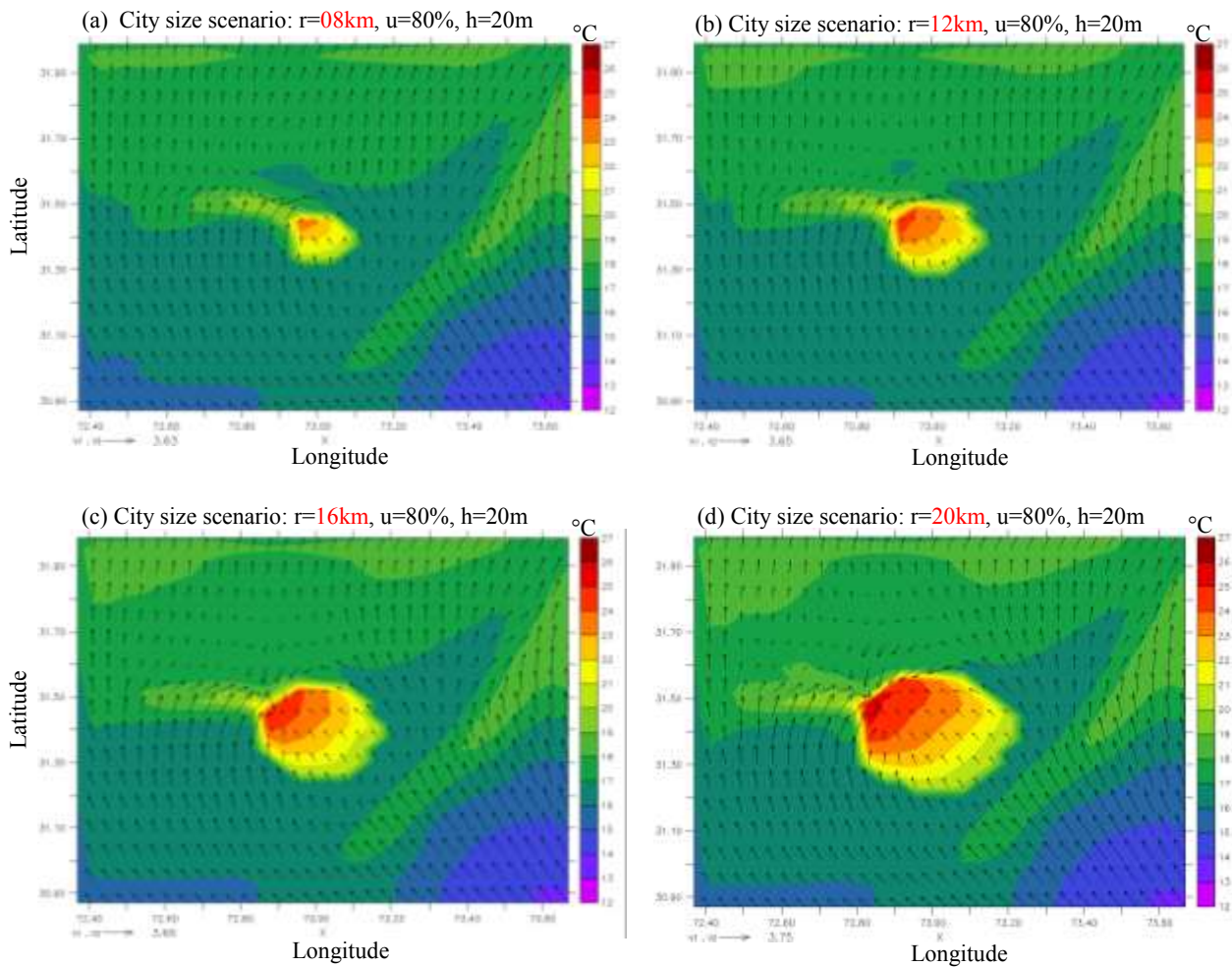


Figure 4.9: Effect of urban areas on local temperature by varying the city size r for 20.04.2005 at 09:00 GMT.

- (a) City size scenario: $r=08\text{km}$, $u=80\%$, $h=20\text{m}$
- (b) City size scenario: $r=12\text{km}$, $u=80\%$, $h=20\text{m}$
- (c) City size scenario: $r=16\text{km}$, $u=80\%$, $h=20\text{m}$
- (d) City size scenario: $r=20\text{km}$, $u=80\%$, $h=20\text{m}$

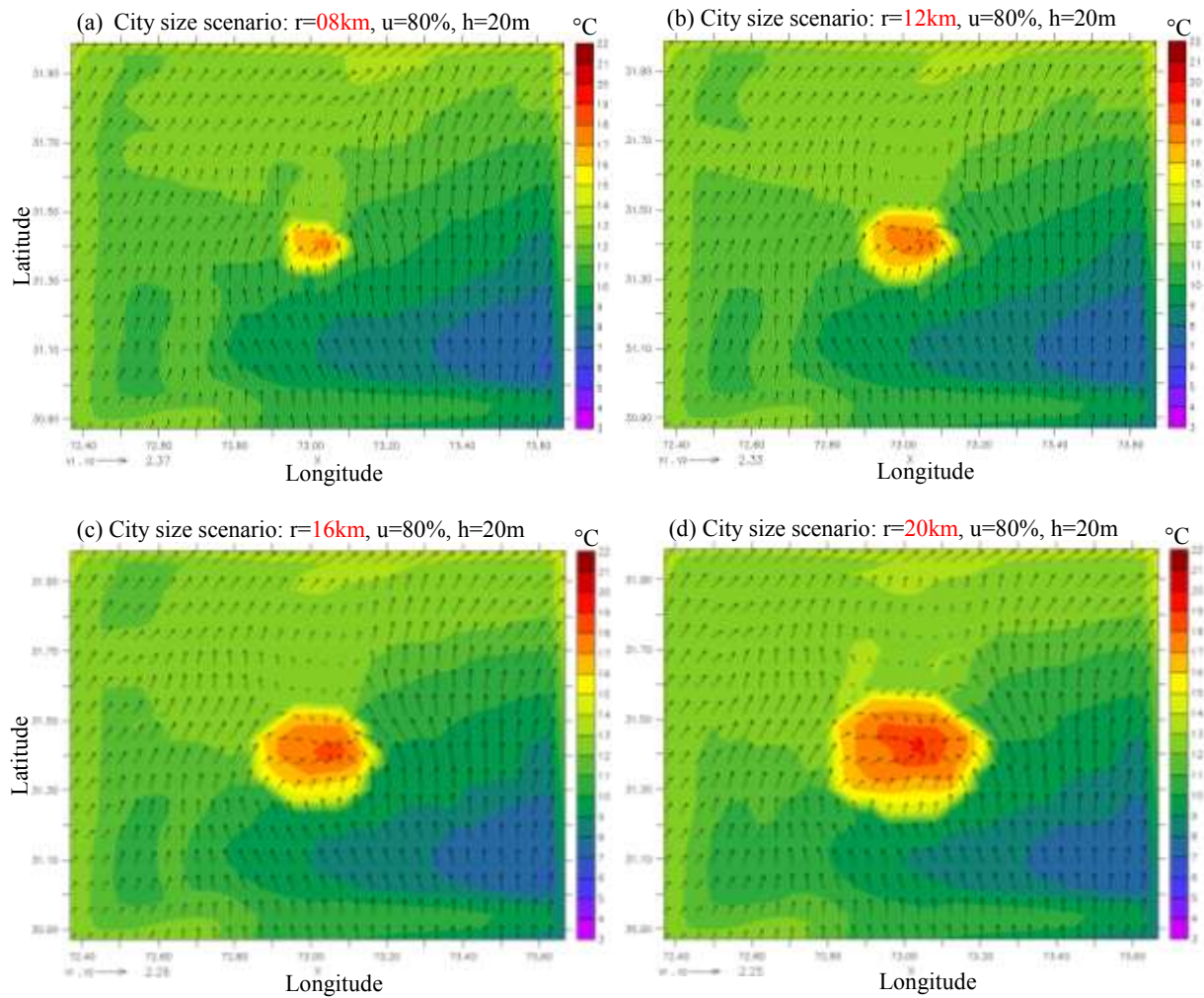


Figure 4.10: Effect of urban areas on local temperature with varying city size r for 20.04.2005 at 17:00 GMT.

- (a) City size scenario: $r=08\text{km}$, $u=80\%$, $h=20\text{m}$
- (b) City size scenario: $r=12\text{km}$, $u=80\%$, $h=20\text{m}$
- (c) City size scenario: $r=16\text{km}$, $u=80\%$, $h=20\text{m}$
- (d) City size scenario: $r=20\text{km}$, $u=80\%$, $h=20\text{m}$

Table 4.2 shows the annual average, maximum value, minimum value and percentage of the total simulations where dT_{min} is found higher than dT_{max} . All the values given in Table 4.2 are based on average of all the simulation scenarios of all the month of a year. The annual average variation in dT_{min}/du and dT_{max}/du is found 0.0201 K and 0.0328 K, respectively; the annual average variation in dT_{min}/dr and dT_{max}/dr is measured 0.1314 K and 0.1090 K, respectively; and the annual average variation in dT_{min}/dh and dT_{max}/dh is found 0.0404 K and -0.0331 K, respectively. As mentioned above that T_{min} and T_{max} increase with increasing urban fraction u and city size r . But T_{min} increases and T_{max} decreases with increasing building height in an urban area.

Further investigations elaborate that among all the simulated scenarios, in 100% cases of the simulations, T_{min} and T_{max} increase with increasing urban fraction u and increasing city size r . However, T_{min} and T_{max} do not increase consistently with increasing building's height. It is observed that with increasing building's height h , T_{min} increased in 95% of the simulation cases and only in 39% of the simulation cases, T_{max} increased.

Table 4.2: Annual averages, minimum and maximum values and % of positive values out of all the simulations for dT_{min}/du , dT_{max}/du , dT_{min}/dr , dT_{max}/dr , dT_{min}/dh and dT_{max}/dh . The values are given in K.

Annual values of all the scenarios	Annual average	Maximum value	Minimum value	% of positive values out of all the simulations
dT_{min}/du	0.0201	0.0265	0.0128	100%
dT_{max}/du	0.0328	0.0525	0.0176	100%
dT_{min}/dr	0.1314	0.1950	0.0957	100%
dT_{max}/dr	0.1090	0.1790	0.0723	100%
dT_{min}/dh	0.0404	0.0771	0.0048	95%
dT_{max}/dh	-0.0331	0.0191	-0.1151	39%

Table 4.3 elaborates the annual average, maximum value and minimum value based on average of all the monthly simulations and the percentage of simulations with positive trends for between variation in minimum and maximum temperature ($dT_{min} - dT_{max}$) for du , dr and dh . It can be seen that with increasing urban fraction T_{max} increases more than T_{min} . However, it can also be noticed that with increasing city size and building's height, T_{min} increases more than T_{max} . The last

column of the Table 4.3 shows that out of 576 simulations, in 7% cases T_{min} increased more than T_{max} when urban fraction increases, in 59% cases T_{min} increased more than T_{max} when city size increases and in 98% cases T_{min} increased more than T_{max} when number of floor increases.

Table 4.3: Net annual temperature difference between $dT_{min}/du - dT_{max}/du$; $dT_{min}/dr - dT_{max}/dr$; $dT_{min}/dh - dT_{max}/dh$ based on average of all the months. The values are given in K.

Annual values of all scenarios	Annual average	Maximum value	Minimum value	% of positive values out of all simulations
$dT_{min}/du - dT_{max}/du$	-0.0127	-0.0024	-0.0264	7%
$dT_{min}/dr - dT_{max}/dr$	0.0223	0.0636	-0.0190	59%
$dT_{min}/dh - dT_{max}/dh$	0.0737	0.1437	0.0213	98%

To summarize, by using the numerical model for simulation of different scenarios of urban fraction (u), city size (r) and building height (h), it is mainly found that:

- T_{min} and T_{max} increase when u increases
- T_{min} and T_{max} increase when r increases
- T_{min} and T_{max} increase when h increases

However, the effect of urban factors (u , r and h) on urban temperature is not homogeneous. The annual average results based on monthly simulation of all the scenarios show that:

- T_{max} increases more than the T_{min} when u increases
- T_{min} increases more than the T_{max} when r increases
- T_{min} increases more than the T_{max} when h increases

By comparing the results based on observational data with these simulations data, it can be said that:

- Urban fraction does not fully explain the objective of the study because when u increases, T_{min} and T_{max} increase but T_{max} increases more than the increase of T_{min} .
- Building's height ' h ' also does not clarify the reason because when h increases, T_{max} does not increase in all the scenarios. With increasing h , T_{max} increases only in 39% cases of all the simulations.

- City size ' r ' well explains the results found in last chapter as in this case T_{min} and T_{max} both increase when r increases and T_{min} increases more than T_{max} as it is found in urban areas trends based on observational data.

The results of the simulation scenarios of r underline and explain the reason of increasing minimum temperature more than maximum temperature in urban areas. The annual average of T_{min} and T_{max} showed that in 100% cases of city size r simulation scenarios, T_{min} and T_{max} increased that correspond to the results which are found in Chapter 3 by using the observational data.

In further explanations and investigations, it is noticed that dT_{min}/dr for all the scenarios is not always greater than dT_{max}/dr . But the variation in dT_{min}/dr and dT_{max}/dr vary from season to season. Table 4.4 explains the monthly and seasonal averages of $dT_{min}/dr - dT_{max}/dr$. It can be easily perceived from Table 4.4 that in general, comparatively in colder months (November, December, January, February, March and April) minimum temperature increases more than maximum temperature with increasing city size. Conversely, comparatively in hot months (May, June, July, August, September and October) minimum temperature does not increase more than maximum temperature with increasing city size. The seasonal variation shows that in winter, in 98% cases of the simulation scenarios of city size r , T_{min} increased more than T_{max} ; in spring, 58% of the total simulation scenarios of city size r showed higher increase in T_{min} than T_{max} ; in autumn, in 51% of the total simulation scenarios of city size r , T_{min} increased more than T_{max} ; and in summer, only 30% of the total cases of simulation scenarios of city size r showed higher increase in T_{min} than T_{max} .

Table 4.4: Monthly average, maximum and minimum value, monthly and seasonal percentage of positive dT_{min} based on all the simulation scenarios of each month. The values are given in K/km.

$dT_{min}/dr - dT_{max}/dr$							
Month	Monthly average	Max. value	Min. value	Monthly % of positive values	Seasons	Seasonal average	Seasonal % of positive values
December	0.088	0.149	0.028	100%	Winter	0.0890	98%
January	0.048	0.124	-0.001	94%			
February	0.131	0.241	0.076	100%			
March	0.016	0.045	-0.020	78%	Spring	0.0122	58%
April	0.062	0.096	-0.001	97%			
May	-0.041	-0.008	-0.118	0%			
June	-0.001	0.076	-0.046	44%	Summer	-0.0236	30%
July	-0.068	-0.019	-0.152	0%			
August	-0.002	0.043	-0.045	44%			
September	-0.005	0.020	-0.042	39%	Autumn	0.0120	51%
October	-0.014	0.030	-0.060	31%			
November	0.055	0.132	-0.078	83%			

In order to compare the modeling results with temperature changes computed in chapter 3 on real cases of urban areas, the data of city size, urban fraction and buildings height of Lahore city is used in our model (given in eq. 4.1). The data of city size of Lahore by considering it as a round city is computed from the data of urbanized land of Lahore given by Khaliq-uz-zaman and Baloch (2010). The surface covered with buildings or covering the artificial material in Lahore is computed from the data provided by Almas et al. (2005) and through personal communication with Amjad S. Almas (2010) (Table 4.5). Due to non-availability of the data about the evolution of building height by a variation of time, the model used two different approximate values for two time periods (1972-1980 and 1980-2010).

Table 4.5: Evolution of urban surface area of Lahore from 1972 to 2010 (After Khaliq-uz-zaman and Baloch, 2011).

Year	Urban area sq.km	Radius (km)		dt	dr/dt
1972	103	5.73		1972 to 1980	0.11
1980	138	6.63		1980 to 1990	0.75
1990	629	14.15		1990 to 2000	0.33
2000	961	17.49		2000 to 2010	0.74
2010	1950	24.91		1980 to 2010	0.61

Table 4.6 represents the per decade change in minimum and maximum temperature for dT/dt by using equation 4.1 for the two periods 1972 to 1980 and 1980 to 2004 obtained through annual average of all the simulation scenarios by using FVM model and the use of the data collected for Lahore. It is highly noticeable that during first and second period, the contribution of city size is the highest among all factors. Overall dT/dt increases over two periods however this increase is the highest during second period.

Table 4.6: Per decade change in minimum and maximum temperature for dT/dt (eq. 4.1) for the two periods 1972 to 1980 and 1980 to 2004 obtained through annual average of all the simulation scenarios by using FVM model.

1972-1980 (P1)	T min	T max	% of contribution in T min	% of contribution in T max
$dT/dr * dr/dt$	0.1447	0.1200	88.26%	117.87%
$dT/du * du/dt$	-0.0010	-0.0016	-0.61%	-1.61%
$dT/df * df/dt$	0.0203	-0.0166	12.36%	-16.25%
dT/dt	0.164	0.102		
1980-2004 (P2)	T min	T max	% of contribution in T min	% of contribution in T max
$dT/dr * dr/dt$	0.8022	0.6655	88.89%	114.52%
$dT/du * du/dt$	-0.0010	-0.0016	-0.11%	-0.28%
$dT/df * df/dt$	0.1013	-0.0828	11.22%	-14.24%
dT/dt	0.902	0.581		

Table 4.7: Comparison of per decade change in minimum and maximum temperature at Lahore based on observational data of Lahore city and the output of the model. Here P1 is representing first period (1972-1980) and P2 is representing for second period (1980-2004).

Lahore	Tmin	Tmax		Model FVM	Tmin	Tmax
1950-1979	0.300	-0.27		1972-1980	0.164	0.102
1980-2004	1.060	-0.15		1980-2004	0.902	0.581
P2-P1	0.760	0.12		P2-P1	0.739	0.479

Table 4.7 represents the comparison of change in minimum and maximum temperature at Lahore city based on observational data and Model output. It highlights that the increase in minimum temperature of Lahore is higher than the maximum temperature and same is found through model observations. The model output for increase in minimum temperature is highly in agreement with increase in minimum temperature at Lahore measured through observational data. However, the increase in maximum temperature simulated through FVM model is higher than the observed data measured at Lahore.

4.4 Conclusion

The results computed in Chapter 3 by using the observational data of several meteorological stations of Pakistan showed that in general, minimum and maximum temperatures are increasing however in recent decades, the minimum temperature at urban areas showed higher increase than the maximum temperature. In this context, the major objective of this part of study was to examine the impact of different urban characteristics such as city size (r), urban fraction (u) and building's height (h) on minimum temperature and maximum temperature and to know that which factor is significantly causing for higher increase in minimum temperature than the maximum temperature in urban areas.

For this purpose, in this part of study different scenarios of city sizes (4), urban fraction (4) and building's height (3) scenarios of the theoretical cities were proposed to study their relative impact on minimum and maximum temperature of urban areas. By taking into account the city size, urban fraction and building's height parameters, 48 possible combinations (4·4·3) of scenarios were designed for each month and then were run for the simulations by using Finite Volume Model (FVM), a mesoscale model (Clappier et al., 1996).

The results based on the simulation scenarios show that the temperature inside urban areas increases with increasing r , u and h (Appendix 4.3, Appendix 4.4, Appendix 4.5). However, the effect of urban factors (u , r and h) on urban temperature is not homogeneous. The results highlights that T_{max} increases more than the T_{min} when u increases; T_{min} increases more than the T_{max} when r increases and T_{min} increases more than the T_{max} when h increases. All the simulation scenarios does not explain the situation of higher increase in minimum temperature and are not fully in agreement of the results which are obtained through observational data at urban areas in chapter 3. As the simulation scenarios results show that with increasing urban fraction T_{max} increased more than the increase in T_{min} and with increasing building's height T_{max} did not increase in all the building height scenarios, these two types of scenarios (u , h) do not explain the results obtained through observational data. However, the city size well explained the results where T_{min} and T_{max} both increase when r increases and T_{min} increases more than T_{max} . This type of behaviour was found on urban areas temperature trends after 1980s through the analysis of observational data in the previous chapter. So it can be concluded that effect of city size is the most prominent fact that cause the minimum temperature to rise higher than the maximum temperature.

The results of analysis of observational data of several cities of Pakistan and the simulations output of several scenarios of theoretical cities show that the minimum and maximum temperature increase at urban areas. But the minimum temperature increases more than the maximum temperature. The results obtained through simulations by using FVM model are in agreement with the results obtained through the observational data for minimum temperature. However the change in maximum temperature obtained through FVM model is higher than the observational data of Pakistan that is to be a perspective of future work.

CHAPTER 5

CONCLUSION

5.1 Major outcome of the study

The extent and the rate of global environmental changes, whether greenhouse gas-induced warming, deforestation, desertification or loss in biodiversity are driven largely by the rapid growth of the Earth's human population. Given the large and ever-increasing fraction of the world's population living in cities, and the disproportionate share of resources used by these urban residents, especially in the global North, cities and their inhabitants are key drivers of global environmental change (Grimmond, 2007). The major part of the energy consumed in the world is produced from combustion of fossil fuels and the burning of fossil fuels in combustion reactions results in emission of number of pollutants and GHGs in the atmosphere. The increasing rate of emission of GHGs such as CO₂ into the atmosphere causes to raise the global mean surface temperature. Global mean surface temperature increased faster in recent decades. During 1906 to 2005, global mean surface temperatures had risen by 0.74°C and during 1956 to

2005, it was measured 0.13°C per decade that was almost double than the period from 1906 to 2005. Although at some extent the global climate changes influence the urban climates, these changes, however, are not only the cause to affect the local urban climate.

Currently, more than half of the world population lives in urban areas. They have major concerns about the degradation of natural environmental and human quality of life. Urban areas are the center of several anthropogenic activities. Different studies highlight that the urban warming has not introduced significant biases into estimates of recent global warming (Easterling et al., 1997; Parker, 2004; Alcoforado and Andrade, 2008) the cities indirectly have an effect to causes global warming because they are the most important source of greenhouse gases. The cities consume a great majority – between 60 to 80% – of energy production worldwide and account for a roughly equivalent share of global CO_2 emissions (OECD, 2010).

The consumption of energy in urban areas causes a higher emission of anthropogenic heat into urban atmosphere. In cities, the buildings, roads and other infrastructure absorb a part of the solar radiation during day time and become warmer. These comparatively warmer surfaces of urban areas emit infra-red radiation which can be trapped by reflection/absorption in the urban canyon. The presence of buildings and artificial surfaces in the cities also influence the wind pattern in these areas. All of these factors lead to change in the urban energy balance of urban areas. In general, these areas become warmer than the areas where there is no artificial land surface. This phenomenon is generally referred as the urban heat island (UHI). Urban heat island has the consequences for human health and thermal comfort. So, the urban areas are being affected through global changes as well as through local changes.

The presence of UHI on urban areas highlights that at urban scale, minimum temperature increases more than maximum temperature and it is recognised by several studies in different parts of the world. However, the information about the reasons of higher increase of minimum temperature than the maximum temperature at urban areas was missing.

Pakistan has about 180 million of population and ranks at number six among top ranked populous countries. Almost 39% of the total population is living in urban areas. According to an estimate, in 2050, the proportion of population living in urban areas of Pakistan will reach to 60% (UNDESA (2011). In future, this huge portion of urban population living in urban areas may be affected by global changes in general and by local changes particularly. Lack of any solid study about changing temperatures on three different types of settlements (urban, town, and rural) of

Pakistan, made this work very important first to understand the real variation in temperature over Pakistan and then the results of this study can be considered as a reference by the policy makers, town planners and government to take actions at local scales to minimize the effects of local climate changes and contribute their part in global efforts to reduce building energy consumption and global warming.

In this context, the objective of this work was to study the urban temperature trends by focusing on to understand the factors that cause of higher increase of minimum temperature compared to the maximum temperature at urban areas by using observational and modelling techniques.

In the Chapter 3 of this thesis, the daily averaged annual and seasonal minimum (T_{min}) and maximum (T_{max}) temperature have been analyzed using the data of 37 meteorological observatories of Pakistan (17 urban, 7 town and 13 rural) was collected from Pakistan Meteorological Department between 1950 and 2004. These data was first homogenized and then analyzed for two different periods, 1950-1979 (period 1) and 1980-2004 (period 2). The data analysis highlighted that during 1980–2004 T_{min} and T_{max} increased faster than the period 1950–1979 at urban areas; T_{min} increased more at urban stations than the smaller cities and rural stations; T_{max} increased more at town and rural stations than the urban stations; T_{min} decreased and T_{max} increased at rural stations and the highest growth in T_{min} and T_{max} at urban and town stations was observed in spring and at rural stations, it was observed in winter for T_{min} and in spring for T_{max} . It was also noticed that during 1980–2004 per decade growth in minimum temperature of urban areas of Pakistan was observed 0.43°C that is 0.14 °C per decade higher than the per decade increase in global minimum temperature (0.29°C/decade) during the same period. However, the increase in T_{max} at urban areas of Pakistan was measured 0.33°C that is close to the per decade increase in global T_{max} (0.285°C/decade).

The main goal of the Chapter 4 is to explain why in urban areas the increase of T_{min} is quite higher than in small cities and rural areas and quite higher than the global change in T_{min} . The Finite Volume Mesoscale Model (FVM) has been used to simulate several theoretical cities to study the effect of the city size, changing land use and the building height. The results of the model have shown that T_{min} and T_{max} increased when urban fraction u , city size r and building height h increased but T_{max} increased more than the T_{min} when u increased, T_{min} increased more than the T_{max} when r increased and T_{min} increased more than the T_{max} when h increased. These

results helped us to conclude that the city size is the major factor among building height and vegetation fraction that causes to increase the minimum temperature in urban areas more than the maximum temperature. Among all the urban characteristics discussed above, city size r alone contributes about 90% in the total increase in minimum temperature at urban areas. More we increase the city size, more we saw the higher increase in minimum temperature as compared to the resulting change in minimum temperature by changing other two factors. So we can conclude that the city size is the major cause of increase of minimum temperature at urban areas.

As more natural surface converts into artificial cover, more space is created for the absorption of a part of solar radiation. As the city size grows, the space of artificial material also grows including the paved roads and streets along with new buildings. The increasing artificial material cause more absorption of the solar radiation that latterly emits the infrared into urban atmosphere. As the emission of infrared dominates when there is no absorption of solar radiation by the material (i.e. during the night), it keep the urban atmosphere warmer. However to fully understand about the higher increase in minimum temperature in urban areas, there is still need to fully understand the mechanism of mechanical and thermal effect on local climate.

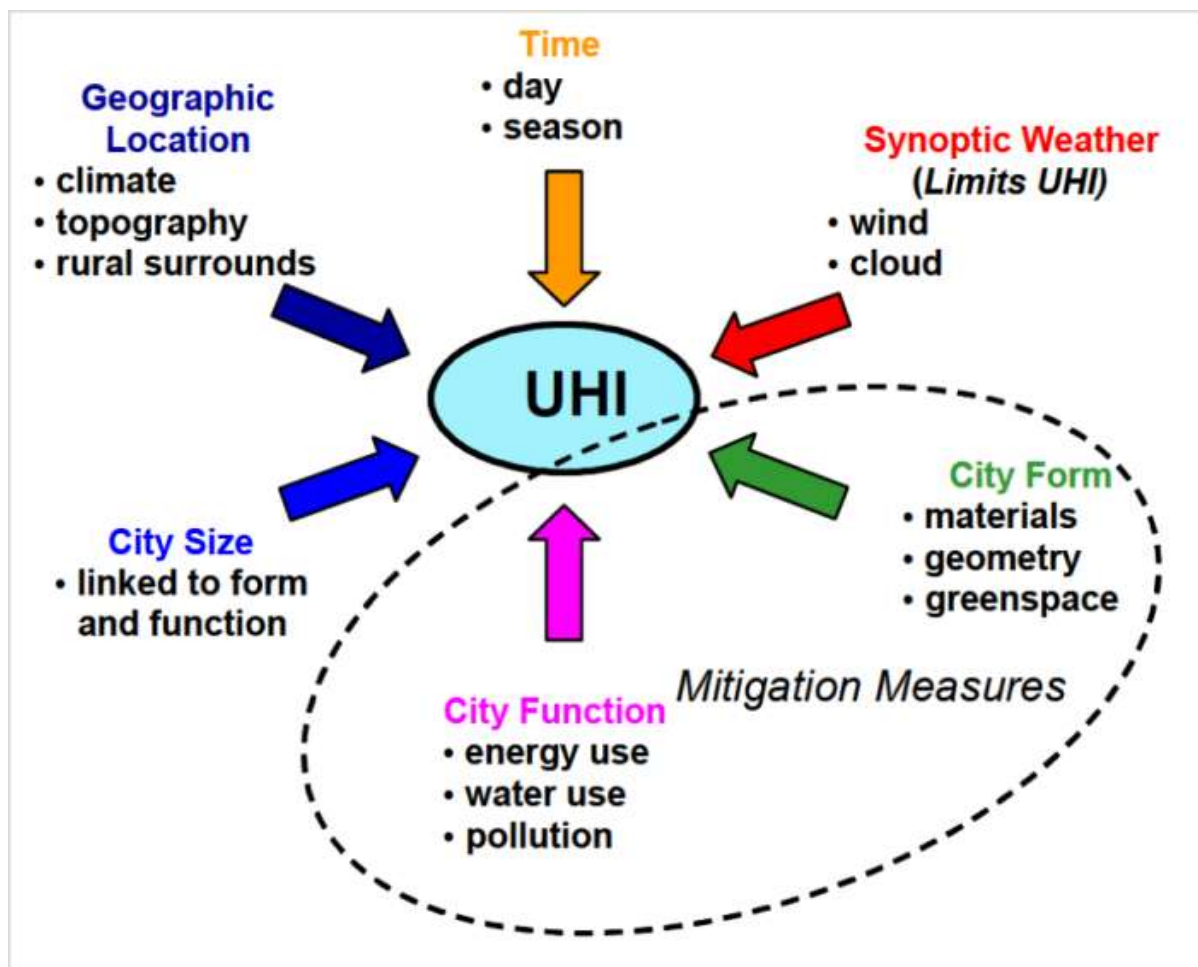
5.2 Future Perspective

- Due to hot weather conditions in Pakistan, the use of air conditioners (ACs) in buildings and vehicles is quite common. Due to lack of data about the timings of use of ACs, in this study the energy consumption and related heat emission from ACs was not considered. The relationship between the use of ACs for human comfort and variation in local urban temperature could be simulated by using models FVM and WRF on real case studies such as mega cities of Pakistan i.e., Lahore and Karachi.
- The emission of greenhouse gases particularly CO₂ into the atmosphere may contribute in urban warming. The CO₂ molecule can absorb infrared radiation and the molecule starts to vibrate. Eventually, the vibrating molecule will emit the radiation again, and it will likely be absorbed by yet another greenhouse gas molecule. This absorption-emission-absorption cycle serves to keep the heat near the surface, effectively insulating the surface from the cold of space. This factor will be studied to distinguish its effect on urban climate especially on real cities.

- Water bodies close to the urban areas play important role in normalizing the local temperatures. Many cities of Pakistan are located close to the water bodies such as Islamabad and Rawalpindi close to the largest dams (Tarbela and Mangla) and many small dams (Simli, Rawal, Khanpur dams), Karachi on coast of Arabian Sea and many cities on river banks (Lahore, Hyderabad etc.).
- The model will be used to study the interactions between urban heat island and sea-breeze circulations during different seasons over Karachi.
- A more complete network of the meteorological sensors to measure the weather parameters such as wind speed, wind direction, relative humidity and temperature in different parts of the city and its surrounding rural areas could help us to properly validate the model simulation. Moreover, the combination of model and measurement results could lead to better understand and study the presence of urban heat island phenomenon in Pakistani cities. This could help to take the decision at local level to apply the strategies to reduce the UHI negative effects.

APENDICES

Appendix 2.1:



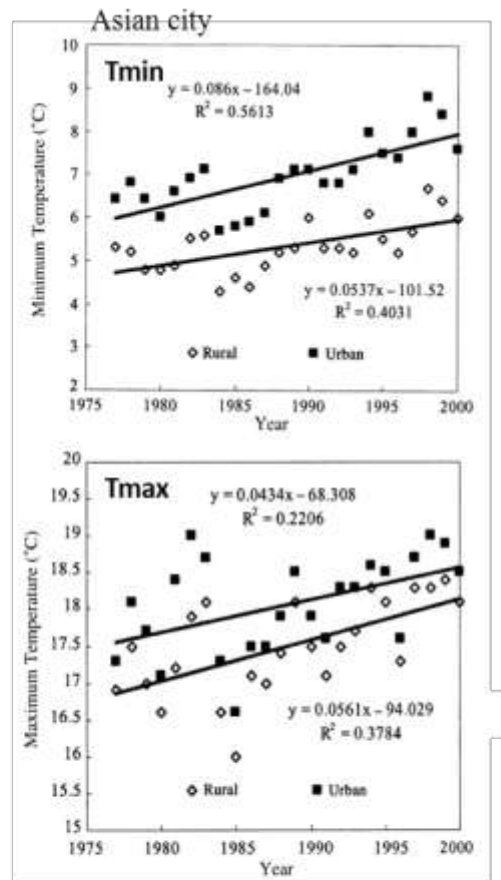
The factors affecting urban heat island (After Voogt, 2007).

Appendix 3.1:

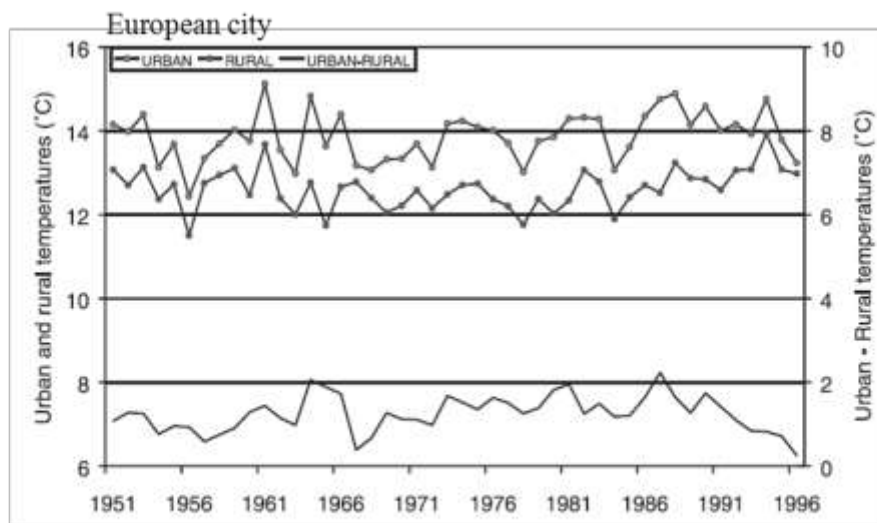
Season	Trend (°C per 100 years)			
	Maximum temp.		Minimum temp.	DTR
	<i>Global</i>			
D-J-F	1.10 (1.31)		2.48 (2.76)	-1.35 (-1.37)
M-A-M	1.25 (1.17)		2.26 (2.27)	-1.04 (-1.09)
J-J-A	0.47 (0.40*)		1.13 (1.12)	-0.65 (-0.69)
S-O-N	0.05* (-0.01*)		0.94 (0.98)	-0.89 (-0.92)
	<i>Northern Hemisphere</i>			
D-J-F	1.26 (1.52)		2.74 (3.04)	-1.44 (-1.48)
M-A-M	1.39 (1.29)		2.28 (2.30)	-0.90 (-1.01)
J-J-A	0.25* (0.25*)		1.05 (1.04)	-0.79 (-0.77)
S-O-N	-0.12* (-0.01*)		0.72* (0.83)	-0.84 (-0.90)
Annual	0.77 (0.87)		1.74 (1.84)	-0.89 (-0.89)
	<i>Southern Hemisphere</i>			
D-J-F	0.66 (0.62)		1.61 (1.66)	-1.00 (-0.93)
M-A-M	0.59* (0.55*)		1.98 (1.97)	-1.37 (-1.31)
J-J-A	1.27 (1.18)		1.41 (1.40)	-0.08* (-0.12*)
S-O-N	0.69* (0.84)		1.74 (1.69)	-1.08 (-1.02)
Annual	0.91 (0.84)		1.81 (1.80)	-0.59 (-0.60)

Annual and seasonal trends from 1950 to 1993 for maximum temperature, minimum temperature, and DTR for the globe and the Northern and Southern hemispheres. Trends calculated using only nonurban stations are given, with the trends using all stations given in parentheses (After Easterling et al., 1997).

Appendix 3.2:



Comparison between urban (Shijingshan in Beijing) and rural minimum and maximum temperatures (Miyun) in China (Liu et al., 2007).



Comparison between urban (Brera) and rural mean temperatures for Milan (Brunetti et al., 2000).

Appendix 3.3:

	Station	dTn_An	dTn_Wi	dTn_Sp	dTn_Su	dTn_Au	dTx_An	dTx_Wi	dTx_Sp	dTx_Su	dTx_Au
Urban	Gilgit	-0.074	-0.101	-0.075	-0.029	-0.110	0.021	-0.013	0.051	0.041	-0.002
	Peshawar	0.005	-0.015	0.026	0.007	-0.004	0.025	0.002	0.052	-0.014	0.049
	Muzaffarabad	-0.007	-0.011	0.006	-0.027	-0.006	0.022	-0.009	0.061	-0.003	0.033
	Kakul	-0.062	-0.079	-0.058	-0.057	-0.070	-0.035	-0.047	-0.007	-0.067	-0.029
	Islamabad	0.000	0.001	0.018	-0.018	-0.008	0.001	-0.005	0.025	-0.042	0.019
	Sargodha	-0.009	-0.042	0.013	-0.011	-0.003	0.018	0.021	0.038	-0.016	0.026
	Jhelum	0.014	0.019	0.021	-0.013	0.023	-0.002	-0.004	0.006	-0.035	0.014
	Sialkot	-0.089	-0.099	-0.095	-0.062	-0.111	-0.041	-0.039	-0.055	-0.061	-0.028
	D.I. Khan	-0.008	-0.020	-0.006	-0.017	0.004	-0.026	-0.029	0.003	-0.064	-0.029
	Faisalabad	-0.049	-0.068	-0.030	-0.051	-0.055	-0.012	-0.025	-0.004	-0.018	-0.011
	Lahore_ur	0.030	0.026	0.043	0.000	0.044	-0.027	-0.027	-0.032	-0.055	-0.002
	Lahore_ap	-0.012	-0.025	0.001	-0.030	-0.001	-0.013	-0.015	-0.021	-0.040	0.012
	Quetta	0.044	0.000	0.039	0.084	0.044	0.015	-0.035	0.036	0.029	0.018
	Multan	-0.001	-0.014	0.008	-0.018	0.005	-0.005	-0.001	0.016	-0.038	-0.006
	Bahawalpur	-0.012	-0.037	-0.005	-0.023	0.000	-0.013	-0.019	-0.016	-0.019	-0.010
	Hyderabad	0.037	0.045	0.044	0.014	0.041	-0.006	-0.028	-0.011	-0.002	0.008
Karachi_ap	0.006	-0.003	-0.001	-0.006	0.026	-0.001	-0.005	-0.012	-0.006	0.013	
Average	-0.011	-0.025	-0.003	-0.015	-0.011	-0.005	-0.016	0.008	-0.024	0.004	
Town	Station	Tn_An	Tn_Wi	Tn_Sp	Tn_Su	Tn_Au	Tx_An	Tx_Wi	Tx_Sp	Tx_Su	Tx_Au
	Risalpur	0.000	0.002	0.009	-0.012	-0.006	-0.023	-0.046	0.002	-0.058	-0.003
	Kohat	-0.012	-0.032	-0.003	-0.013	-0.010	-0.024	-0.042	0.013	-0.058	-0.018
	Jacobabad	0.009	-0.005	0.015	-0.004	0.022	-0.028	-0.032	-0.009	-0.033	-0.040
	Nawabshah	-0.006	-0.027	0.004	-0.006	-0.007	0.000	-0.011	0.000	-0.005	0.009
	Badin	0.001	-0.033	0.003	0.004	0.016	-0.061	-0.094	-0.069	-0.033	-0.058
	Panjgur	0.080	0.028	0.126	0.094	0.067	0.018	-0.019	0.037	0.028	0.015
	Sibbi	0.010	-0.019	0.017	0.003	0.032	-0.008	-0.028	0.001	-0.003	-0.018
	Average	0.012	-0.012	0.024	0.009	0.016	-0.018	-0.039	-0.004	-0.023	-0.016
Rural	Station	Tn_An	Tn_Wi	Tn_Sp	Tn_Su	Tn_Au	Tx_An	Tx_Wi	Tx_Sp	Tx_Su	Tx_Au
	Gupis	0.014	0.016	0.024	0.023	-0.014	0.026	0.015	0.038	0.036	0.008
	Skardu	0.022	0.032	0.028	0.030	-0.006	0.018	0.020	0.039	0.018	-0.008
	Bunji	-0.008	-0.004	0.020	-0.003	-0.048	-0.005	-0.027	0.046	-0.005	-0.045
	Chilas	0.037	0.014	0.053	0.047	0.027	0.025	-0.004	0.044	0.026	0.021
	Astore	0.035	0.026	0.030	0.058	0.019	0.010	0.006	0.026	0.020	-0.022
	Cherat	-0.007	-0.016	0.008	-0.029	0.004	-0.054	-0.063	0.012	-0.088	-0.088
	Chhor	0.004	-0.017	0.003	-0.002	0.022	-0.002	-0.008	-0.012	-0.006	0.010
	Kalat	0.049	-0.023	0.065	0.087	0.054	0.002	-0.020	0.008	0.006	0.007
	Dalbandin	0.025	-0.054	0.038	0.052	0.044	0.009	-0.030	0.022	0.019	0.014
	Lasbella	-0.007	-0.032	0.010	-0.005	-0.010	-0.012	-0.031	-0.015	-0.023	0.003
	Padidan	0.016	0.004	0.012	0.019	0.016	0.003	-0.011	0.006	-0.002	0.012
	Jiwani	0.010	0.004	0.012	0.018	-0.001	-0.002	-0.015	-0.001	0.000	0.003
	Pasni	0.014	-0.036	0.014	0.032	0.039	0.010	0.008	0.007	0.007	0.021
Rural_mean	0.016	-0.007	0.024	0.025	0.011	0.002	-0.012	0.017	0.001	-0.005	

Annual and seasonal per year trends ($^{\circ}\text{C}$) of T_{min} and T_{max} at urban, town and rural stations from 1950 – 1979.

Appendix 3.4:

Station	dTn_An	dTn_Wi	dTn_Sp	dTn_Su	dTn_Au	dTx_An	dTx_Wi	dTx_Sp	dTx_Su	dTx_Au
Gilgit	-0.038	-0.019	-0.023	-0.069	-0.050	0.076	0.113	0.080	0.025	0.083
Peshawar	0.060	0.046	0.087	0.039	0.060	0.015	0.008	0.105	-0.023	-0.036
Muzaffarabad	0.029	0.003	0.050	0.030	0.025	0.100	0.129	0.144	0.040	0.094
Kakul	0.024	0.021	0.050	0.016	0.001	0.079	0.099	0.135	0.040	0.041
Islamabad	0.068	0.039	0.100	0.055	0.075	0.031	0.039	0.112	0.000	-0.026
Sargodha	0.029	0.018	0.035	0.033	0.025	0.011	-0.010	0.067	-0.007	-0.013
Jhelum	0.053	0.031	0.082	0.045	0.047	0.037	0.019	0.124	0.006	-0.004
Sialkot	0.040	0.017	0.056	0.019	0.058	0.022	0.013	0.090	-0.016	0.000
D.I. Khan	0.040	0.058	0.051	0.001	0.049	0.024	0.007	0.110	-0.019	-0.001
Faisalabad	0.061	0.050	0.069	0.038	0.085	0.037	0.000	0.120	0.009	0.014
Lahore_ur	0.106	0.105	0.138	0.062	0.114	-0.015	-0.041	0.074	-0.059	-0.037
Lahore_ap	0.048	0.032	0.090	0.027	0.038	0.019	-0.005	0.099	-0.030	0.008
Quetta	0.085	0.083	0.089	0.092	0.076	0.070	0.104	0.113	0.026	0.037
Multan	0.041	0.045	0.063	0.015	0.032	0.004	-0.015	0.089	-0.036	-0.022
Bahawalpur	0.014	0.015	0.023	-0.022	0.023	0.052	0.044	0.118	0.004	0.038
Hyderabad	0.000	0.010	-0.001	-0.016	-0.001	-0.021	-0.004	0.010	-0.033	-0.054
Karachi_ap	0.066	0.116	0.057	0.011	0.069	0.032	0.053	0.057	0.001	0.017
Urban_mean	0.043	0.039	0.060	0.022	0.043	0.034	0.032	0.097	-0.004	0.008
Station	Tn_An	Tn_Wi	Tn_Sp	Tn_Su	Tn_Au	Tx_An	Tx_Wi	Tx_Sp	Tx_Su	Tx_Au
Risalpur	0.021	-0.011	0.043	0.015	0.032	0.019	0.022	0.107	-0.020	-0.037
Kohat	-0.005	-0.022	0.035	-0.016	-0.023	0.094	0.083	0.151	0.067	0.072
Jacobabad	0.032	0.024	0.041	0.024	0.031	0.036	0.052	0.094	-0.016	0.012
Nawabshah	0.025	0.031	0.030	-0.003	0.033	0.054	0.047	0.079	0.036	0.054
Badin	0.022	0.053	0.016	-0.006	0.016	0.037	0.051	0.041	0.027	0.030
Panigur	0.045	0.032	0.054	0.028	0.065	0.057	0.100	0.084	0.015	0.031
Sibbi	0.046	0.059	0.069	0.025	0.026	0.045	0.092	0.094	-0.025	0.018
Town_mean	0.027	0.024	0.041	0.010	0.026	0.049	0.064	0.093	0.012	0.026
Station	Tn_An	Tn_Wi	Tn_Sp	Tn_Su	Tn_Au	Tx_An	Tx_Wi	Tx_Sp	Tx_Su	Tx_Au
Gupis	-0.042	-0.022	-0.043	-0.079	-0.034	0.047	0.087	0.049	-0.006	0.056
Skardu	0.009	0.035	0.004	0.008	-0.020	0.056	0.082	0.068	0.011	0.059
Bunji	0.022	0.062	0.048	-0.026	-0.004	0.013	0.063	0.032	-0.061	0.016
Chilas	0.025	0.061	0.017	-0.014	0.027	-0.002	0.006	0.000	-0.019	-0.005
Astore	0.038	0.079	0.028	0.003	0.028	0.041	0.064	0.048	-0.001	0.048
Cherat	-0.080	-0.010	-0.050	-0.164	-0.090	0.011	0.003	0.063	0.011	-0.036
Chhor	0.002	0.016	0.009	-0.030	0.000	0.046	0.055	0.069	0.033	0.026
Kalat	0.043	0.045	0.053	0.020	0.046	0.047	0.031	0.080	0.017	0.058
Dalbandin	-0.001	-0.006	-0.005	-0.023	0.021	0.071	0.104	0.112	0.015	0.056
Lasbella	-0.017	-0.024	-0.015	-0.047	0.011	0.029	0.052	0.052	-0.001	0.010
Padidan	0.014	0.011	0.009	-0.008	0.033	-0.007	0.033	0.042	-0.054	-0.047
Jiwani	-0.083	-0.069	-0.088	-0.118	-0.066	0.020	0.052	0.037	-0.013	0.006
Pasni	0.009	0.011	-0.022	-0.002	0.043	0.024	0.050	0.034	-0.008	0.027
Rural_mean	-0.005	0.015	-0.004	-0.037	0.000	0.030	0.052	0.053	-0.006	0.021

Annual and seasonal per year trends ($^{\circ}\text{C}$) of T_{min} and T_{max} at urban, town and rural stations from 1980 – 2004.

Appendix 4.1:

No.	City	Country	Population	Area*	Density/dam*	Region
1	Dhaka	Bangladesh	12797000	324	39496.91	Asia
2	Mumbai	India	21200000	777	27284.43	Asia
3	Faisalabad	Pakistan	5081000	207	24545.89	Asia
4	Karachi	Pakistan	18000000	881	20431.33	Asia
5	Kolkata	India	15420000	803	19202.99	Asia
6	Tehran	Iran	13450000	777	17310.17	Asia
7	Lahore	Pakistan	10000000	583	17152.66	Asia
8	Yangon	Myanmar	5500000	350	15714.29	Asia
9	Kabul	Afghanistan	4000000	259	15444.02	Asia
10	Chittagong	Bangladesh	2579107	168	15351.83	Asia
11	Mashhad	Iran	3000000	207	14492.75	Asia
12	Izmir	Turkey	3796000	272	13955.88	Asia
13	Seoul	South Korea	24472000	2163	11313.92	Asia
14	Baghdad	Iraq	6500000	596	10906.04	Asia
15	Delhi	India	16713000	1567	10665.60	Asia
16	Manila	Philippines	13503000	1425	9475.79	Asia
17	Tianjin	China	11750000	1295	9073.36	Asia
18	Istanbul	Turkey	12600000	1399	9006.43	Asia
19	Bangalore	India	6562000	738	8891.60	Asia
20	Ho Chi Minh	Vietnam	7396446	842	8784.38	Asia
21	Jakarta	Indonesia	24100000	2784	8656.61	Asia
22	Tokyo	Japan	32542946	3925	8291.20	Asia
23	London	United Kingdom	12200000	1623	7516.94	Europe
24	Ankara	Turkey	4000000	583	6861.06	Asia
25	Shanghai	China	19200000	2914	6588.88	Asia
26	Madrid	Spain	5300000	945	5608.47	Europe
27	Osaka	Japan	17590000	3212	5476.34	Asia
28	Bangkok	Thailand	11970000	2202	5435.97	Asia
29	Beijing	China	17550000	3302	5314.96	Asia
30	Barcelona	Spain	4210000	803	5242.84	Europe
31	Athens	Greece	3074160	684	4494.39	Europe
32	Munich	Germany	1353186	311	4351.08	Europe
33	Zurich	Switzerland	372047	88	4227.81	Europe
34	Manchester	UK	2240000	558	4014.34	Europe
35	Berlin	Germany	3490445	892	3913.05	Europe
36	Paris	France	11769000	3043	3867.56	Europe
37	Vienna	Austria	1714142	453	3783.98	Europe
38	Stockholm	Sweden	1372565	382	3593.10	Europe
39	Amsterdam	Netherlands	780152	219	3562.34	Europe
40	St Petersburg	Russia	4879566	1439	3390.94	Europe
41	Kiyev	Ukraine	2797553	839	3334.39	Europe
42	Warsaw	Poland	1716855	517	3320.80	Europe
43	Moscow	Russia	14800000	4533	3264.95	Europe
44	Glasgow	Scotland	1199629	368	3259.86	Europe
45	Lisbon	Portugal	2815851	958	2939.30	Europe
46	Los Angeles	USA	14940000	5812	2570.54	N. America
47	Prague	Czech Republic	1262106	496	2544.57	Europe
48	Lódź	Poland	742387	293	2533.74	Europe
49	Dublin	Ireland	1045769	453	2308.54	Europe
50	Toronto	Canada	5100000	2279	2237.82	N. America
51	Copenhagen	Denmark	1199224	549	2184.38	Europe
52	Rome	Italy	2761477	1285	2149.01	Europe
53	Oslo	Norway	611491	285	2145.58	Europe
54	Phoenix	USA	4192887	2069	2026.53	N. America
55	Montréal	Canada	3316615	1677	1977.71	N. America
56	Budapest	Hungary	1733685	894	1939.24	Europe
57	New York City	USA	20090000	11264	1783.56	N. America
58	Ottawa	Canada	883391	512	1725.37	N. America
59	Houston	USA	5946800	3463	1717.24	N. America
60	Chicago	USA	8711000	5498	1584.39	N. America
61	Lyon	France	1422331	954	1490.91	Europe
62	Brussels	Belgium	1089538	751	1450.78	Europe
63	San Antonio	USA	1327407	1056	1257.01	N. America
64	Marseille	France	1420000	1204	1179.40	Europe
65	Philadelphia	USA	5325000	4661	1142.46	N. America
66	Pyongyang	North Korea	3255388	3194	1019.22	Asia
67	Vancouver	Canada	2313328	2700	856.79	N. America

*Represents the data source of *Demographia World Urban Areas: 7th Annual Edition (2011.04)* except italic numbers. The italic numbers represent the data sources of Wikipedia for individual cities.

Population density of the largest cities selected from Asia, Europe and North America in 2010-2011. Source: City Mayors Statistics 2011.

Appendix 4.2:

The mesoscale model governing equations (Martilli et al., 2002; Mauree, 2011).

1. Conservation of Mass

This principle states that mass can neither be created nor destroyed, that is the total mass of air will remain constant in an enclosed volume (this being true if there is no chemical or physical processes that affect the air inside that volume).

Equation 4.2 represents this principle, written in partial differential equations,

$$\frac{\partial \rho}{\partial t} + \frac{\partial \rho U_i}{\partial x_i} = 0 \quad (4.2)$$

I II

where ' ρ ' is the air density (kg.m^{-3}), and ' U_i ' the wind velocity for each of the three directions in space ($i=1,2,3$). The term I represents the mass storage and the term II represents the mean transport.

2. Conservation of Momentum

This principle asserts that the variation of momentum in time is equal to the sum of external forces. It is derived from Newton's Second Law of Motion and states that the acceleration of a body due to a force is proportional to the force, inversely proportional to its mass and in the direction of the force. Equation 4.3 takes into account this principle and is written as follows:

$$\frac{\partial \rho U_i}{\partial t} = - \frac{\partial \rho U_i U_j}{\partial x_j} - \frac{\partial \overline{\rho u_i u_j}}{\partial x_j} - \frac{\partial P}{\partial x_i} - \rho g \delta_{i3} - 2 \varepsilon_{ijk} \Omega_j U_k + D_{ui} \quad (4.3)$$

I II III V V VI VII

where ' P ' is the air pressure, ' g ' the acceleration due to gravity and ' Ω_j ' the rotational angular velocity of the Earth.

Term I is the storage of momentum, term II is the mean transport and term III is the turbulent transport and term V is the pressure-gradient force. The term V represents the action of gravity

while the term II relates to the Coriolis force (due to the rotation of the Earth). The term III corresponds to the forces due to the interactions between the Earth surface and the airflow.

FVM being at present a non-hydrostatic mesoscale model assumes that the air pressure (P) and density (ρ) can be expressed as follows:

$$P = P_0 + P'; P' \ll P_0 \quad (4.4)$$

$$\rho = \rho_0 + \rho'; \rho' \ll \rho_0 \quad (4.5)$$

where ' P_0 ' and ' ρ_0 ' are the air pressure and density at hydrostatic equilibrium and ' P' ' and ' ρ' ' are the related perturbations.

For a hydrostatic reference state, equations 4.6 and 4.7 can be used:

$$\frac{\partial P_0}{\partial x_3} = -\rho_0 g \quad (4.6)$$

$$\frac{\partial P_0}{\partial x_i} = -2\Omega_{ijk} U_k^G \quad i = 1, 2 \quad (4.7)$$

where ' U_k^G ' represents the geostrophic wind.

The pressure gradient term (I) in equation 4.3 can be expressed as follows when taking into account the hydrostatic balance equations (4.6 and 4.7)

$$-\frac{\partial P}{\partial x_3} = -\frac{\partial P_0}{\partial x_3} - \frac{\partial P'}{\partial x_3} = \rho_0 g - \frac{\partial P'}{\partial x_3} \quad (4.8)$$

$$-\frac{\partial P}{\partial x_i} = -\frac{\partial P_0}{\partial x_i} - \frac{\partial P'}{\partial x_i} = 2\Omega_{ijk} U_k^G - \frac{\partial P'}{\partial x_i} \quad i = 1, 2 \quad (4.9)$$

Equation 4.8 and 4.9 can then be substituted in equation 4.3 to give:

$$\frac{\partial \rho U_i}{\partial t} = \underbrace{-\frac{\partial \rho U_i U_j}{\partial x_i}}_I - \underbrace{\frac{\partial \overline{\rho u_i u_j}}{\partial x_j}}_{III} - \underbrace{\frac{\partial P'}{\partial x_i}}_{IV} - \underbrace{\rho g \delta_{i3}}_V - \underbrace{2\varepsilon_{ijk} \Omega_j (U_k - U_k^G)}_{VI} + \underbrace{D_{ui}}_{VII} \quad (4.10)$$

The term ' $\rho'g$ ' represents the buoyancy. Taking into account the equation of state and that of the potential temperature:

$$\Theta = T \left(\frac{P_{z=0}}{P} \right)^{\frac{R}{C_p}} \quad (4.11)$$

we can then write the buoyancy term in the following form:

$$\rho' g = \rho_0 \left(\frac{\Theta'}{\Theta_0} \right) g \quad (4.12)$$

where ' Θ_0 ' is the temperature for the reference hydrostatic state and ' Θ' ' represents the difference of temperature ($\Theta' = \Theta - \Theta_0$).

The momentum conservation partial differential equation can finally be written as follows from equation 4.10 and 4.12:

$$\begin{array}{ccccccc} \frac{\partial \rho U_i}{\partial t} & = & - \frac{\partial \rho U_i U_j}{\partial x_i} & - \frac{\partial \overline{\rho u_i u_j}}{\partial x_j} & - \frac{\partial P'}{\partial x_i} & - \rho \frac{\Theta'}{\Theta_0} \delta_{i3} & - 2\varepsilon_{ijk} \Omega_j (U_k - U_k^G) + D_{ui} \end{array} \quad (4.13)$$

I II III IV V VI VII

A simplified form of this equation can be expressed as:

$$\frac{\partial \rho U_i}{\partial t} = - \frac{\partial P'}{\partial x_i} + F_i \quad (4.14)$$

Where

$$F_i = - \frac{\partial \rho U_i U_j}{\partial x_i} - \frac{\partial \overline{\rho u_i u_j}}{\partial x_j} - \rho \frac{\Theta'}{\Theta_0} \delta_{i3} - 2\varepsilon_{ijk} \Omega_j (U_k - U_k^G) + D_{ui} \quad (4.15)$$

3. Conservation of Energy

The conservation of energy equation (4.16), which is derived from the first law of thermodynamics and states that energy per unit mass transferred from an air parcel to its environment (δQ) is equal to the change in internal energy (dU) of the parcel and the work done (δW) by or on the parcel.

$$\delta Q = dU + \delta W \quad (4.16)$$

Since the entropy (S) can be defined as follows:

$$dS = \frac{\delta Q}{T} \quad (4.17)$$

$$dS = \frac{1}{T}(dU + \delta W) \quad (4.18)$$

where T (Kelvin) is the air temperature, we can write, based on the definition of the potential temperature:

$$dS = C_p \frac{d\Theta}{\Theta} \quad (4.19)$$

When taking equations 4.18 and 4.19, we can transform the energy conservation equation to an equation that shows the temporal evolution of potential temperature. The following form of the conservation of energy equation is used in FVM:

$$\underbrace{\frac{\partial \rho \Theta}{\partial t}}_I = - \underbrace{\frac{\partial \rho \Theta U_i}{\partial x_i}}_{II} - \underbrace{\frac{\partial \overline{\rho u_j \Theta}}{\partial x_j}}_{III} - \underbrace{\frac{1}{C_p} \left(\frac{P^0}{P} \right)^{\frac{R}{C_p}} \frac{\partial R_{lw}}{\partial z}}_{IV} + \underbrace{D_{\Theta}}_V \quad (4.20)$$

where ' R ' is the gas constant, ' R_{lw} ' is the longwave radiation flux and ' P^0 ' is the reference pressure at 1000 (mbar), i.e. at ground level. The term I is the storage of heat (potential temperature), the term II is the mean transport while the term III is the turbulent transport. The term IV represents the loss from the surface by long wave radiations and lastly the term V represents the influence of sensible heat fluxes from solid surfaces.

Note that the evolution of temperature will impact the atmospheric stability, pressure, density and turbulence among other parameters.

4. Conservation of Humidity

The law of conservation of humidity represents the variation of moisture in the air and is given by the following equation:

$$\underbrace{\frac{\partial \rho H}{\partial t}}_I = - \underbrace{\frac{\partial \rho H U_i}{\partial x_i}}_{II} - \underbrace{\frac{\partial \overline{\rho u_j h}}{\partial x_j}}_{III} + \underbrace{D_h}_{IV} \quad (4.21)$$

where ' H ' is the absolute humidity. The term I represents the humidity stored by a given air parcel over a period of time, the term II represents the mean transport of moisture while the term

$///$ represents the turbulent transport of moisture. Finally the term IV gives the impact of latent heat fluxes from solid surfaces.

5. Equation of State

From the above equations (4.2, 4.14, 4.20 and 4.21) we can see that we have a set of 6 partial differential equations but have 7 meteorological unknown variables (ρ , U_i ($i=1, 2, 3$), P' , θ , H) and three turbulent fluxes (term $///$ in equation 4.14, 4.20 and 4.21).

The equation of state is thus used to link the air pressure to other meteorological variables, in order to close the above system.

$$P = \rho RT \quad (4.22)$$

where T is the temperature in Kelvin.

Using the equation of the speed of sound in the air ($c = \sqrt{RT}$), the equation of state becomes:

$$P = \rho c^2 \quad (4.23)$$

6. Equation for Pressure

The equation for the conservation of mass and momentum and the equation of state are used to solve implicitly the pressure perturbation using a partial differential equation.

First, equation 4.2 is derived with respect to time (dt):

$$\frac{\partial}{\partial t} \left(\frac{\partial p}{\partial t} \right) + \frac{\partial}{\partial x_i} \left(\frac{\partial \rho U_i}{\partial t} \right) = 0 \quad (4.24)$$

Substituting in equation 4.14:

$$\frac{\partial}{\partial t} \left(\frac{\partial p}{\partial t} \right) - \frac{\partial}{\partial x_i} \left(\frac{\partial P'}{\partial x_i} \right) = - \frac{\partial F_i}{\partial x_i} \quad (4.25)$$

Deriving the equation of state (4.23):

$$\frac{\partial P}{\partial t} = c^2 \frac{\partial \rho}{\partial t} \quad (4.26)$$

Replacing equation 4.26 in 4.25, the following relation more commonly known as the acoustic equation is obtained:

$$\frac{\partial^2}{\partial t^2} \left(\frac{P}{c^2} \right) - \frac{\partial^2 P'}{\partial x_i^2} = \frac{\partial F_i}{\partial x_i} \quad (4.27)$$

I II III

If barotropic atmospheric conditions are assumed, the speed of sound is constant and the pressure is considered to depend only on the density. Equation 4.27 becomes:

$$\frac{1}{c^2} \frac{\partial^2 P}{\partial t^2} - \frac{\partial^2 P'}{\partial x_i^2} = - \frac{\partial F_i}{\partial x_i} \quad (4.28)$$

If inelastic atmospheric conditions are assumed, the term *I* can be neglected since it can be assumed that c^2 is much greater than P . Equation 4.28 then becomes the following Poisson's equation:

$$\frac{\partial^2 P'}{\partial x_i^2} = \frac{\partial F_i}{\partial x_i} \quad (4.29)$$

7. Turbulent Transport

The resolution of the transport of turbulence is not possible due to the higher number of unknowns as compared to the number of available equations. This is more commonly known as the closure problem (Stull, 1988).

So as to solve this issue, different approaches have been described. The one that is used in FVM is called the K-theory or gradient-transport theory. This method parameterizes the vertical turbulent transport, so that approximated values are used instead of calculated ones. For a given meteorological variable 'N', a diffusion coefficient, ' K_j ' changes according to the following equations:

$$\overline{u_j n} = -K_j \frac{dN}{dx_j}; j = 1, 2, 3 \quad (4.30)$$

This diffusion coefficient is calculated with a prognostic equation for the turbulent kinetic energy (T.K.E, 'E'):

$$\frac{\partial \rho E}{\partial t} = \underbrace{-\frac{\partial \rho E U_i}{\partial x_i}}_I - \underbrace{\frac{\partial \rho \overline{u_j e}}{\partial x_j}}_{III} + \underbrace{\rho K_z \left[\left(\frac{\partial U_1}{\partial x_3} \right)^2 + \left(\frac{\partial U_2}{\partial x_3} \right)^2 \right]}_{IV} - \underbrace{\frac{g}{\Theta_0} \rho K_z \frac{\partial \Theta}{\partial x_3}}_V - \underbrace{\rho C_\varepsilon \frac{E^2}{l_\varepsilon}}_{VI} + \underbrace{D_E}_{VII} \quad (4.31)$$

The diffusion coefficients, 'K_j', can then be calculated for a value of T.K.E with:

$$K_j = C_j l_j \sqrt{E}; j = 1, 2, 3 \quad (4.32)$$

where 'C_ε' and 'C_j' are numerical constants and 'l_ε' and 'l_j' are characteristics length scales. Term I is the storage of T.K.E, term II and III are the mean and turbulent transport of the T.K.E. Term IV and V characterize the buoyant and shear production of T.K.E and term VI represents the dissipation of the T.K.E. Finally the impact of solid surfaces on the T.K.E is given by the term VII.

Bougeault and Lacarrère (1989) described the k-l closure technique that is used to compute the parameters 'C_k' and 'l_k' for the vertical direction. The vertical distance that an air parcel can travel before the buoyancy term is the driving force, is referred to 'l_k' here. Martilli et al., (2002) further illustrate how the model parameters ('C_k', 'C_ε') are calculated.

When high horizontal resolution are considered (such as here for better representation of urban scale), it is important to take into account horizontal diffusion and in such cases the characteristic length scales are of the order of the horizontal resolution of the grid.

8. Generalized FVM equation

The mesh of the mesoscale meteorological model is divided into cells. Each of the equations, corresponding to the different meteorological variables are integrated over a finite volume. From the previous section, the different equations for each of the meteorological variables (humidity, velocity, temperature...) can be generalized to give the following equation:

$$\Phi \frac{\partial \rho N}{\partial t} + \vec{\nabla} \phi (\vec{u}, \rho N) = \vec{\nabla} (\phi \lambda_t \vec{\nabla} N) + \Phi S_a + \Phi S_s \quad (4.33)$$

/
//
///
///

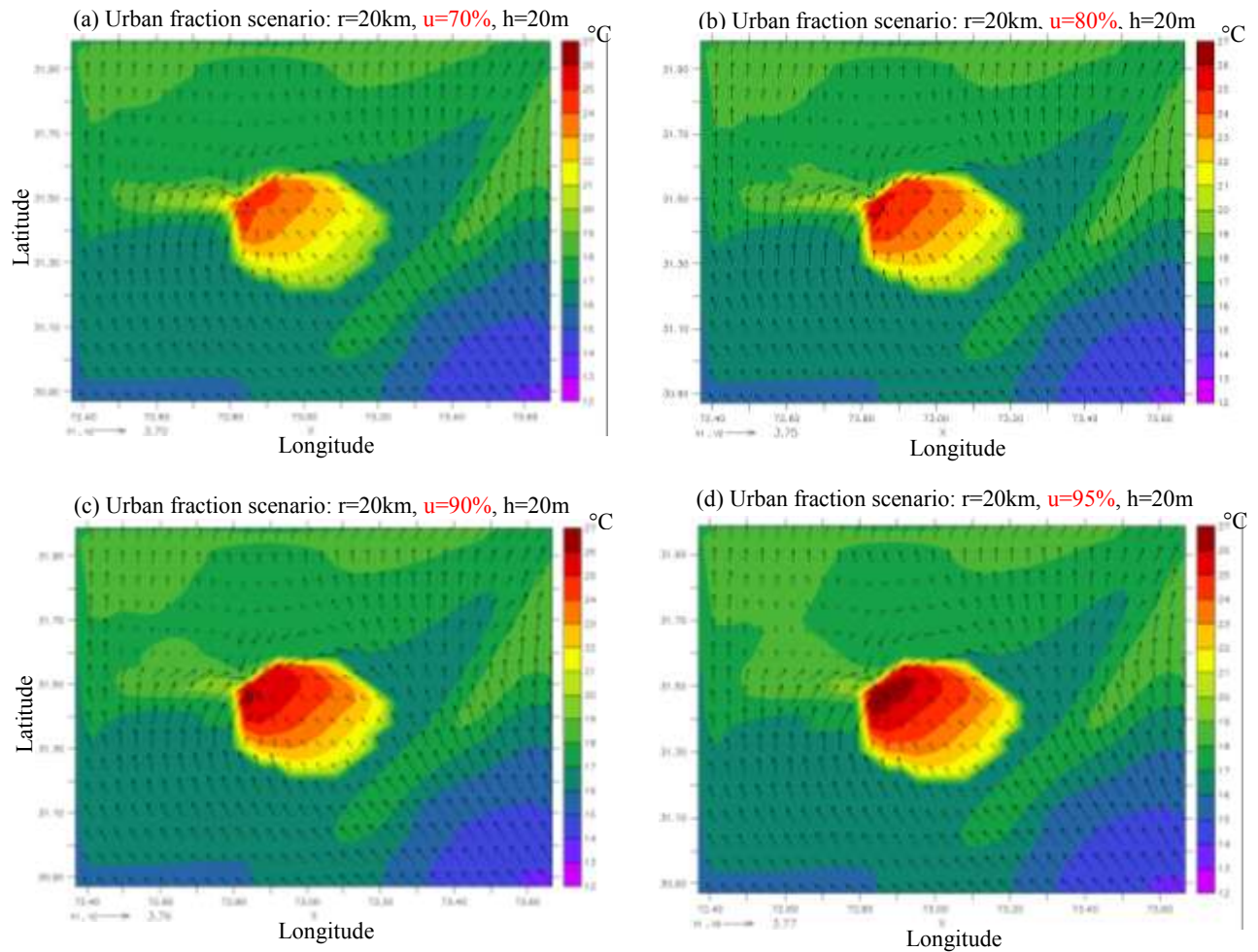
where N can be either the velocity (\vec{u}) or the temperature (θ) or 'r' a mixing ratio (humidity or pollutants)

ϕ is the surface porosity, which is the ratio of free surface in each directions divided by the surface of the cell in that same direction

Φ is the volume porosity, which is the ratio of free volume in each cell divided by the volume of the cell.

The term / represent the storage term for N, the term // represents the Advection, term /// the diffusion and term /// the source from the atmosphere (S_a) and from the surface (S_s). The source terms are computed at the cell volume while the advection and diffusion term are treated at the cell face.

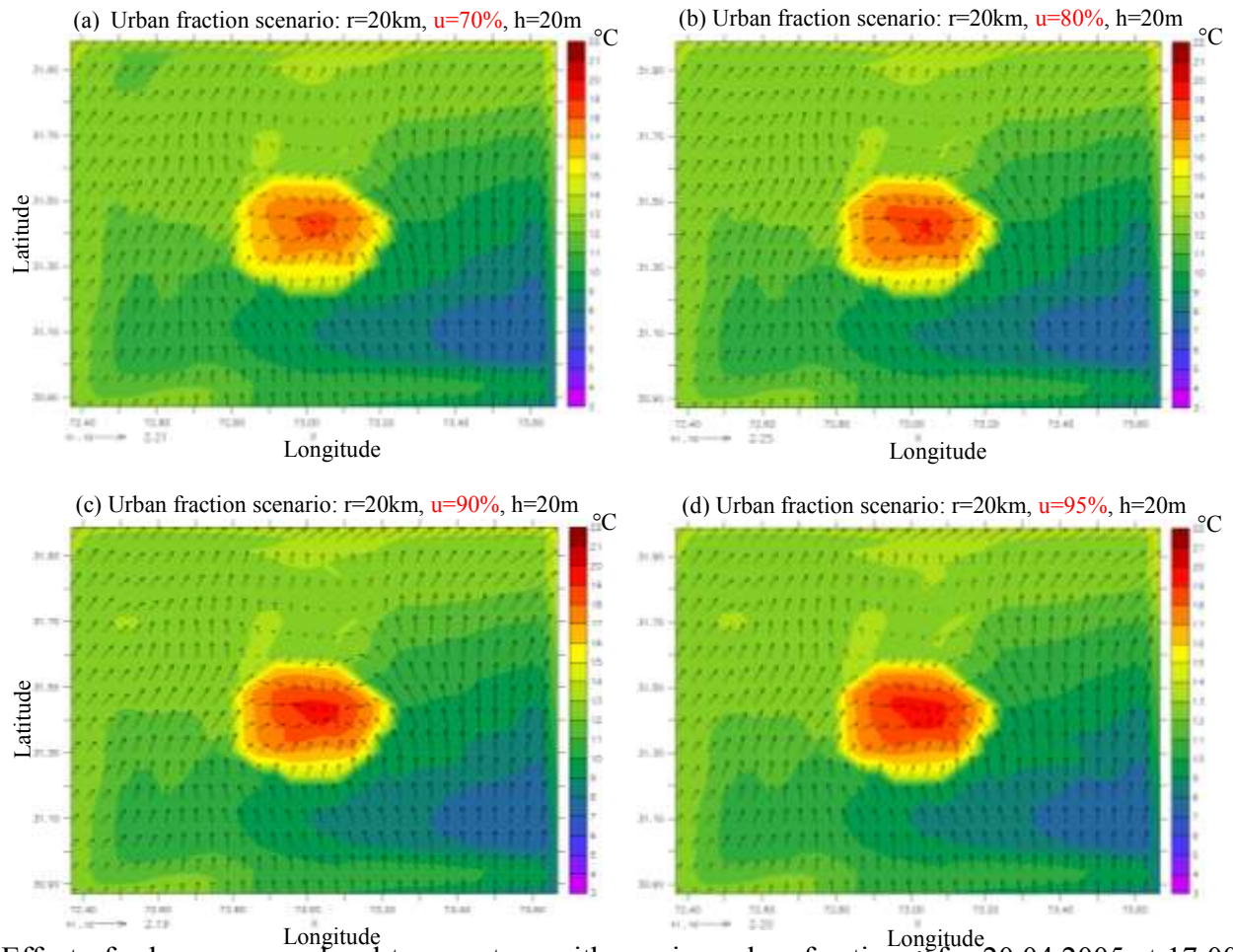
Appendix 4.3:



Effect of urban areas on local temperature with varying urban fraction u for 20.04.2005 at 09:00 GMT

- (a) Urban fraction scenario: $r=20\text{km}$, $u=70\%$, $h=20\text{m}$
- (b) Urban fraction scenario: $r=20\text{km}$, $u=80\%$, $h=20\text{m}$
- (c) Urban fraction scenario: $r=20\text{km}$, $u=90\%$, $h=20\text{m}$
- (d) Urban fraction scenario: $r=20\text{km}$, $u=95\%$, $h=20\text{m}$

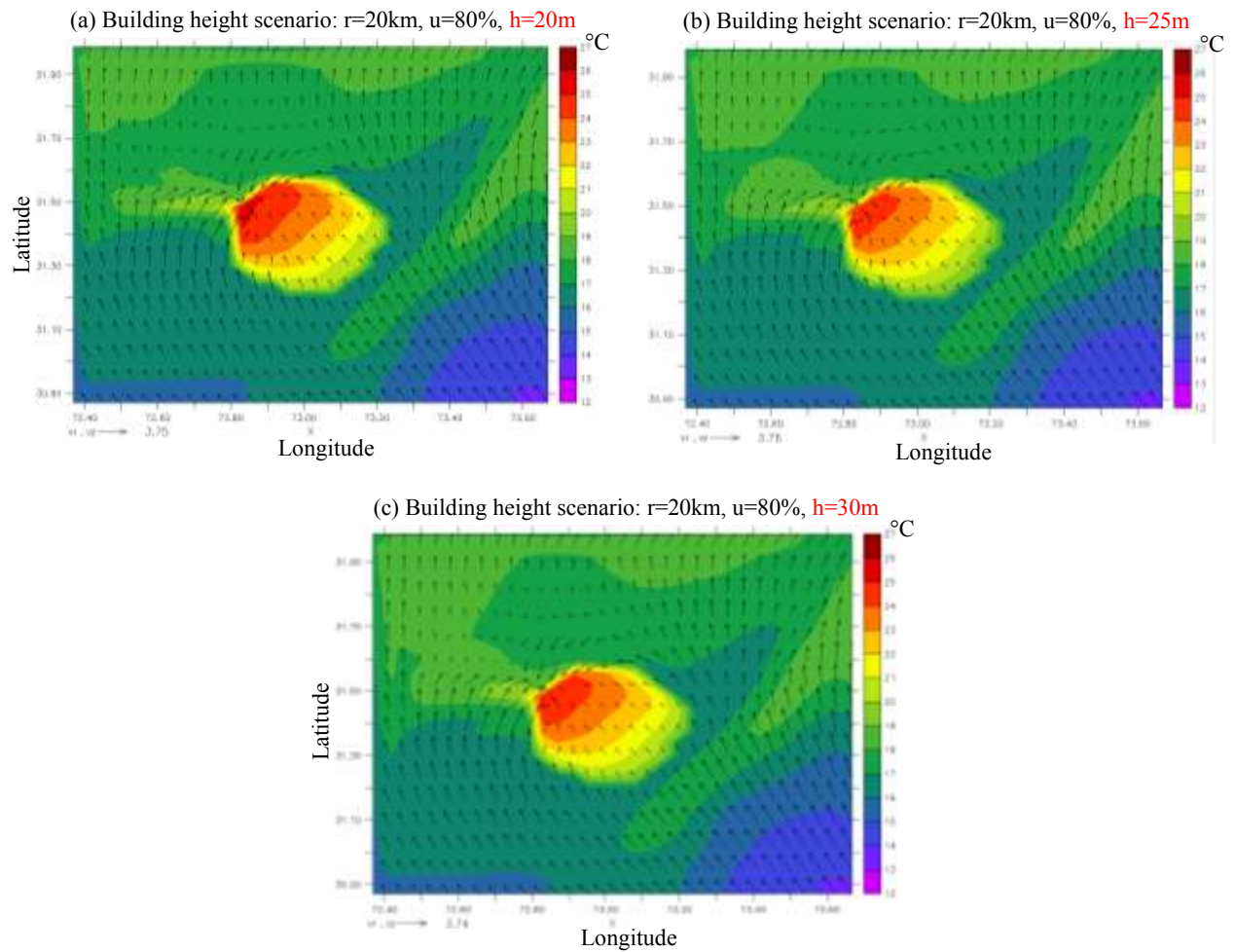
Appendix 4.4:



Effect of urban areas on local temperature with varying urban fraction u for 20.04.2005 at 17:00 GMT

- (a) Urban fraction scenario: $r=20\text{km}$, $u=70\%$, $h=20\text{m}$
- (b) Urban fraction scenario: $r=20\text{km}$, $u=80\%$, $h=20\text{m}$
- (c) Urban fraction scenario: $r=20\text{km}$, $u=90\%$, $h=20\text{m}$
- (d) Urban fraction scenario: $r=20\text{km}$, $u=95\%$, $h=20\text{m}$

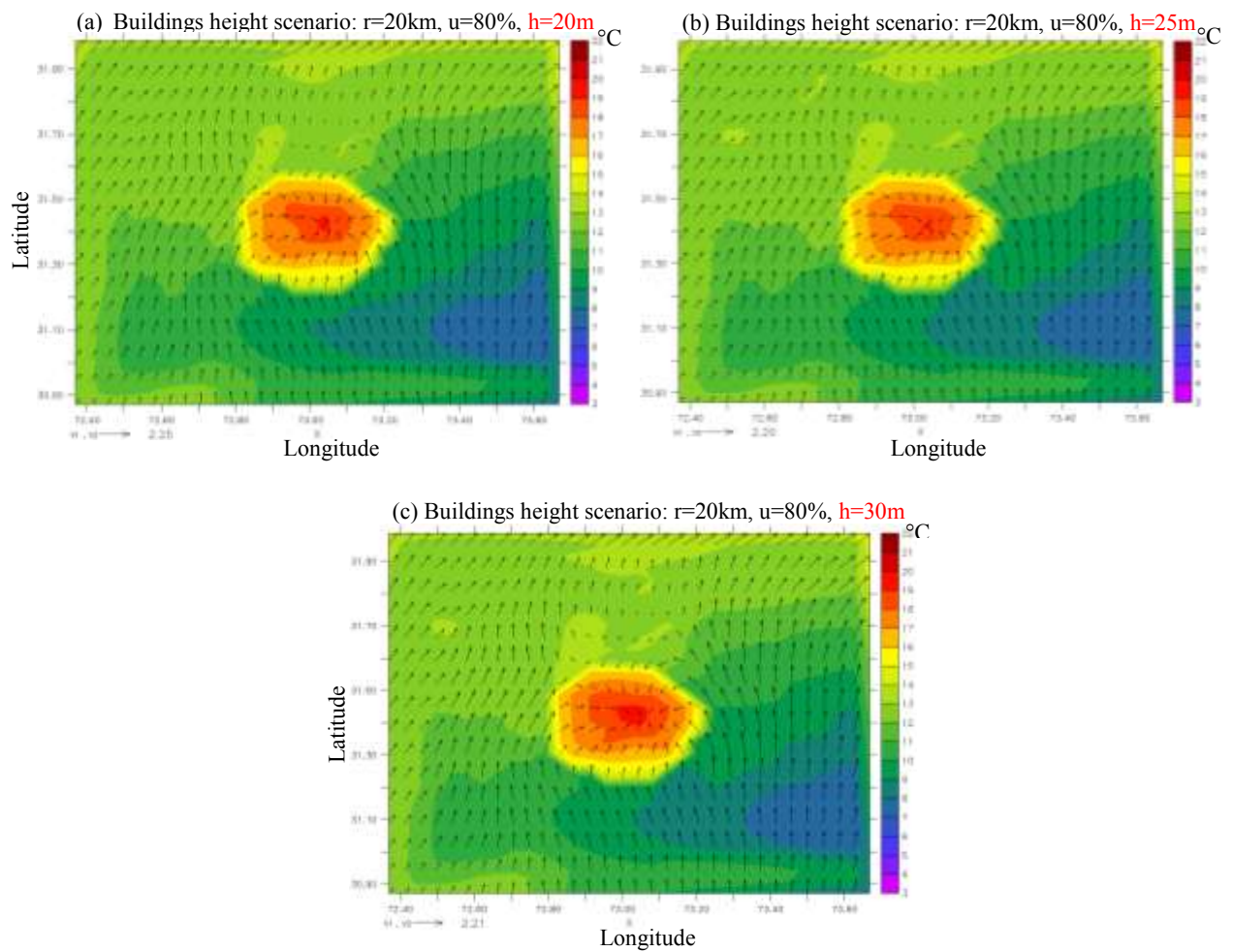
Appendix 4.5:



Effect of urban areas on local temperature with varying building height h for 20.04.2005 at 09:00 GMT.

- (a) Building height scenario: $r=20\text{km}$, $u=80\%$, $h=20\text{m}$
- (b) Building height scenario: $r=20\text{km}$, $u=80\%$, $h=25\text{m}$
- (c) Building height scenario: $r=20\text{km}$, $u=80\%$, $h=30\text{m}$

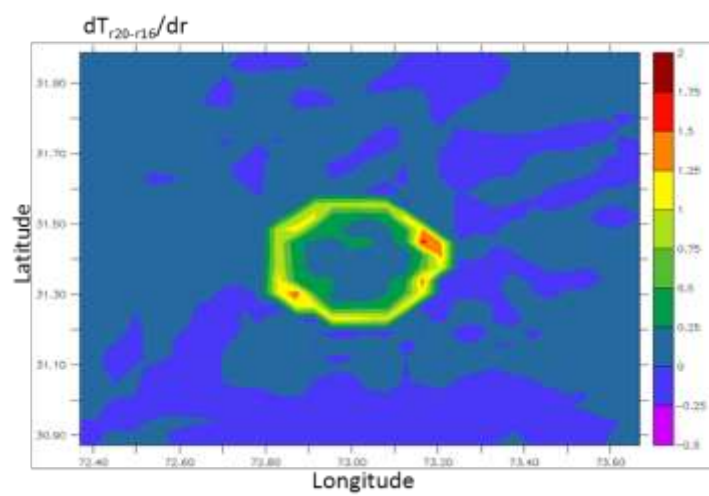
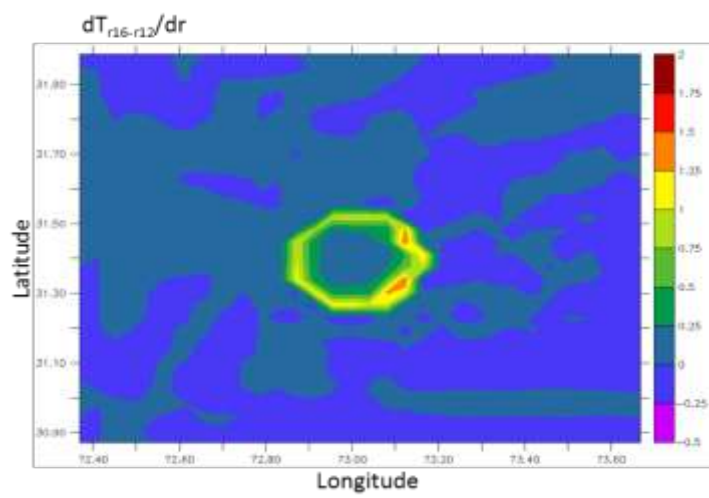
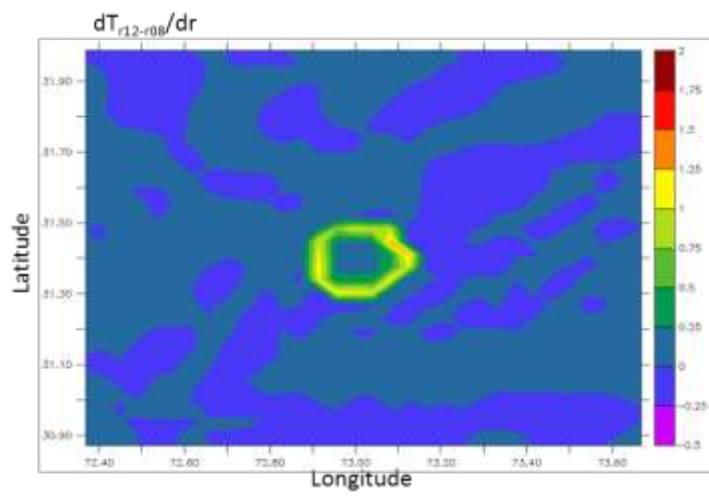
Appendix 4.6:



Effect of urban areas on local temperature with varying building's height h for 20.04.2005 at 17:00 GMT.

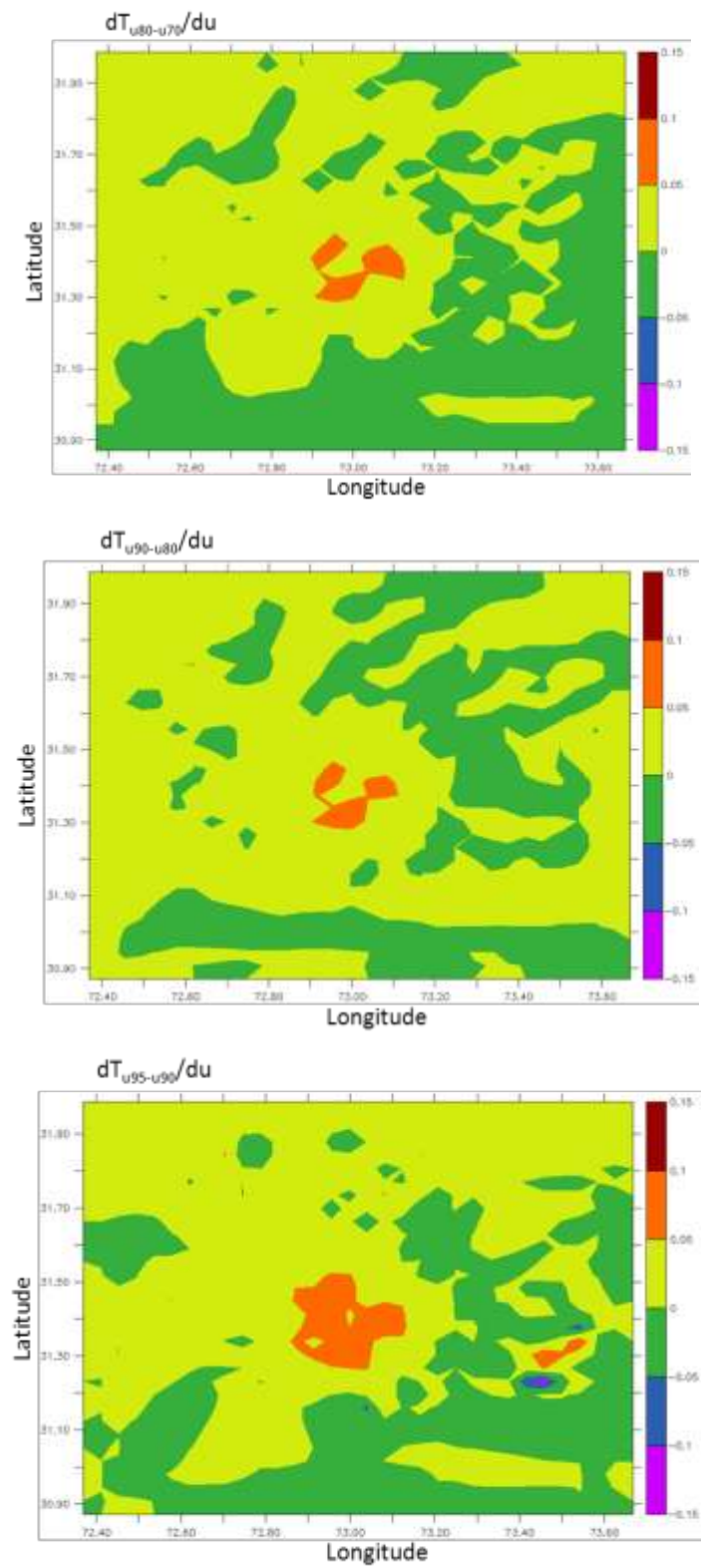
- (a) Building height scenario: $r=20\text{km}$, $u=80\%$, $h=20\text{m}$
- (b) Building height scenario: $r=20\text{km}$, $u=80\%$, $h=25\text{m}$
- (c) Building height scenario: $r=20\text{km}$, $u=80\%$, $h=30\text{m}$

Appendix 4.7:



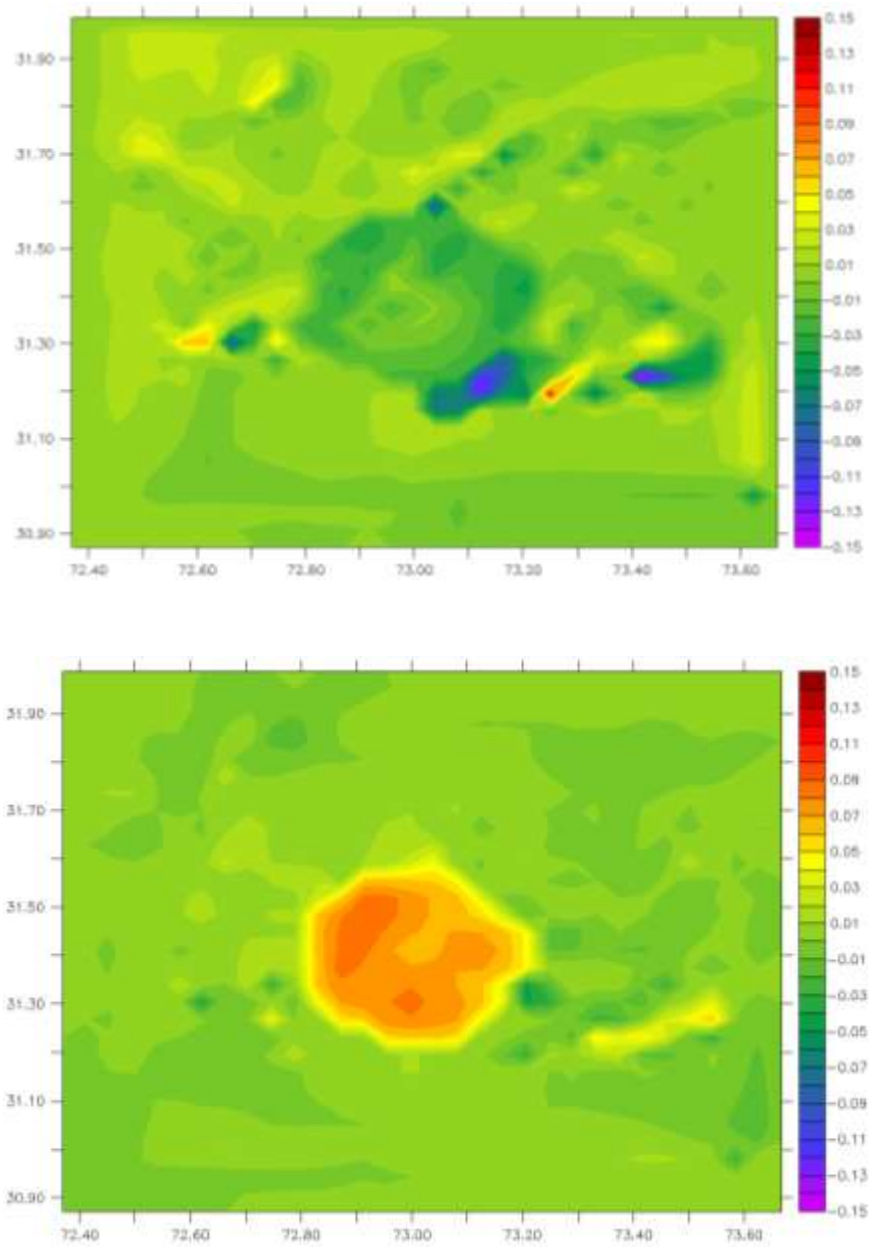
$dT_{r12-r08}/dr$; $dT_{r16-r12}/dr$ and $dT_{r20-r16}/dr$ with urban fraction 80% and building height 20 meter.

Appendix 4.8:



$dT_{u80-u70}/du$; $dT_{u90-u80}/du$ and $dT_{u95-u90}/du$ with city size 20 km of radius and building height 20 meter.

Appendix 4.9:



$dT_{h30-h25}/dh$ and $dT_{h25-h20}/dh$ with 20 km radius of the city and 80% of the urban fraction.

REFERENCES

- Adinna E. N, Christian E. I, Okolie A. T (2009) Assessment of urban heat island and possible adaptations in Enugu urban using landsat-ETM. *Journal of Geography and Regional Planning*, 2(2): 030–036.
- Aguilar E, Auer I, Brunet M, Peterson TC, Weringa J. (2003) Guidelines on Climate Metadata and Homogenization, World Climate Programme Data and Monitoring, WMO/TD No. 1186, World Meteorological Organization, Geneva, 51 pp
- Akbari et al. (2010) Reducing Urban Heat Islands: Compendium of Strategies, Urban Heat Island Basics. Climate Protection Partnership Division in the U.S. Environmental Protection Agency's Office of Atmospheric Programs, p. 1–22.
- Akbari H (2005) Energy Saving Potentials and Air Quality Benefits of Urban Heat Island Mitigation. <http://escholarship.org/uc/item/4qs5f42s>
- Akbari H et al. (2008) Reducing Urban Heat Islands: Compendium of Strategies – Urban Heat Island Basics. U. S. Environmental Protection Agency. Chapter 1: 1–22. <http://www.epa.gov/heatislands/resources/compendium.htm>.
- Akbari H, Pomerantz M, Taha H (2001) Cool surfaces and shade trees to reduce energy use and improve air quality in urban areas. *Sol Energy* 70: 295–310.
- Alcoforado M.J, Andrade H (2008) Global warming and the urban heat island. *Urban Ecology*, 3: 249–262.
- Alexandersson H (1984) A Homogeneity Test Based on Ratios and Applied to Precipitation. Report 79, Department of Meteorology, Uppsala, Sweden, 55 pp. (PhD dissertation)
- Alexandersson H (1986) A homogeneity test applied to precipitation data. *J. Climatol.*, 6: 661–675.
- Alexandersson H, Moberg A (1997) Homogenization of Swedish temperature data. Part I: A homogeneity test for linear trends. *Int. J. Climatol.*, 17: 25–34.
- Almas A.S, Rahim C.A, Butt M.J, Shah T.I (2005) Metropolitan growth monitoring and landuse classification using geospatial technique. ISPRS Workshop on Service and Application of Spatial Data Infrastructure, XXXVI(4/W6), October 14-16, 2005, Hangzhou, China.
- Anandakumar K (1999) A study on the partition of net radiation into heat fluxes on a dry asphalt surface. *Atmospheric Environment* 33:3911–3918.

- Aniello C, Mogan K, Busbey A, Newland L (1995) Mapping micro-urban heat island using LANDSAT TM and GIS. *Computers & Geoscience*. 21:965–969.
- APN CAPaBLE (2005) Enhancement of National Capacities in the Application of Simulation Models for the Assessment of Climate Change and its Impacts on Water Resources and Food and Agricultural Production. 2005-CRP1CMY-Khan, Asia Pacific Network for Global Change Research. Pp. 25–28.
- Arnfield A.J (2003) Review two decades of urban climate research: a review of turbulence, exchanges of energy and water, and the urban heat island. *International Journal of Climatology*; 23: 1–26.
- Arnfield AJ (1984) Simulating radiative energy budgets within the urban canopy layer. *Modeling and Simulation* 15: 227–233.
- Arnfield AJ (2000) A simple model of urban canyon energy budget and its validation. *Physical Geography* 21: 305–326.
- Arnfield AJ (2003) Two decades of urban climate research: a review of turbulence, exchanges of energy and water, and the urban heat island. *Int. J. Climatol.* 23: 1–26.
- Arya S. P (2001) Introduction to micrometeorology. Second Eds. International Geophysics Series, Volume 79. Academic Press, p. 11–45.
- Asaeda T, Ca VT, Wake A (1996) Heat storage of pavement and its effect on the lower atmosphere. *Atmospheric Environment* 30: 413–427.
- Assimakopoulos MN, Mihalakakou G, Flocas HA (2007) Simulating the thermal behaviour of a building during summer period in the urban environment. *Renew Energy* 32(11): 1805–1816.
- Auer I (1992) Experiences with the Completion and Homogenization of Long-term Precipitation Series in Austria, Centr. Europ. Research. Initiative, Proj. Gr. Meteorology, Wp. 1, Vienna.
- Auliciems A (1997) Comfort, Clothing and Health. In Thompson R.D., and Perry A. (Eds.), *Applied climatology: principles and practices*. New York: Routledge, pp. 155-174.
- Bacci P, Maugeri M (1992) The urban heat island of Milan. *Il Nuovo Cimento* 15C:417-424.
- Baik J.J, Kim Y.H, Kim J.J, Han J.Y (2007) Effects of boundary-layer stability on urban heat island-induced circulation. *Theor. Appl. Climatol.* 89: 73–81.
- Bonan G (1997) Effects of land use on the climate of United States. *Climatic Change*, 37: 449–486.

- Bornstein R, Lin Q (2000) Urban heat islands and summertime convective thunderstorms in Atlanta: three case studies. *Atmos Environ* 34: 507–516.
- Bornstein R. D (1975) The two dimensional URBMET urban boundary layer model. *J. Appl. Meteor.*, 14: 1459–1477.
- Bottyan Z, Kircsi A, Szegedi S, Unger J (2005) The relationship between built-up areas and the spatial development of the mean maximum urban heat island in Debrecem, Hungary. *Int J Climatol* 25: 405–418.
- Bottyan Z; Unger J (2003) A multiple linear statistical model for estimating the mean maximum urban heat island. *Theor. Appl. Climatol.* 75: 233–243.
- Bounoua L, Defries R, Collatz G.J, Sellers P, Khan H (2002) Effects of land cover conversion on surface climate. *Climatic Change* 52: 29–64.
- Bounoua L, Safia A, Masek J, Peters-Lidarad C, Imhoff ML (2009) Impacts of urban growth on surface climate: A case study in Oran, Algeria. *J. Appl. Meteorol.*, 48: 217–231.
- Brázdil R, Budíková M (1999) An urban bias in air temperature fluctuations at the Klementinum, Prague, the Czech Republic. *Atmospheric Environment*, 33 (24–25): 4211–4217.
- Brunet M (2012) The Development of the Spanish Daily Adjusted Temperature Series (SDATS): A Case-Study Discussing from Integrated Data Rescue Procedures to Calculation of Area-Averaged Climate Series. *Proceedings of the Second WMO/MEDARE International Workshop: Addressing climate data sources and key records for the Mediterranean Basin in support of an enhanced detection, prediction and adaptation to climate change and its impacts.* 10-12 pp.
- Brunetti M, Mangianti F, Maugeri M, Nanni T (2000) Urban heat island bias in Italian air temperature series. *Il Nuovo Cimento*, 23: 423–431.
- Busishand T.A (1982) Some methods for testing the homogeneity of rainfall records. *Journal of Hydrology* 58: 11-27.
- Camilloni I, Barros V (1997) On the urban heat island effect dependence on temperature trends. *Climatic Change* 37: 665–681.
- Caussinus H, Lyazrhi F (1997) Choosing a linear model with a random number of change-points and outliers. *Ann. Inst. Stat. Math.*, 49: 761–775.

- Caussinus H, Mestre O (1996) New mathematical tools and methodologies for relative homogeneity testing', Proceedings of the Seminar for Homogenization of Surface Climatological Data, Budapest, 6–12 October, pp. 63–82.
- Caussinus H, Mestre O (2004) Detection and correction of artificial shifts in climate series. *Appl. Statist.* 53(3): 405–425.
- Cermak JE (1996) Thermal effects on flow and dispersion over urban areas: capabilities for prediction by physical modeling. *Atmospheric Environment*, 30: 393–401.
- Chandler T.J (1960) Wind as a factor of urban temperatures: A survey in north-east London, *Weather*, 25: 204.
- Changnon S.A (1968) The La Porte weather anomaly—Fact or fiction? *Bull. Amer. Meteor. Soc.* 49: 4–11.
- Charles T (1983) Improving street climate through urban design, American Planning Association.
- Chemel C, Chollet J-P, Chaxel E (2008) On the Suppression of the Urban Heat Island over Mountainous Terrain in Winter. C. Borrego and A.I. Miranda (eds.), *Air Pollution Modeling and Its Application XIX?* PP. 46–53.
- Chen L, Zhu W, Zhou X, Zhou Z (2003) Characteristics of the Heat Island Effect in Shanghai and Its Possible Mechanism. *Advances in Atmospheric Sciences*, Vol. 20(6): 991–1001.
- Chen L.X, Li W.L, Zhu W.Q, Zhou X.J, Zhou Z.J, Liu H.L (2006b) Seasonal trends of climate change in the Yangtze Delta and its adjacent regions and their formation mechanisms. *Meteorol. Atmos. Phys.*, 92: 11–23.
- Chen X-L, Zhao H-M, Li P-X, Yin Z-Y (2006a) Remote sensing image-based analysis of the relationship between urban heat island and land use/cover changes. *Remote Sensing of Environment*, 104: 133–146.
- Cheval S, Dumitrescu A (2009) The July urban heat island of Bucharest as derived from modis images. *Theor Appl Climatol.*, 96: 145–153.
- Cheval S, Dumitrescu A, Bell A (2009) The urban heat island of Bucharest during the extreme high temperatures of July 2007. *Theor Appl Climatol* 97: 391–401.
- Childs P.P, Raman S (2005) Observations and Numerical Simulations of Urban Heat Island and Sea Breeze Circulations over New York City. *Pure appl. geophys.* 162: 1955–1980.
- Ching JKS, Clarke JF, Godowitch JM (1983) Modulation of heat flux by different scales of advection in an urban environment. *Boundary-Layer Meteorology* 25: 171–191.

- Chung U, Choi J, Yun J.I (2004) Urbanization effect on the observed change in mean monthly temperatures between 1951-1980 and 1971-2000 in Korea, *Climatic Change* 66: 127–136.
- Clappier A, Perrochet P, Martilli A, Muller F, Krueger B. C (1996) A New Non- Hydrostatic Mesoscale Model Using a CVFE (Control Volume Finite Element) Discretisation Technique’, in P. M. Borrell et al. (eds.), *Proceedings of EUROTRAC Symposium ’96*, Computational Mechanics Publications, Southampton, pp. 527–531.
- Collier C.G (2006) The impact of urban areas on weather. *Q. J. R. Meteorol. Soc.*, 132: 1–25.
- Costa AC, Soares A (2009) Homogenization of climate data: Review and new perspectives using geostatistics. *Math Geosci.*, 41: 291–305.
- Craddock J.M (1979) Methods of comparing annual rainfall records for climatic purposes. *Weather*, 34: 332–346.
- Dale V.H (1997) The relationship between land-use change and climate change. *Ecological Applications*, 7(3): 753–769.
- Decker E.H, Elliott S, Smith F.A, Blake D.R, Rowland F.S. (2000) Energy and material flow through the urban ecosystem. *Annu. Rev. Energy Environ.* 25: 685–740.
- Demographia (2011): *World Urban Areas (World Agglomerations)*, 7th Annual Edition April 2011. <http://www.demographia.com/db-worldua.pdf>
- Doll D, Ching JKS, Kaneshiro J (1985) Parameterization of subsurface heating for soil and concrete using net radiation data. *Boundary-Layer Meteorology* 32: 351–372.
- Dziubinski O, Chipman R (1999) *Trends in Consumption and Production: Household Energy Consumption*. United Nations Department of Economic and Social Affairs. ST/ESA/1999/DP. 6, DESA Discussion Paper No. 6.
- Easterling D.R, Horton B, Jones P.D, Peterson T.C, Karl T.R, Parker D.E, Salinger M.J, Razuvayev V, Plummer N, Jamason P, Folland C.K (1997) Maximum and minimum temperature trends for the globe. *Science* 277: 364–367.
- Easterling D.R, Peterson T.C (1995a) A new method for detecting and adjusting for undocumented discontinuities in climatological time series. *Int. J. Climatol.*, 15: 369–377.
- Easterling D.R, Peterson T.C (1995b) The effect of artificial discontinuities on recent trends in minimum and maximum temperatures. *Atmos. Res.*, 37: 19–26.
- Economic Survey of Pakistan, 2008-2009, p. 226

- Eliasson I, Holmer B (1990) Urban Heat Island Circulation in Goteborg, Sweden. *Theor. Appl. Climatol.* 42: 187–196.
- ENERDATA (2010) World energy demand down for the first time in 30 years. June 8, 2010.
- Erell E, Williamson T (2007) Intra-urban differences in canopy layer air temperature at a mid-latitude city. *Int J Climatol.*, 27: 1243–1255.
- Esteban P, Prohom M, Aguilar E, Mestre O (2010) Annual and seasonal analysis of temperature and precipitation in Andorra (Pyrenees) from 1934 to 2008: quality check, homogenization and trends. *Geophysical Research Abstracts*, Vol. 12, EGU2010-1885, 2010. EGU General Assembly 2010.
- Fan G, Lu S, Luo S (1998) The influence of the NW China afforestation on regional climate in East and South Asia. *Plateau Meteorology*, 17(3): 300–308.
- Fan H, Sailor D.J (2005) Modeling the impacts of anthropogenic heating on the urban climate of Philadelphia: a comparison of implementations in two PBL schemes. *Atmospheric Environment*, 39: 73–84.
- Fenichel A (1979) *Quantitative Analysis of the Growth and Diffusion of Steam Power in Manufacturing in the United States, 1838–1919*. Arno Press.
- Forland E.J, Allerup P, Dahlstrom B, Elomaa E, Jonsson T, Madsen H, Per J, Rissanen P, Vedin H, Vejen F (1996) *Manual for Operational Correction of Nordic Precipitation Data*, DNMI-Reports 24/96 KLIMA, 66 pp.
- Free M, Durre I, Aguilar E, Seidel D, Peterson T.C, Eskridge R.E, Luers J.K, Parker D, Gordon M, Lanzante J, Klein S, Christy J, Schroeder S, Soden B, McMillin L, Weatherhead E (2001) *Creating Climate Reference Datasets. CARDS Workshop on Adjusting Radiosonde Temperature Data for Climate Monitoring*. *Bull. Amer. Meteor. Soc.* 83: 891-899.
- Freitas E.D, Rozoff C.M, Cotton W.R, Dias P.L.S (2007) Interactions of an urban heat island and sea-breeze circulations during winter over the metropolitan area of São Paulo, Brazil. *Boundary-Layer Meteorol.* 122: 43–65.
- Fu C.B (2003) Potential impacts of human-induced land cover change on east Asia monsoon. *Global Planet. Change*, 37: 219–229.
- Fujibe F (2003) Long-term surface wind changes in the Tokyo metropolitan area in the afternoon of sunny days in the warm season. *J. Meteor. Soc. Japan*, 81: 141-149.

- Gaffin, S.R, Rosenzweig C, Khanbilvardi R, Parshall L, Mahani S, Glickman H, Goldberg R, Blake R, Slosberg R.B, Hillel D (2008) Variations in New York City's urban heat island strength over time and space. *Theor. Appl. Climatol.*, 94: 1-11,
- Gallo K.P, Owen T.W (1998) Assessment of urban heat islands: A multi sensor perspective for the Dallas Ft Worth, USA region. *Geocarto International*, 13: 35–41.
- Gao X, Luo Y, Lin W, Zhao Zongci, Filippo G (2003) Simulation of effects of land use change on climate in China by a Regional Climate Model. *Advances in Atmospheric Sciences*, 20(4): 583–592.
- Geiger R, Aron R.H, Todhunter P (1995) *The climate near the ground*. 5th ed. Vieweg & Sohn Verlagsgesellschaft mbH, Wiesbaden. p. 5–50.
- Global Security (2011) Pakistan Climates (2013) Climate classification and associated rainfall. http://www.globalsecurity.org/jhtml/jframe.html#http://www.globalsecurity.org/military/world/pakistan/images/PAK_Climate.jpg
- Gray K.A, Finster M.E (1999) *The Urban Heat Island, Photochemical Smog, and Chicago: Local Features of the Problem and Solution*. Atmospheric Pollution Prevention Division U.S. Environmental Protection Agency. Pp. 1–41.
- Grimmond C.S, King T.S, Cropley F.D, Novak D.J, Souch C (2002) Local-scale fluxes of carbon dioxide in urban environments: Methodological challenges and results from Chicago. *Environ. Pollut.*, 116: S243–S254.
- Grimmond C.S.B (2006) Progress in measuring and observing the urban atmosphere. *Theoretical and Applied Climatology*, 84 (1–3): 3–22.
- Grimmond C.S.B (2007) Urbanization and global environmental change: local effects of urban warming. *Cities and global environmental change*, 173(1): 83–88.
- Grimmond C.S.B, Cleugh H.A, Oke T.R (1991) An objective heat storage model and its comparison with other schemes. *Atmos. Environ.*, 25B, 311–326.
- Grimmond C.S.B, Souch C, Hubble MD (1996) Influence of tree cover on summertime surface energy balance fluxes, San Gabriel Valley, Los Angeles. *Climate Research* 6: 45–57.
- Gullett D.W, Vincent L, Malone L.H (1991) Homogeneity Testing of Monthly Temperature Series. Application of Multiple-Phase Regression Models with Mathematical Change points, CCC Report No. 91–10. Atmospheric Environment Service, Downsview, Ontario. 47 pp.

- Hansen J, Ruedy R, Glascoe J, Sato M (1999) GISS analysis of surface temperature change. *J Geophys Res.*, 104: 30997–31022
- Hansen J.E, Ruedy R, Sato M, Imhoff M, Lawrence W, Easterling D, Peterson T, Karl T (2001) A closer look at United States and global surface temperature change. *J Geophys Res.*, 106: 23947–23963.
- Hanssen-Bauer I, Forland E (1994) Homogenizing long Norwegian precipitation series. *J. Climate*, 7: 1001-1013.
- Harman I.N (2003) The energy balance of urban areas. A PhD thesis, Department of Meteorology, The University of Reading. Pp. 1–18.
- Hart M.A, Sailor D.J (2009) Quantifying the influence of land-use and surface characteristics on spatial variability in the urban heat island. *Theor Appl Climatol* 95: 397–406.
- Hassid S, Santamouris M, Papanikolaou N, Linardi A, Klitsikas N, Georgakis C, Assimakopoulos D.N (2000) The effect of the Athens heat island on air conditioning load. *Energy and Buildings* 32: 131–141.
- Hawkins P.M (1977) Testing a sequence of observations for a shift in random location. *J. Am. Statist. Assoc.*, 73: 180-185.
- He C-Y, Shi P-J, Chen J, Zhou Y-Y (2001) A study on land use/cover change in Beijing area. *Geographical Research*, 20(6): 679–687.
- He J.F, Liu J.Y, Zhuang D.F, Zhang W, Liu M.L (2007) Assessing the effect of land use/land cover change on the change of urban heat island intensity. *Theor. Appl. Climatol.* 90: 217–226.
- Heck P, Luthi D, Wernli H, Schar G (2001) Climate impacts of European-scale anthropogenic vegetation changes: A sensitivity study using a regional climate model. *J. Geophys. Res.*, 106: 7817–7835.
- Heino R (1994) Climate in Finland during the period of Meteorological observations, Finnish Meteorological Institute Contributions 12 Academic dissertation, Helsinki, 209 pp.
- HIG (2005) Heat Island Group world-wide web: <http://HeatIsland.LBL.gov> . Lawrence Berkeley National Laboratory, Berkeley, CA.
- Hinkel K.M, Nelson F.E, Klene A.E, Bell J.H (2003) The urban heat island in winter at Barrow, Alaska. *Int. J. Climatol.* 23: 1889–1905.
- Howard L (1833) The climate of London. Vol. I-III, London.

- Hu Y, Jia G (2010) Influence of land use change on urban heat island derived from multi-sensor data. *Int. J. Climatol.* 30: 1382–1395.
- Hua L.J, Ma Z.G, Guo W.D (2008) The impact of urbanization on air temperature across China. *Theor. Appl. Climatol.* 93: 179–194.
- Huang H, Ooka R, Kato S (2005) Urban thermal environment measurements and numerical simulation for an actual complex urban area covering a large district heating and cooling system in summer. *Atmos Environ* 39:6362–6375. DOI 10.1016/j. atmosenv.2005.07.018.
- Huff F.A, Changnon S.A (1972) Climatological assessment of urban effects on precipitation at St. Louis. *J. Appl. Meteor.*, 11: 823–842.
- Hung T, Uchihama D, Ochi S, Yasuoka Y (2006) Assessment with satellite data of the urban heat island effects in Asian mega cities. *International Journal of Applied Earth Observation and Geoinformation* 8: 34–48.
- IMF and World Bank (2006) Clean energy and development: towards an investment framework. DC2006–0002. Environmentally and Socially Sustainable Development Vice-Presidency and Infrastructure Vice-Presidency, The World Bank, Washington, DC, page viii.
- Imhoff M.L, Lawrence W.T, Stutter D.C, Elvidget C.D (1997) A technique for using composite DMSP/OLS “City Lights” satellite data to map urban area. *Remote Sens. Environ* 61: 361–370.
- Jacobson M.Z (2005) *Fundamentals of Atmospheric Modeling*. Cambridge University Press 2005, Cambridge United Kingdom.
- Jauregui E (1997) Heat island development in Mexico city. *Atmospheric Environment*, 31(22): 3821–3831.
- Jauregui E, Romales E (1996) Urban effects on convective precipitation in Mexico City. *Atmos Environ* 30: 3383–3389.
- Jiang Z, Chen Y Li J (2006) On urban heat island of Beijing based on Landsat TM Data. *Geospatial Information*, 9(4): 293–297.
- Johnson G.T, Oke T.R, Lyons T.J, Steyn D.G, Watson I.D, Voogt J.A (1991) Simulation of surface urban heat islands under ‘ideal’ conditions at night part 1: Theory and tests against field data. *Boundary-Layer Meteorology*, 56: 275–294.
- Jones B.G, Kandel W.A (1992) Population growth, urbanization and disaster risk vulnerability in metropolitan areas: A conceptual framework. *Environmental management and urban*

- vulnerability, edited by Alcira Kreimer, Mohan Munasinghe. Washington, D.C., World Bank, 1992: 51-76. (World Bank Discussion Papers 168).
- Jones P.D, Groisman P.Y, Coughlan M, Plummer N, Wang W-C, Karl T.R (1990) Assessment of urbanization effects in time series of surface air temperature over land. *Nature*, 347: 169–172.
- Jones P.D, Raper S.C.B, Bradley R.S, Diaz H.F, Kelly P.M, Wigley T.M.L (1986) Northern Hemisphere Surface Air Temperature Variations: 1851–1984. *J. Climate Appl. Meteorol.*, 25: 161–179.
- Jusuf S.K, Wong N.H, Hagen E, Anggoro R, Hong Y (2007) The influence of land use on the urban heat island in Singapore. *Habitat International* 31: 232–242.
- Kahn, M.E (2006) *Green cities. Urban growth and the environment*. Brookings Institution Press, Washington, D.C, 160 p.
- Kalnay E, Cai M (2003) Impact of urbanization and land-use change on climate. *Nature*, 423: 528–531.
- Kalnay E. et al. (1996) The NCEP/NCAR 40-year reanalysis project. *Bull. Am. Meteorol. Soc.* 77(3): 437–431.
- Karl T, Jones P (1989) Urban biases in area-averaged surface air temperature trends. *Bull. Am. Meteorol. Soc.*, 70: 265; *Environ. Rep. 2*, WMO No. 312, Geneva, pp. 101-106.
- Karl T.R et al., (1991) Global Warming: Evidence for asymmetric diurnal temperature change. *Geophysical Research Letter* 18(12): 2253–2256.
- Karl T.R, Diaz H, Kukla G (1988) Urbanization: Its detection in the U.S Climate record. *J. Clim.*, 1: 1099–1123.
- Karl T.R, Diaz H.F, Kukla G (1988) Urbanization: Its detection and effect in the United States climate record. *Journal of Climate*, 1(11): 1099–1123.
- Karl T.R, Jones P.D, Knight R.W, Kukla G, Plummer N, Razuvayev V, Gallo K. P, Lindsey J, Charlson R, Peterson T.C (1993) A new perspective on Recent Global Warming: Asymmetric trends of daily maximum and minimum temperature. *Bull. Am. Meteorol. Soc.* 74: 1007–1023.
- Karl TR, Jones PD (1989) Urban bias in area-averaged surface air temperature trends. *Bull Amer Met Soc* 70: 265-270.

- Kato S, Yamaguchi Y (2005) Analysis of urban heat island effect using ASTER and ETM+ Data: separation of anthropogenic heat discharge and natural heat radiation from sensible heat flux. *Remote Sensing of Environment* 99: 44–54.
- Khaliq M.N, Ouarda T.B.M.J (2007) On the critical values of the standard normal homogeneity test (SNHT). *Int. J. Climatol.* 27: 681 – 687.
- Khaliq-uz-Zaman, Baloch A.A (2011) Urbanization of arable land in Lahore city in Pakistan: A case study. *JABSD*, 3(7): 126–135.
- Khambhammettu P (2005) Mann-Kendall Analysis for the Fort Ord Site. HydroGeoLogic, Inc. – OU-1 Annual Groundwater Monitoring Report –Former Fort Ord, California.
- Kim S (2005) Industrialization and urbanization: Did the steam engine contribute to the growth of cities in the United States? *Explorations in Economic History* 42: 586–598.
- Kim Y.H, Baik J.J (2004) Daily maximum urban heat island intensity in large cities of Korea. *Theor. Appl. Climatol.* 79: 151–164.
- Kim Y.H, Baik J.J (2005) Spatial and Temporal Structure of the Urban Heat Island in Seoul. *Journal of Applied Meteorology*, 44: 591–605.
- Kim Y.H, Baik J.J, (2002) Maximum urban heat island intensity in Seoul. *J. Appl. Meteorol.*, 41: 651–659.
- Kjelgren R, Montague T (1998) Urban tree transpiration over turf and asphalt surfaces. *Atmospheric Environment* 32: 35–41.
- Kobysheva N, Naumova L (1979) Works of the Main Geophysical Observatory, 425, Saint Petersburg, Russia.
- Kolokotroni M, Zhang Y, Watkins R (2007) The London heat island and building cooling design. *Sol Energy* 81:102–110. DOI 10.1016/j.solener.2006.06.005.
- Kondo H, Asahi K, Tomizuka T, Suzuki M (2006) Numerical analysis of diffusion around a suspended expressway by a multi-scale CFD model. *Atmospheric Environment*, 40: 2852–2859.
- Kusaka H, Chen F, Tewari M, Hirakuchi H (2005) Impact of the urban canopy model on the simulation of the heat island. *WRF/MM5 user’s workshop 2005*.
- Kuttler W, Barlag A-B, Roßmann F (1996) Study of the thermal structure of a town in a narrow valley. *Atmospheric Environment* 30: 365–378.

- Lai L-W, Cheng W-L (2010) Urban heat island and air pollution – An emerging role for hospital respiratory admissions in an urban area. *J Environ Health*. 72(6): 32-5.
- Landsberg H.E (1970) Man-made climate changes. *Science*, 170: 1265–1274.
- Landsberg H.E (1981) *The urban climate*. Academic, New York.
- Lanzante J.R (1996) Resistant, robust and nonparametric techniques for the analysis of climate data. Theory and examples, including applications to historical radiosonde station data. *Int. J Climatol.*, 16: 1197–1226.
- Lean J, Rowntree P (1997) Understanding the sensitivity of a GCM simulation of Amazonian deforestation to the specification of vegetation and soil characteristics. *J. Clim.*, 10: 1216–1235.
- Lee C-C (2006) The causality relationship between energy consumption and GDP in G-11 countries revisited. *Energy Policy* 34: 1086–1093.
- Lee S.H, Baik J.J (2010) Statistical and dynamical characteristics of the urban heat island intensity in Seoul. *Theor Appl Climatol* 100: 227–237.
- Lemonsu A, Masson V (2002) Simulation of a summer urban breeze over Paris. *Boundary-Layer Meteorology*, 104(3): 463-490.
- Liu W, Ji C, Zhong J, Jiang X, Zheng Z (2007) Temporal characteristics of the Beijing urban heat island, *Theor. Appl. Climatol.* 87: 213–221.
- Lo C.P, Quattrochi D.A (2003) Land-Use and Land-Cover Change, Urban Heat Island Phenomenon, and Health Implications, a Remote Sensing Approach. *Photogrammetric Engineering and Remote Sensing*, 69(9): 1053–1063.
- Lo C.P, Quattrochi D.A (2003) Land-Use and Land-Cover Change, Urban Heat Island Phenomenon, and Health Implications: A Remote Sensing Approach. *Photogrammetric Engineering & Remote Sensing*, 69(9): 1053–1063.
- Magee N, Curtis J, Wendler G (1999) The Urban Heat Island Effect at Fairbanks, Alaska. *Theor. Appl. Climatol.* 64, 39–47.
- Martilli A (2001) Development of an urban turbulence parameterisation for mesoscale atmospheric models. PhD thesis, Ecole Polytechnique Fédérale de Laussane.
- Martilli A (2002) Numerical Study of Urban Impact on Boundary Layer Structure: Sensitivity to Wind Speed, Urban Morphology, and Rural Soil Moisture. *Journal of Applied Meteorology*, 41: 1247–1266.

- Martilli A (2003) A Two-dimensional numerical study of the impact of a city on atmospheric circulation and pollutant dispersion in a coastal environment. *Boundary Layer Meteorol.*, 108: 91–119.
- Martilli A, Roulet Y.A, Junier M, Kirchner F, Rotach M, Clappier A (2003) On the impact of urban surface exchange parameterisations on air quality simulations: the Athens case, *Atmos. Environ.*, 37: 4217–4231.
- Masson V (2000) A Physically-based scheme for the Urban Energy Budget in atmospheric models. *Boundary-Layer Meteorol.*, 94: 357-397.
- Mathews E (1983) Global vegetation and land use: New high resolution data bases for climate studies. *J. Clim. Appl. Meteorol.*, 22: 474–487.
- Mauree D (2011) Development of a multi-scale model to evaluate building energy consumption in urban areas. 2nd ADEME Report 2011.
- Mestre O (2000) Methodes statistiques pour l’homogeneisation de longues series climatiques. PhD thesis, L’universite Paul Sabatier de Toulouse.
- Mestre O, Caussinus H (2001) A Correction Model for Homogenisation of Long Instrumental Data Series, in Brunet, M. and López, D., *Detecting and Modelling Regional Climate Change*, Springer, pp13-19.
- Miao S, Chen F, Lemone M. A, Tewari M (2009) An Observational and Modeling Study of Characteristics of Urban Heat Island and Boundary Layer Structures in Beijing. *Journal of Applied Meteorology and Climatology*, Vol. 48: 484–501.
- Mills G (2007) Cities as agents of global change. *Int. J. Climatol.* 27: 1849–1857.
- Mirzaei P.A, Haghghat F (2010) Approaches to study Urban Heat Island – Abilities and limitations. *Building and Environment*, 45(10): 2192–2201.
- Mochida A, Lun IYF (2008) Prediction of wind environment and thermal comfort at pedestrian level in urban area. *Journal of Wind Engineering and Industrial Aerodynamics*, 96: 1498–527.
- Mohan M, Kikegawa Y, Gurjar B.R, Bhati S Kollu N.R (2012) Assessment of urban heat island effect for different land use–land cover from micrometeorological measurements and remote sensing data for megacity Delhi. *Theor Appl Climatol.* DOI 10.1007/s00704-012-0758-z.
- Mohsin T, Gough W.A (2010) Trend analysis of long-term temperature time series in the Greater Toronto Area (GTA). *Theor Appl Climatol.*, 101:311–327

- Montavez J.P, Rodriguez A, Jimenez J.I (2000) A Study of the urban heat island of Granada. *Int. J. Climatol.*, 20: 899-911.
- Nichols N, Tapp R, Burrows K, Richards D (1996) Historical thermometer exposures in Australia, *Int. J. Climatol.*, 16: 705-710.
- Nunez M, Oke TR (1977) The energy balance of urban canyon. *Journal of Applied Meteorology*, 16: 11–19.
- OECD (2010) *Cities and Climate Change*, OECD Publishing. <http://dx.doi.org/10.1787/9789264091375-en>
- Oke T. R (1973) City size and the urban heat island. *Atmospheric Environment Pergamon Press*, 7: 769–779.
- Oke T. R (1976) The distinction between canopy and boundary-layer urban heat islands. *Atmosphere*, 14,268-277.
- Oke T. R (1976) The distinction between canopy and boundary-layer urban heat islands. *Atmosphere*, 14: 268-277.
- Oke T. R (1979) Advectively-assisted evapotranspiration from irrigated urban vegetation. *Boundary-Layer Meteorology* 17: 167–173.
- Oke T. R (1982) The energetic basis of the urban heat island. *Q J Roy Meteor Soc.*, 108: 1–24.
- Oke T. R (1987) *Boundary layer climates*. Metuen & Co. Ltd. British Library Cataloguing in Publication Data, Great Britain.
- Oke T. R (1988) The urban energy balance. *Progress in Physical Geography*, 12: 471–508.
- Oke T. R (1989) The micrometeorology of the urban forest. *Philosophical Transactions of the Royal Society of London, Series B* 324: 335–349.
- Oke T. R (1995) The heat island of the urban boundary layer: characteristics, causes and effects. In J.E Cermak, A.G Davenport, E.J Plate and D.X Viegas (eds), *Wind Climate in Cities*, Dordrecht: Kluwer Academic, pp. 81–107.
- Oke T. R (1997) Urban climate and global environmental change. In Thompson R.D., and Perry A. (Eds.), *Applied climatology: principles and practices*. New York: Routledge, pp. 273-287.
- Oke T. R, Johnson G.T, Steyn D.G, Watson I. D (1991) Simulation of surface urban heat islands under ‘ideal’ conditions at night part 2: Diagnosis of causation. *Boundary-Layer Meteorology* 56: 339–358.

- Ouyang Z, Xiao R.B, Schienke E.W, LI W.F, Wang X, Miao H, Zheng H (2008) Beijing urban spatial distribution and resulting impacts on heat islands. Springer Science+ Business Media B.V. 2008, Chapter 27: 459–478.
- Park H-S (1986) Features of the heat island in Seoul and its surrounding cities. *Atmospheric Environment*, 20(10): 1859–1866.
- Parker D.E (2004) Large-scale warming is not urban. *Nature*, 432 (7015): 290.
- Paterson D.A, Apelt C.J (1989) Simulation of wind flow around three-dimensional buildings. *Building and Environment* 24: 39–50.
- Pauleit S, Ennos R, Golding Y (2005) Modeling the environmental impacts of urban land use and land cover change – a study in Merseyside, UK. *Landscape and Urban Planning* 71: 295–310.
- Petralli M, Massetti L, Orlandini S (2011) Five years of thermal intra-urban monitoring in Florence (Italy) and application of climatological indices. *Theor Appl Climatol*. 104: 349–356.
- Pettit A.N (1979) A non-parametric approach to the change-point detection. *Applied Statistics* 28: 126-135.
- Pielke R.A (1974) A three dimensional numerical model of the sea breeze over South Florida. *Mon. Weather Rev.*, 102: 115–139.
- Plummer N, Lin Z, Torok S (1995) Trends in the diurnal temperature range over Australia since 1951. *Atmos. Res.*, 37: 79–86.
- Poreh M (1996) Investigation of heat islands using small scale models. *Atmospheric Environment*, 30: 467–474.
- Potter K.W (1981) Illustration of a new test for detecting a shift in mean in precipitation series. *Mon. Wea. Rev.*, 109: 2040–2045.
- Quattrochi D.A, Ridd M.K (1994) Measurement and analysis of thermal energy responses from discrete urban surfaces using remote sensing data. *Int J Remote Sens.*, 15: 1991–2022.
- Quayle R.G, Easterling D.R, Karl T.R, Huges P.Y (1991) Effects of recent thermometer changes in the cooperative station network. *Bull. Amer. Meteor. Soc.*, 72: 1718–1723.
- Qureshi S (2010) The fast growing megacity Karachi as a frontier of environmental challenges: Urbanization and contemporary urbanism issues. *JGRP*, 3(11): 306-321.
- Qureshi S, Breuste J.H (2010) Prospects of biodiversity in the mega city Karachi, Pakistan: potentials, constraints and implications. In: Muller N, Werner P, Kelcey J (Eds.), *Urban*

Biodiversity and Design – Implementing the Conservation on Biological Diversity in Towns and Cities. Wiley-Blackwell Academic Publishing, Oxford, p. 497-517, DOI: 10.1002/9781444318654.ch27.

Ramanathan V (1987) Atmospheric general circulation and its low frequency variance: radiatives influences. *J. Meteor. Soc. Jpn.*, 65: 151–175.

Ramanathan V, Barkstrom B, Harrison E (1989) Climate and the earth's radiation budget. *Physics Today*, 42: 22–32.

Rasheed A (2009) Multiscale Modelling of urban climate. PhD Thesis, Swiss Federal Institute of Technology, Lausanne – Switzerland (2009).

Revi A, Dronin N, Vries B (2002), “Population and environment in Asia since 1600 AD”, in B deVries and J Goudsblom (editors), *Mappae Mundi: Humans and their Habitats in a Long-Term Socioecological Perspective*, Amsterdam University Press.

Rhoades D.A, Salinger M.J (1993) Adjustment of temperature and rainfall records for site changes. *Int. J. Climatol.*, 13, 899–913.

Ripley EA , Archibold OW, Bretell DL (1996) Temporal and spatial temperature patterns in Saskatoon. *Weather*, 51: 398–405.

Rizwan A.M, Dennis Y.C.L, Liu C (2008) A review on the generation, determination and mitigation of Urban Heat Island. *Journal of Environmental Sciences* 20(1): 120–128.

Roches A. (2007). D'veloppement d'un pr'eprocasseur de mod`eles m'et'eorologiques. MSc. Thesis, Swiss Federal Institute of Technology lausanne.

Rosenberg N, Trajtenberg M (2004) A general purpose technology at work: the Corliss steam engine in the late-nineteenth-century United States. *Journal of Economic History* 64 (1): 61–99.

Rotach M.W, Vogt R, Bernhofer C, Batchvarova E, Christen A, Clappier A, Feddersen B, Gryning S-E, Martucci G, Mayer H, Mitev V, Oke T.R, Parlow E, Richner H, Roth M, Roulet Y-A, Ruffieux D, Salmond J.A, Schatzmann M, Voogt J.A (2005) BUBBLE – an Urban Boundary Layer Meteorology Project. *Theor. Appl. Climatol.* 81: 231–261.

Roth M (2000) Review of atmospheric turbulence over cities. *Q. J. R. Meteorol. Soc.*, 126: 941–990.

Rotty R.M, Mitchell J.M. Jr. (1974) Man's energy and the World's climate. Paper to 67th Annual Meeting Amer. Instit. Chem. Engineers, Washington, D.C.

- Saitoh TS, Shimada T, Hoshi H (1996) Modeling and simulation of the Tokyo urban heat island. *Atmos Environ* 30: 3431–3442.
- Sajjad S.H, Blond N, Clappier A, Raza A, Shirazi S.A, Shakrullah K (2010) The preliminary study of urbanization, fossil fuels consumptions and CO₂ emission in Karachi. *African Journal of Biotechnology*, 9(13): 1941–1948.
- Salamanca F, Krpo A, Martilli A, Clappier A (2010) A new building energy model coupled with an urban canopy parameterization for urban climate simulations—part I. formulation, verification, and sensitivity analysis of the model. *Theor Appl Climatol* 99: 331–344.
- Salamanca F, Martilli A (2010) A new Building Energy Model coupled with an Urban Canopy Parameterization for urban climate simulations—part II. Validation with one dimension off-line simulations. *Theor Appl Climatol*. 99: 345–356.
- Salamanca F, Martilli A, Yagüe C (2012) A numerical study of the Urban Heat Island over Madrid during the DESIREX (2008) campaign with WRF and an evaluation of simple mitigation strategies. *International Journal of Climatology*. Volume 32(15): 2372–2386.
- Salby M.L (1996) *Fundamentals of Atmospheric Physics*. Elsevier Science (USA), pp. 1-53.
- Sarrat C, Lemonsu A, Masson V, Guedalia D (2006) Impact of urban heat island on regional atmospheric pollution. *Atmos Environ* 40:1743–1758. DOI 10.1016/j.atmosenv.2005.11.037.
- Schmugge T.J, Jackson T.J, O'Neill P.E, Parlange M.B (1998) Observations of coherent emissions from soils. *Radio Science* 33(2): doi: 10.1029/97RS02614. issn: 0048-6604.
- Seinfeld J.H, Pandis S.N (2006) *Atmospheric Chemistry and Physics: From Air Pollution to Climate Change*. 2nd Ed. John Wiley & Sons, Inc.
- Shahbaz M, Lean1 H-H, Shabbir M.S (2010) Environmental kuznets curve and the role of energy consumption in Pakistan. *Development Research Unit, Discussion Paper DEVDP 10/05*, Pp. 1–23.
- Sheikh M.A (2010) *Renewable and Sustainable Energy Reviews*, Renewable and Sustainable Energy Reviews, 14: 354–363.
- Shepherd J.M (2005) A Review of Current Investigations of Urban-Induced Rainfall and Recommendations for the Future. *Earth Interactions*, 9(12): 1–27.
- Shepherd J.M (2006) Evidence of urban-induced precipitation variability in arid climate regimes. *Journal of Arid Environments*, 67: 607–628.

- Shepherd J.M, Burian S.J (2003) Detection of urban-induced rainfall anomalies in a major coastal city. *Earth Interactions*, 7: 1–17.
- Shrestha K.L, Kondo A, Maeda C, Kaga A, Inoue Y (2009) Numerical simulation of urban heat island using gridded urban configuration and anthropogenic heat data generated by a simplified method. The seventh International Conference on Urban Climate. 29 June - 3 July 2009, Yokohama, Japan.
- Siegel S, Castellan N (1988) *Nonparametric Statistics for the Behavioural Sciences*, McGraw-Hill, New York, 399 pp.
- Solecki W.D, Oliveri C (2004) Downscaling climate change scenarios in an urban land use change model. *Journal of Environmental Management*, 72: 105–115.
- Solow A (1987) Testing for climatic change: an application of the two-phase regression model. *J. Climate Appl. Meteorol.*, 26: 1401–1405.
- Steinecke K (1999) Urban climatological studies in the Reykjavik subarctic environment, Iceland. *Atmospheric Environment*, 33: 4157–62 .
- Storvold R et al. (1998) Boundary-layer structure obtained with a Tethered Balloon System and Large-Scale Observations of the Arctic basin obtained with a Satellite Data Acquisition System at the SHEBA Ice Camp. Proceedings of the Eighth Atmospheric Radiation Measurement (ARM) Science Team Meeting, ARM-CONF-1998, March 1998 Tucson, Arizona.
- Stull R.B (1988) *An introduction to boundary layer meteorology*. Kuwer Academic Publishers, Netherland.
- Suckling PW (1980) The energy balance microclimate of a suburban lawn. *Journal of Applied Meteorology* 19: 606–608.
- Suh M-S, Lee D-K (2004) Impacts of land use/cover changes on surface climate over east Asia for extreme climate cases using RegCM2. *J. Geophysical Research*, 109: 1–14.
- Szentimrey T (1996) Statistical procedure for joint homogenization of climatic time series, Proceedings of the Seminar for Homogenization of Surface Climatological Data, Budapest, Hungary, pp. 47–62.
- Szentimrey T (1999) Multiple Analysis of Series for Homogenization (MASH)', Proceedings of the Second Seminar for Homogenization of Surface Climatological Data, Budapest, Hungary; WMO, WCDMP-No. 41, pp. 27-46.

- Szentimrey T (2000) Multiple Analysis of Series for Homogenization (MASH). Seasonal application of MASH (SAM), Automatic using of Meta Data, Proceedings of the Third Seminar for Homogenization of Surface Climatological Data, Budapest, Hungary.
- Taha H (1996) Modeling impacts of increased urban vegetation on ozone air quality in the south coast air basin. *Atmos Environ* 30: 3423–3430.
- Taha H (1997) Urban climates and heat islands: albedo, evapotranspiration, and anthropogenic heat. *Energy and Buildings*, 25: 99–103.
- Taha H, Akbari H, Rosenfeld A (1989) Vegetation microclimate measurements: the Davis project, Lawrence Berkeley Lab. Rep. 24593.
- Taha H, Akbari H, Rosenfeld A (1991) Heat island and oasis effects of vegetative canopies: Micrometeorological field measurements, *Theor. Appl Climat.*, 44(2): 123–138.
- Tan J, Zheng Y, Tang X, Guo C, Li L, Song G, Zhen X, Yuan D, Kalkstein A.J, Li F, Chen H (2010) The urban heat island and its impact on heat waves and human health in Shanghai. *Int J Biometeorol* 54: 75–84.
- Thom E.C (1959) The discomfort index. *Weatherwise*, 12, 57-60.
- Tominaga Y, Mochida A, Yoshie R, Kataoka H, Nozu T, Yoshikawa M, Shirasawa T (2008) AIJ guidelines for practical applications of CFD to pedestrian wind environment around buildings. *Journal of Wind Engineering and Industrial Aerodynamics*, 96:1749–1761.
- Toreti A, Kuglitsch F. G, Xoplaki E, Della-Marta P. M, Aguilar E, Prohomf M, Luterbacherg J (2011) A note on the use of the standard normal homogeneity test to detect inhomogeneities in climatic time series. *Int. J. Climatol.* 31: 630–632.
- Trenberth, K.E., P.D. Jones, P. Ambenje, R. Bojariu, D. Easterling, A. Klein Tank, D. Parker, F. Rahimzadeh, J.A. Renwick, M. Rusticucci, B. Soden and P. Zhai (2007) Observations: Surface and Atmospheric Climate Change. In: *Climate Change 2007: The Physical Science Basis*. Contribution of Working Group I to the Fourth Assessment Report of the Intergovernmental Panel on Climate Change [Solomon, S., D. Qin, M. Manning, Z. Chen, M. Marquis, K.B. Averyt, M. Tignor and H.L. Miller (eds.)]. Cambridge University Press, Cambridge, United Kingdom and New York, NY, USA.
- Tuomenvirta H (2002) Homogeneity Testing and Adjustment of Climatic Time Series in Finland. *Geophysica*, 38(1-2): 15-41.

- U.S. Energy Information Administration (2008) Energy statistics on Pakistan during 1980 to 2008. <http://www.eia.gov/countries/country-data.cfm?fips=PK#undefined>
- UNDESA (2011) World Population Prospects: The 2010 Revision, United Nations, Department of Economic and Social Affairs, Population Division, New York, <http://esa.un.org/unpd/wup/index.htm>
- Unger J, Bottyan Z, Sumeghy Z, Gulyas A (2000) Urban heat island development affected by urban surface factors. *Idojaras* 104: 253–268.
- Vedal S (1997) Ambient particles and health: Lines that divide. *J. Air & Waste Manage. Assoc.*, 47: 551–581.
- Verseghy D.L, Munro D.S (1989a) Sensitivity studies on the calculation of the radiation balance of urban surfaces: I. Shortwave radiation. *Boundary-Layer Meteorology* 46: 309–331.
- Verseghy D.L, Munro D.S (1989b) Sensitivity studies on the calculation of the radiation balance of urban surfaces: II. Longwave radiation. *Boundary-Layer Meteorology* 48: 1–18.
- Vincent L (1998) A technique for the identification of inhomogeneities in Canadian temperature series, *J Climat.*, 11: 1094–1104.
- Voogt J.A (2002) Urban heat island: causes and consequences of global environmental change, vol 2. Wiley, Chichester, NY, pp 660–666.
- Voogt J.A (2003) Urban Heat Island. Volume 3, Causes and consequences of global environmental change, pp 660–666. Edited by Professor Ian Douglas in *Encyclopedia of Global Environmental Change*. John Wiley & Sons, Ltd, Chichester, 2002.
- Voogt J.A (2007) How researchers measure urban heat islands. Washington: USEPA. http://www.epa.gov/hiri/resources/pdf/EPA_How_to_measure_a_UHI.pdf.
- Voogt J.A, Oke T.R (1998) Effects of urban surface geometry on remotely-sensed surface temperature. *International Journal of Remote Sensing*, 19(5): 895–920.
- Voogt J.A, Oke T.R (2003) Thermal remote sensing of urban climates. *Remote Sens. Environ.* 86: 370–384.
- Vose R.S, Easterling D.R, Gleason B (2005) Maximum and minimum temperature trends for the globe: An update through 2004. *Geophys. Res. Lett.*, 32, L23822, doi:10.1029/2004GL024379.
- Vose R.S, Karl T ;R, Easterling D.R, Williams C.N, Menne M.J (2004) Impact of land-use change on climate. *Nature*, 427:213–214.

- Wallace J.M, Hobbs P.V (2006) Atmospheric Science: An Introductory Survey. 2nd Ed. Academic Press Elsevier, p. 1–505.
- Wan Z, Dozier J (1996) A Generalized Split- Window Algorithm for Retrieving Land-Surface Temperature from Space. IEEE Trans. Geosci. Remote Sens, 34(4): 892–905.
- Wan Z, Li Z.L (1997) A physics-based algorithm for retrieving land-surface emissivity and temperature from EOS/MODIS data. IEEE Trans. Geosci. Remote Sens. 35 (4): 980–996.
- Wang H-J (1999) Role of vegetation and soil in the Holocene megathermal climate over China. J. Geophysical Research, 104(D8): 9361–9367.
- Wehrli C (1985) Extra-terrestrial solar spectrum. Publication Number 615, World Radiation Centre, Davos Dorf.
- Weng Q, Lub D, Schubring J (2004) Estimation of land surface temperature–vegetation abundance relationship for urban heat island studies. Remote Sensing of Environment 89: 467–483.
- Weng Q, Yang S (2004) Managing the Adverse Thermal Effects of Urban Development in a Densely Populated Chinese City. Journal of Environmental Management, 70(2): 145-156.
- Wijngaard J.B, Klein Tank, A.M.G, Können G.P (2003) Homogeneity of 20th century European daily temperature and precipitation series. Int. J. Climatol., 23: 679-692.
- Wikipedia (2012) Faisalabad the city information. Wikipedia, the free encyclopedia. <http://en.wikipedia.org/wiki/Faisalabad>
- Wikipedia (2012): Demographics of Pakistan. <http://en.wikipedia.org/wiki/Pakistan>
- World of Maps (2013) Map of Pakistan (Topographic Map). Online maps and travel information. <http://www.worldofmaps.net/uploads/pics/topographische-karte-pakistan.jpg>.
- World Urbanization Prospects (2005) World Urbanization Prospects: The 2005 Revision, Department of Economic and Social Affairs, United Nation Population Division, <http://www.un.org/esa/population/publications/WUP2005/2005wup.htm>
- World urbanization Prospects (2011) World urbanization Prospects: The 2009 Revision. Department of Economic and Social Affairs, United Nations, ESA/P/WP/215, 1–55.
- Xiao H, Weng O (2007) The impact of land use and land cover changes on land surface temperature in a karst area of China. Journal of Environmental Management 85: 245–257.
- Xie X, Liu C-H, Leung DYC (2007) Impact of building facades and ground heating on wind flow and pollutant transport in street canyons. Atmospheric Environment, 41: 9030–9049.

- Yagüe C, Zurita E, Martinez A, (1991) Statistical analysis of the Madrid urban heat island. *Atmos Environ.*, 25: 327–332.
- Yin D, Zhiqing X, Yan Z, Yafeng S., Jingang W (2007) Impact of urban expansion on regional temperature change in the Yangtze River Delta. *J Geog Sci.*, 17: 387–398.
- Zhang G.J, Cai M, Hu Aixue (2013) Energy consumption and the unexplained winter warming over northern Asia and North America. *Nature Climate Change*, doi:10.1038/nclimate1803.
- Zhang J, Dong W, Wu L, Wei J, Chen P, Lee D-K (2005) Impact of land use changes on surface warming in China. *Advances in Atmospheric Sciences*, 22(3): 343–348.
- Zhang K, Wang R, Shen C, Da L (2010) Temporal and spatial characteristics of the urban heat island during rapid urbanization in Shanghai, China. *Environ Monit Assess.* 169: 101–112.
- Zhao M, Pitman A.J, Chase T (2001) The impact of land cover change on the atmospheric circulation. *Climate Dynamics*, 17: 467–477.
- Zhao S, Da L, Tang Z, Fang H, Song K, Fang J (2006) Ecological consequences of rapid urban expansion: Shanghai, China. *Front Ecol Environ* 4(7): 341–346.
- Zhou L, Dickinson R.E, Tian Y, Fang J, Li Q, Kaufmann R.K, Tucker C.J, Myneni R.B (2004) Evidence for a significant urbanization effect on climate in China. *PNAS*, 101: 9540–9544.

CURRICULUM VITAE

Mr. Sajjad Hussain SAJJAD

Date of birth: 14.09.1977

Birth place: District Muzaffargarh

Country of birth: Pakistan

Address (Home)

House No. 01, 24 rue de Milan

67000 Strasbourg, FRANCE

Tel mobile: 0033. 06.25.95.39.76

Tel Res.: 0033.3.69.36.25.26

Email: shsajjad@hotmail.com

-

-

-

-

-

-

Address (Work place)

Department of Earth Sciences

University of Sargodha

40100 Sargodha - PAKISTAN

Phone: 0092.333.42.83.023

Email: shsajjad@hotmail.com

EDUCATION

PhD (2009 – 2013)

From Laboratoire Image ville et Environnement, Faculté de Géographie, Université de Strasbourg – 67000 Strasbourg, France.

Thesis Title: “*Observational and Modelling approaches to study urban climate*”

Skills acquired: Finite volume method, urban parameterization, model simulations, homogenization of time series data, use of SPSS, Tanagra.

Operating systems: Windows, Linux

Programming languages: FORTRAN, R

Master of Geography (2008 – 2009)

Master of Geography (Research) from Department of Geography, Université de Nancy2, France

Thesis Title: “*Use of Finite Volume Mesoscale (FVM) model to study urban heat island of Karachi*”

M. Phil South Asian Studies (2002 – 2004)

M. Phil South Asian Studies (Research) with specialization in Geography from Center for South Asian Studies, University of the Punjab, Lahore – Pakistan

Thesis Title: “*Impact of climate changes on South Asia*”

Master of Geography (1998 – 2000)

Master of Geography (Professional) from Department of Geography, University of the Punjab, Lahore – Pakistan

Bachelor of Arts (B.A) (1995 – 1998)

Bachelor of Arts (B.A) with major subject of Geography from Bahauddin Zakariya University Multan – Pakistan

COURSES

French Language Courses (19.05.2008 – 12.09.2008)

Langue, Communication et Culture Française. From Centre d'Approches Vivantes des Langues et des Médias, CAVILAM, Vichy, France.

Other Courses

- Sep. 2012: Energy Transition: global concerns and local Responses. Course attended at Pôle Européen de Gestion et d'Économie (PEGE), Université de Strasbourg, France.
- Apr. 2012: Climate, Pollution and Energy. Organized by Forum Réseau Alsace des Laboratoires en Ingénierie et Sciences pour l'Environnement (REALISE).
- Feb. 2012: New and Renewable Energies, Course attended at Collège Doctorale Européen (CDE), Strasbourg, France.
- Feb. 2011: Protection du patrimoine scientifique et sécurité d'information, Faculté de Géographie, Université de Strasbourg, France.
- Jan. 2011: Science and Society, Course attended Collège Doctorale Européen (CDE), Strasbourg, France.
- Oct. 09 à feb. 2010: Introduction of numerical modeling of fluids as well as atmospheric sciences. Course attended Faculté de Géographie, Université de Strasbourg, France.
- Oct. 2005: American History, Consulate general of United States of America, Lahore, Pakistan.
- Juin, 2002: Intel Teach to the Future, Intel Microsoft Company, Lahore, Pakistan
- 1996–1997: Certificate of Teaching (CT), from Allama Iqbal Open University, Islamabad – Pakistan.

Workshops Attended

- Jan. 2011: Application of Zotero, Université de Strasbourg, France
- Dec. 2010: Homogenization of Time Series Data by using SNHT and PRODIGE, at Centre for Climate Change, Université Rovira I Virgili, Tarragona – Espagne.
- Jun. 10-11, 2010: Analysis of qualitative data and classifications of data, Faculté de Géographie, Université de Strasbourg, France.
- Feb. 20 to May 17, 2006: Faculty Development Course from Higher Education Commission Islamabad, Pakistan.
- Sept. 20-25, 2004: In-Service Teacher Training in Geography from Higher Education Commission, Islamabad, Pakistan.

PROFESSIONAL EXPERIENCE

Research

- 2009 – 2013: Doctorate (Ph.D) from Laboratoire Image Ville Environnement, Centre National de la Recherche Scientifique, Faculté de Géographie, Université de Strasbourg, 67000 Strasbourg – France.
- Aug. 06–30, 2012: Participating researcher, Centre Interdisciplinaire d'Analyse des Processus Humains et Sociaux. Université Rennes 2, Rennes – France.

Teaching

- Jan 30 to Jun 30, 2011: *Tuteur* Espace réussite, Faculté de Géographie, l'Université de Strasbourg, France.
- Sep 05, 2005 to Jan. 2008: *Lecturer* Physical Geography, Department of Earth Sciences, University of Sargodha, 40100 Sargodha – Pakistan.

Administrative jobs

- Oct. 01, 2012 to Mar. 29, 2013: Vacataire Administrative, Service Alumni, Université de Strasbourg, France.
- Feb. 13 to Jun. 30, 2012: Vacataire Administrative, Service Alumni, Université de Strasbourg, France.
- Oct. 17, 2011 to Jan. 17, 2012: Vacataire Administrative, Service Internationale for foreign researchers, Université de Strasbourg, France.

Workshops Coordinator / Organizer:

- Mar. 26-31, 2007: Six Days Workshop on Research Methodology at University of Sargodha. Sponsored by Higher Education Commission Government of Pakistan.
- Dec. 06-08, 2007: Three Day Workshop on Project Management at University of Sargodha. Sponsored by Higher Education Commission Government of Pakistan.
- Feb. 03-07, 2008: Six Days Workshop on Research Methodology at University of the Punjab Lahore. Sponsored by Higher Education Commission Government of Pakistan.

RECHERCHE INTEREST

Mesoscale climates, Urban Heat Island, Relationship between global warming and urban climate, Energy consumption effects on UHI, Regional and global climate changes and effects, Climate vulnerabilities, adaptabilities and resiliences, Environmental degradation and effect on human health, landuse change effect on local urban climates.

PUBLICATION

International Journals

- Sajjad S.H, Blond N, Clappier A (2013) Urban size, landuse change and building height effect on urban temperature (Submitted for possible publication).
- Sajjad S.H, Blond N, Clappier A (2013) A comparative analysis of the change in temperature on urban, town and rural areas (Submitted for possible publication).
- Sajjad S.H, Blond N, Clapier A, Raza A, Shirazi S.A, Shakrullah K (2010) The preliminary study of urbanization, fossil fuels consumption and CO₂ emission in Karachi. *African Journal of Biotechnology*, 9(13): 1941-1948.
- Sajjad S.H, Hussain B, Khan M.A, Raza A, Zaman B, Ahmed I (2009) On rising temperature trends of Karachi in Pakistan. *Climatic Change*, 96: 539-547.
- Sajjad S.H, Shirazi S.A, Khan M.A, Raza A (2009) Urbanization effects on temperature trends of Lahore during 1950-2007. *Int. J. of Climate Change Strategies and Management*, Vol 1:274-281.

Oral Communication in Conferences

- Sajjad S.H, Blond N, Clappier A (2013) A comparative analysis of the change in temperature on urban, town and rural areas. International Conference on urban climate and history of meteorology. 25 to 26 February 2013, Florence – Italy.
- Sajjad S.H, Blond N, Clappier A (2012) Urban size and landuse change effect on urban heat island. 8th International Conference on Urban Climate – ICUC8 and 10th Symposium on the Urban Environment, Dublin – Ireland from 6 – 10 August 2012.
- Blond N, Kohler M, Mauree D, Sajjad S.H, Clappier A (2012) Development of a new canopy model to improve urban meteorology modeling. European Geosciences Union (EGU) General Assembly 2012, Vienna – Austria 22 – 27 April 2012.
- Sajjad S.H, Blond N, Clappier (2011) Observed temperature changes of Quetta City, Pakistan from 1961-2006. Pakistan Urban Forum, Lahore – Pakistan on 01 – 05 March 2011.
- Shirazi S.A, Sajjad S.H (2008) Urbanization and its effect on temperatures of Lahore. 13th All Pakistan Geographical Conference, 21 – 23 December 2008, Karachi – *Pakistan*.
- Sajjad S.H, Khan M.A, Raza A (2007) Urbanization and temperature trends of Karachi in Pakistan. 3rd International Conference on Urbanization, Agriculture and Environment at Science City of Munõz – Philippines on 04 – 07 November, 2007.
- Sajjad S.H, Khan M.A, Raza A (2007) Prevailing drought conditions in Sind and Balochistan provinces of Pakistan. 9th Asian Urbanization Conference, Kangwon-do National University, Kangwon National University, Chuncheon, Republic of Korea (South Korea) on 18 – 23 August 2007.

- Prof. Dr. Safdar Ali Shirazi, Department of Geography, University of the Punjab Lahore, Lahore, Pakistan. Phone: 0092 (0) 3004210213. Email: geoshirazi@hotmail.com